SOME SYSTEMATICS OF URANIUM AND LEAD DISTRIBUTION IN RELATION TO THE PETROLOGY OF THE MT. RUBIDOUX GRANITES, RIVERSIDE COUNTY, CALIFORNIA

Thesis by

Philip Oren Banks

In Partial Fulfillment of the Requirements

For the Degree of

Doctor of Philosophy

California Institute of Technology

Pasadena, California

1963

ACKNOWLEDGEMENTS

I am indebted to many people for providing a stimulating environment in which to carry out this work, especially Dr. Hugh T. Millard, Dr. R. E. Zartman, Mr. C. R. McKinney, and Mr. Lisle Jory. I owe an additional debt of gratitude to Dr. M. A. Lanphere for assistance in learning the techniques of Rb-Sr analysis, and to Dr. M. Tatsumoto for advice on the ion-exchange method of lead extraction. Mr. A. A. Chodos generously provided his time to assist and advise on x-ray analytical techniques. For assistance in performing many of the manual operations I am grateful to Mrs. G. Baenteli, Mr. G. Cebula, and Mr. N. Shields. I particularly wish to acknowledge discussions, criticism, and advice provided by Dr. G. J. Wasserburg. Above all, I am indebted to my advisor, Dr. L. T. Silver, for his continued support and interest, and for providing much of the information on which this project has been based. His knowledge and ideas have been a constant source of stimulation and encouragement.

This work was supported by United States Atomic Energy Commission Contract AT(04-3)-427. A portion of the equipment used was bought through a grant from the Society of the Sigma Xi.

ABSTRACT

Field and petrologic studies and uranium-lead isotope geochemistry investigations have been made of the Mt. Rubidoux granites, Riverside Co., Calif. The coarse-grained granite was emplaced earlier than the fine-grained granite, and both were intruded by later dikes of pyroxene granodiorite. The two rocks are very similar quartz monzonites with an unusual assemblage of iron-rich silicates including biotite, hornblende, hypersthene, and fayalite. The composition of the fine granite corresponds very nearly to a natural minimum in the Q-Or-Ab-water system. Data from published experimental studies suggest a temperature of 700-760°C and a water vapor pressure of 1000-1500 bars during crystallization. The presence of fayalite and hypersthene is attributed to late-stage loss of water pressure.

U-Pb isotopic analyses of accessory minerals, potash feldspar, and whole rock samples were performed to investigate the behavior of these isotopes in the coarse granite. Zircon, uranothorite, allanite, and apatite constitute the principal sites of U and radiogenic Pb in the rock. Apatite was not analyzed. Systematic analyses of the other minerals have provided a criterion for recognizing discordance in young U-Pb systems. The granites are at least 116 m.y. old and possibly as old as 130 m.y. Variations in the degree of discordance for equivalent zircon fractions from different localities suggest that an unrecognized episodic event less than 100 m.y. ago may have caused the discordance.

Zircon fractions from other rocks of the southern California batholith gave the following minimum ages: Woodson Mtn. granodiorite 119 m.y.; pyroxene granodiorite 108 m.y.; Crestmore quartz monzonite porphyry 106 m.y. Zircons from a soil profile over the coarse granite contained older zircons which have a minimum age of 1730 m.y. and are thought to be from metasedimentary wall rocks.

The isotopic composition of common lead was determined by several analyses of potash feldspar. Analyses of whole rock material and acid leaches of the fresh granite indicate that the total rock is discordant to the same extent as the principal minerals, and that the abundance and leachability of U and radiogenic Pb in the rock are governed strongly by the mineral uranothorite. Similar analyses of C-zone weathered granite indicate that the chief effect of weathering is to make available to acid leaching a higher proportion of common lead from the feldspar and radiogenic Pb^{208} from allanite.

Isotopic analyses of radiogenic Pb have been utilized to evaluate the decay constant of U^{235}. The presently accepted constant is believed to be accurate to within 1%, relative to the accepted constant for U^{238}.

The effects of intermediate daughter losses in contributing to discordance in natural U-Pb systems have been considered in a series of model calculations. It is suggested that such losses may be of significance where the degree of discordance is relatively small and/or where the apparent time of episodic disturbance is very young.

TABLE OF CONTENTS

Chapter 1

INTRODUCTION

The project reported herein was undertaken primarily to investigate the distribution and behavior of uranium and lead in a single body of granitic rock. It was desired to know if the major sources of these elements within the rock could be isolated and systematically studied with regard to their mineralogy and isotopic character and if the characteristics of these sources were adequate to account for the characteristics of the total rock system. It was desired to explain the availability of acid-leachable uranium and lead, and to investigate at least preliminarily the effects of weathering in disrupting and redistributing the isotopic systems within the rock.

This work represents part of a long-range investigation of the geochemical behavior of uranium and lead being carried out at the California Institute of Technology (Brown and Silver, 1). Earlier studies of detailed mineral separates from several different rocks and many acid leaching experiments on whole-rock powders, performed largely by L. T. Silver and co-workers, had indicated the need for a critical evaluation of the influence of accessory minerals in determining the properties of total rock uranium-lead systems. In particular, three factors of importance in

undertaking such an evaluation had been established: 1) Analyses of individual mineral separates can be meaningfully interpreted only if care is taken to insure mineralogical purity. 2) Individual mineral species may show a range of isotopic properties, the extent of which should be known in order to adequately judge the contribution of that species to the total rock system. 3) A significant fraction of the uranium (and thorium) in a given rock may reside in mineral species whose abundance is far too small to measure accurately, thereby placing a limit on the use of material balance calculations for estimating isotopic imbalance in the whole rock. These considerations suggested that isotopic systematics alone might provide a sensitive way of determining the relative contributions of the various components to the total rock system, if sufficiently different properties existed among the components.

In basic outline, the project has consisted of five parts: 1) the selection and geological evaluation of a suitable body of rock, 2) the identification, isolation, and isotopic analysis of those mineral species which contribute significant amounts of uranium and radiogenic lead to the rock, with emphasis on the range of variation within each species, 3) a determination of the isotopic composition of original or "common" lead in the rock and an investigation of the sampling and analytical problems involved in obtaining this figure, 4) the isotopic analysis of samples of whole

rock, and 5) the extraction and measurement of acid-soluble uranium and lead. Analytical work was performed on mineral separates, whole rock samples and leaches of both fresh and weathered materials.

Each analysis consisted of a measurement of the isotopic composition of lead and a determination, by isotope dilution, of the concentrations of lead and uranium in the sample. These parameters were then employed as a means of estimating the isotopic balance in the total rock system, without attempting to measure the weight percent contribution of each mineral species. The strength of this sort of approach depends on the number of contributing sources and the number of available parameters. Results of the present study, for example, would have been augmented, though probably not significantly changed, by the determination of thorium as well as uranium and lead, but facilities were not available for doing so.

The rock selected for this work is the coarse-grained leucogranite of Mt. Rubidoux, Riverside County, California, which is part of the Cretaceous batholith of southern California (Larsen, 2). A considerable number of analyses were also performed on samples of the fine-grained leucogranite of the same locality. Several factors contributed to this choice. Primarily it was desired to study a young rock situated in a simple geologic setting so that complexities due to possible secondary events would be minimized.

It was known (Larsen, 2; Silver, personal communication; Larsen and Gottfried, 3) that the Rubidoux granites contain a relatively large amount of radioactivity distributed in several different mineral phases, and hence that it would be possible, in spite of the young age of the system, to detect and accurately measure the accumulated radiogenic lead. It was believed that definitive field relationships could be worked out, and it was known that samples of very fresh rock were readily accessible (Silver, personal communication). Moreover, the fact that these rocks were postulated by Larsen to be the last differentiates of the batholith made them interesting from several geochemical points of view, and had resulted in a large body of data accumulated from a number of earlier investigations.

In addition to the central objective of the work, three other goals were pursued. One necessary consequence of the analytical work was a determination of the approximate age of the rock. It was found that all radioactive systems in the rock showed evidence of having been isotopically disturbed. This matter was investigated in some detail, particularly with regard to the mineral zircon. Age determinations were made on zircon samples from other rocks in the local area to place the Rubidoux granites in geochronological perspective.

A second consequence of the analytical work was the accumulation of many analyses of young radiogenic lead, which made possible an evaluation of the half-life of U^{235} relative

to that of U^{238}. The age of the Rubidoux granites is such that mass spectrometric errors in determining the isotopic composition of radiogenic lead are more significant than the uncertainty of determining the true age of a slightly disturbed system from the Pb^{206}/U^{238} ratio, and the precision of mass spectrometry suffices to give a closer estimate of the relative half-lives than has been established previously.

Finally, it was desired to investigate possible theoretical models of intermediate daughter loss as a cause of discordance in natural radioactive systems.

Chapter 2

GEOLOGY AND PETROLOGY OF THE MOUNT RUBIDOUX GRANITES

Introduction

The two granites chosen for the present investigation were first mapped and described by Larsen (2) in his classic study of the batholith of southern California. He called them the coarse-grained and fine-grained leucogranites of Mt. Rubidoux and showed that they are very similar leucocratic quartz monzonites; that they contain several iron-rich minerals including hypersthene, biotite, and hornblende; that their compositions are consistent with the hypothesis that they were among the last materials of the batholith to crystallize; and that they are limited in occurrence to a few isolated hills in the vicinity of the city of Riverside, California. His mapping, however, was not sufficiently detailed to permit him to establish a definite intrusive relationship between the coarse and fine granites or between these rocks and other rock types of the batholith.

Several subsequent investigations concerning various geochemical features of the batholith have contributed to a growing body of data on the Rubidoux granites. Larsen and Draisin (4) analyzed the chemical composition of the mafic minerals and determined their optical properties. Patterson, Silver and McKinney (5) measured the isotopic composition of lead from a whole-rock sample of the coarse

granite. Larsen, Gottfried, Jaffe and Waring (6) performed age determinations on zircon by the lead-alpha method. Whitfield, Rogers and Adams (7) determined the concentrations of uranium and thorium in the fine granite by gamma spectrometry, and Larsen and Gottfried (3) measured by fluorimetry the concentration of uranium in whole-rock samples and in mineral separates from both granites. Finally, Taylor and Epstein (8) investigated the oxygen isotopic composition of the coarse granite and its major minerals.

None of the later studies, however, included an attempt to supplement Larsen's original field work, and definitive criteria for determining time relationships in the development of the Rubidoux granites therefore remained lacking. The first portion of the present work was devoted to this problem and to the problem of evaluating, insofar as possible, the petrogenic history of the rocks; i.e. their mode of emplacement, the probable temperature and pressure conditions that prevailed during their crystallization, and the nature of identifiable secondary events, if any. Pertinent information was obtained by field work, thin section examination, and chemical, optical, and x-ray analyses of individual mineral separates.

The investigation has proven to be petrologically interesting and valuable. Field mapping has shown that simple and straightforward intrusive relationships exist in the areas accessible to study, and comparison of the two granites with experimentally studied systems has permitted a

close estimate to be made of the temperature and pressure during crystallization. Two factors have made this possible: 1) The rocks are composed predominantly of quartz, microcline perthite, and oligoclase, with a relatively small percentage of anorthite and other minerals. The natural systems are thus similar to the "Residua" system studied by Tuttle and Bowen (9). 2) The presence of several iron-rich silicates, including fayalite in addition to the phases identified by Larsen, places severe restrictions on possible equilibrium P-T conditions of crystallization. Although experimental studies of the iron-magnesium silicate systems are far from complete, enough information is available to complement and reinforce conclusions based on the work of Tuttle and Bowen.

Location and Geologic Setting

Detailed mapping of the Rubidoux granites was undertaken at Mt. Rubidoux itself. Reconnaissance visits to other exposures of the granites were made to verify or, where necessary, alter the distribution mapped by Larsen. Mt. Rubidoux is an elongate, northeast-southwest trending monadnock situated in Riverside County, California. It is bounded on the northwest by the Santa Ana River and on the southeast by an alluvial plain upon which has been built the city of Riverside (Fig. 1). U.S. Highway 60 crosses a saddle which divides Mt. Rubidoux from a topographically lower extension to the northeast known as Little Rubidoux.

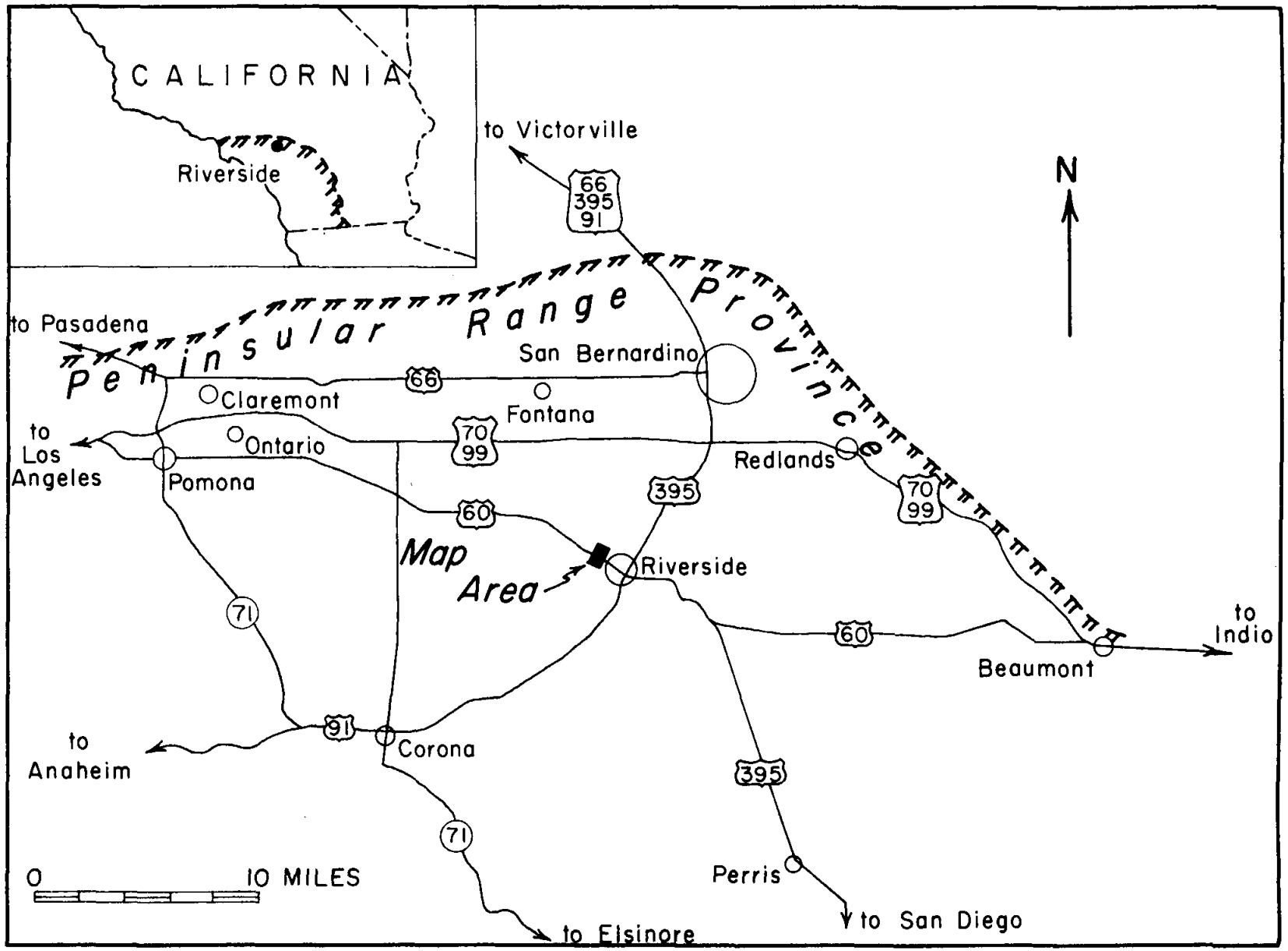

Figure 1. Location Map

Mt. Rubidoux comprises one of the northernmost exposures of rocks of the Peninsular Range province. Boundaries of the province are defined by the Sierra Madre fault system on the north, the San Andreas fault system on the east, and the Pacific Ocean on the west. To the south the province extends throughout Baja California.

In southern California the oldest rocks of the province are comprised of two principal groups of lithologies: 1) variably metamorphosed clastic sediments with minor marbles (Bedford Canyon formation), generally of unknown age but including some middle and upper Jurassic units, and 2) weakly to moderately metamorphosed volcanic flows, tuffs, and breccias (Santiago Peak volcanics), predominantly andesitic in composition, and younger than at least part of the Bedford Canyon formation. Intrusion of the batholith into these rocks in Middle and Late Cretaceous time generally followed the classical scheme of evolution: gabbros were the first to be emplaced, followed by quartz diorites, tonalites, granodiorites, and finally quartz monzonites. Uplift and erosion during the Tertiary was accompanied by thick accumulations of both marine and non-marine clastic sediments in local basins such as the Los Angeles basin. Considerable volcanic activity characterized the Miocene epoch. Repeated faulting during much of the Tertiary along the Elsinore, San Jacinto, and many smaller fault systems has given the province an overall northwest-southeast physiographic pattern, which essentially coincides with older structural trends in the

crystalline rocks.

More locally, a sequence of quartz-biotite gneisses and schists, interlayered with minor quartzites, amphibolites, and marbles is exposed in the Jurupa Mountains, west of Mt. Rubidoux (MacKevett, 10). The Bonsall tonalite intrudes these rocks in the southern portion of the mountains. Small bodies of other quartz diorites and granodiorites are present and aplite and pegmatite dikes are locally abundant. At the eastern end of the Jurupa Mountains, about two miles north of Mt. Rubidoux, is the famous Crestmore quarry, where an unusual suite of contact metamorphic minerals was produced by the intrusion of quartz monzonite porphyry into magnesian limestone (Burnham, 11).

The hills to the east and south of Mt. Rubidoux, including the Box Springs Mountains, are underlain chiefly by the Bonsall tonalite. Screens and roof pendants of metasedimentary rocks are present, as well as small bodies of other batholithic rocks.

Areal Geology of Mt. Rubidoux

Four rock types were distinguished as mappable units. The coarse-grained and fine-grained leucogranites underlie most of Mt. Rubidoux. Both rocks are leucocratic quartz monzonites and are separable in the field chiefly on the basis of their difference in grain size. The coarse granite, where fresh, has an unusual blue-green color which readily

disappears upon weathering. Scattered mafic inclusions, up to a foot or so across and of variable shape are distributed throughout the coarse granite. The fine granite, where fresh, has a more typical light gray color. Its grain size actually varies from medium to medium-coarse, whereas the coarse granite varies from coarse to very coarse. No mafic inclusions have been found in the fine granite. A third rock type has been called miscellaneous granodiorite and is somewhat like the fine granite but has a greater abundance of dark minerals and a slightly higher proportion of plagioclase. The fourth type, called pyroxene-bearing granodiorite, is a medium-grained rock containing a moderate but variable amount of pyroxene (both monoclinic and orthorhombic) and a higher proportion of more calcic plagioclase than the two leucogranites.

A geologic map of Mt. Rubidoux is shown in Plate 1, and Fig. 2 shows an interpreted cross section. Larsen tentatively believed that the fine-grained variety was the earlier of the two granites to be emplaced, but the detailed mapping clearly shows that this is not the case; the coarse granite is the oldest unit underlying the mountain. The fine granite intrudes the coarse as a thick, arcuate dike, convex to the northwest. On the concave side of this dike the structure is complicated by a branching network of subsidiary dikes of the fine granite which have in part surrounded and isolated blocks of the coarse granite. Relationships of this sort were not found on the convex side of the central dike.

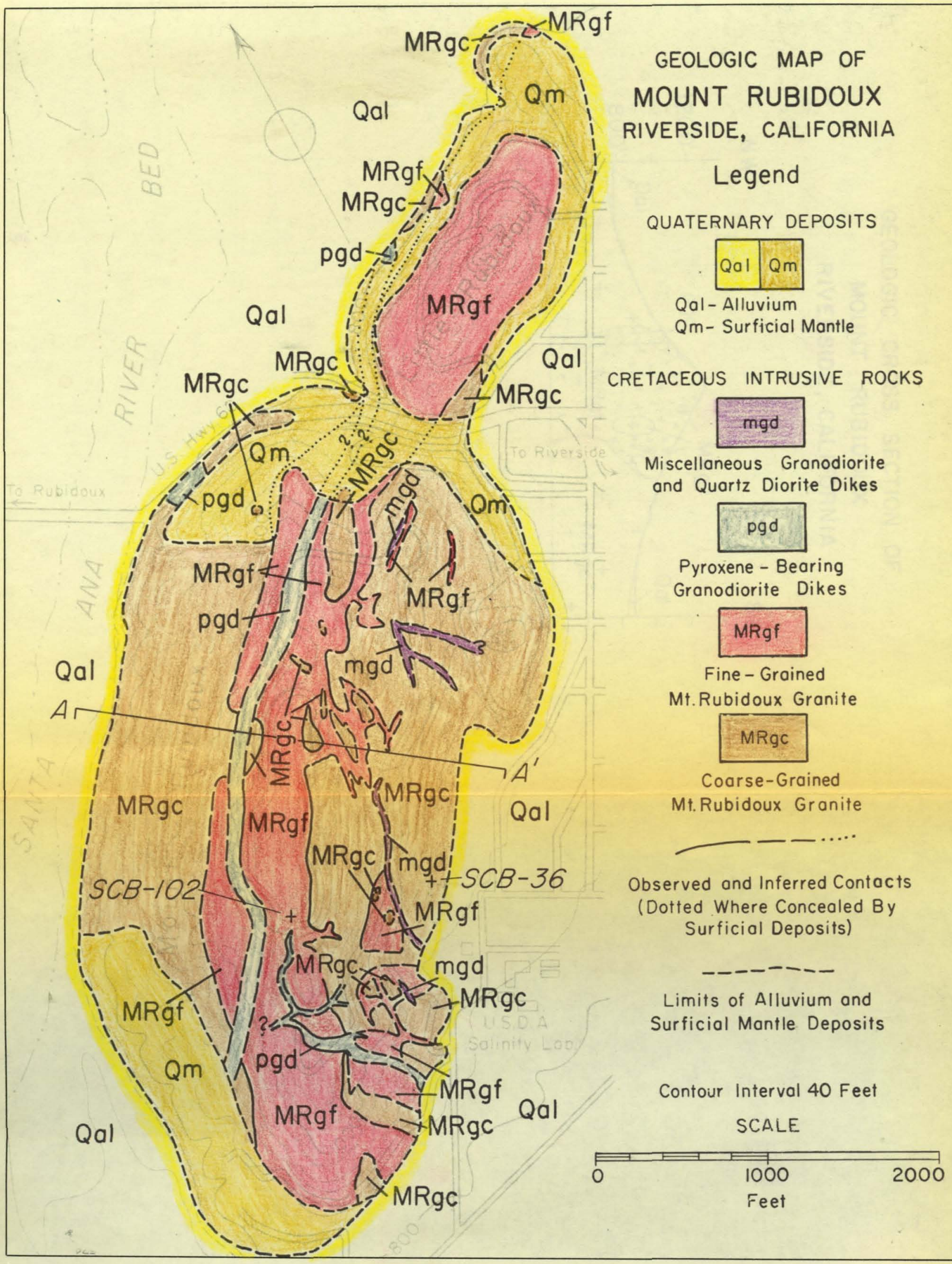
GEOLOGIC MAP OF
MOUNT RUBIDOUX
RIVERSIDE, CALIFORNIA
Legend
QUATERNARY DEPOSITS
Qal
Qm
Qal - Alluvium
Qm - Surficial Mantle
CRETACEOUS INTRUSIVE ROCKS
mgd
Miscellaneous Granodiorite and Quartz Diorite Dikes
pgd
Pyroxene - Bearing Granodiorite Dikes
MRgf
Fine - Grained Mt. Rubidoux Granite
MRgc
Coarse-Grained Mt. Rubidoux Granite
Observed and Inferred Contacts (Dotted Where Concealed By Surficial Deposits)
Limits of Alluvium and Surficial Mantle Deposits
Contour Interval 40 Feet
SCALE
0
1000
2000
Feet
A
A'
SCB-102
SCB-36
To Rubidoux
To Riverside
SANTA ANA RIVER BED
U.S. Hwy 60
U.S.D.A Salinity Lab

Plate 1.

GEOLOGIC CROSS SECTION OF
MOUNT RUBIDOUX
RIVERSIDE, CALIFORNIA

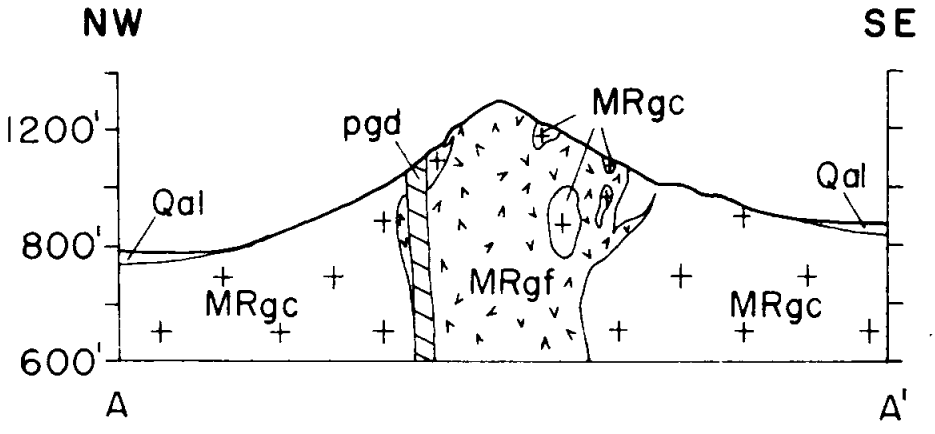

Figure 2

On the lower northwestern flank of the mountain rather prominent masses of fine granite are present, but careful study has shown that they are not in place and must have acquired their position through the influence of gravity.

Where the contact between the coarse and fine granites can be seen it is commonly sharply defined as a sudden change of dominant grain size, but without any apparent chilling of the fine granite (Photograph 1, Appendix B). In many places the contact is a zone, two or three feet wide, in which bands of the coarse and fine grained rocks alternate. On the concave side of the central dike the attitudes of the contacts are quite variable, but on the convex side they are vertical or have a steep dip to the southeast.

In general, the fine granite is more resistant to weathering than the coarse, and this fact influences the overall aspect of Mt. Rubidoux. The crest of the mountain displays huge bouldery outcrops of texturally uniform, light gray to flesh colored fine-grained granite. The subsidiary dikes on the southeast flank of the mountain are less uniform in texture and in places become almost aplitic. Resistance to weathering is apparently reduced where this occurs. On both flanks of Mt. Rubidoux the coarse granite locally develops massive bouldery outcrops similar to those on the crest, but their color is more nearly ruddy brown rather than pink. Elsewhere on the flanks deep weathering has produced

superficial deposits which completely obscure the underlying rock. This material has been shown on the geologic map (Plate 1) as surficial mantle.

The surface deposits appear to be the product of weathering and slope wash in response to present-day topography and climate. A topographic bench on the southwest flank of the mountain was the only feature found which could be related to a previous erosional or depositional environment.

In a few places near the base of Mt. Rubidoux irregular masses, up to a few feet in maximum dimension, of fine grained, gray-green, slightly schistose amphibolitic rock were found in contact with the coarse granite. They are composed largely of calcic oligoclase, hornblende, and hypersthene, and are probably remnants of pre-batholithic rocks into which the granite was intruded. Their small size suggests that they are portions of screens or wholly included masses and thus cannot be taken as evidence for the limit of extent of the coarse granite at this locality.

Many small dikes and stringers of aplite and pegmatite crosscut the two granites. It is possible to distinguish two generations, one which is younger than the coarse granite but older than the fine, and the other which is younger than both granites. These bodies are typical of late-stage development of such material and are composed almost exclusively of quartz, potash feldspar, and soda-rich plagioclase, with minor amounts of muscovite and biotite.

The rock which has been mapped as miscellaneous granodiorite is obviously younger than the coarse granite as it occurs as thin dikes within that rock. The contacts are sharp and without evidence of chilling, although some banding or streaking can be seen in places. The relationship of the granodiorite to the fine granite is more obscure. The fact that it is in some respects similar to the fine granite, and the fact that it appears to be limited in occurrence to the southeast flank of the mountain where the fine granite also occurs, suggest that the two may be closely related genetically.

The youngest intrusive unit at Mr. Rubidoux is the pyroxene granodiorite, which occurs primarily as a relatively thin, continuous dike traversing the length of the mountain and crosscutting both granites. It is more susceptible to weathering than the granites and good exposures are rare. Contacts with the host rocks are sharp, but show slight chilling of the granodiorite and evidence for some reaction, indicated in the field by an increased abundance of biotite in the granites near the contact.

In order to learn more about possible relationships with other rocks of the batholith, exposures of the Rubidoux granites elsewhere in the Riverside area were visited. In all cases except one, Larsen's original conclusions were supported. The exception is the body of coarse granite shown by him to be intruding the Bonsall tonalite northeast of

Quarry Hill. The rock exposed at this site is texturally unlike the coarse granite and contains a higher proportion of less perthitic potash feldspar. It is therefore not considered to be immediately related to the Rubidoux granites. This means that exposures of the coarse granite are limited solely to Mt. Rubidoux, whereas the fine granite occurs at several other localities including Pachappa Hill, Victoria Hill, and Quarry Hill. At one of the small hills just beyond the eastern end of Arlington Avenue the fine granite is in intrusive contact with metasedimentary rocks. At Quarry Hill the fine granite must be in contact with a quartz diorite body, but the actual contact is obscured by soil cover.

To the northeast of Little Rubidoux recent roadcuts show that North Hill is underlain at least in part by deeply weathered fine-grained Rubidoux granite. A dike of quartz diorite crosscuts the granite at this locality. Between North Hill and Little Rubidoux a body of quartz diorite containing screens of metasedimentary rocks is exposed, but its contact with the granites cannot be seen.

Evidence from field work thus leads to several important conclusions regarding the genesis and history of the Rubidoux granites:

1) There is clear evidence, both at Mt. Rubidoux and at the eastern end of Arlington Avenue, that the granites were intruded into metasedimentary rocks. On the other hand, there is no positive evidence that they were intruded into any of the other rocks of the batholith.

2) The presence of scattered inclusions in the coarse granite indicates that emplacement was accomplished in part by stoping of the wall rock.

3) The coarse granite was emplaced earlier and must have been largely crystallized when the fine granite was intruded. However, the similarity of the two rocks, the lack of chilled margins, and the degree of intermixing along the contacts indicate that complete solidification of the coarse granite probably had not occurred.

4) The intrusion of the pyroxene granodiorite represents a significant younger event in the history of the granites. It is difficult to believe that the grandiorite is related in any simple way to the granites. Its occurrence in a somewhat different structural geometry than the other rocks and the presence of chilled margins suggest that the granites were completely solidified when it was emplaced.

5) The occurrence of a body of quartz diorite northeast of Little Rubidoux, from which the pyroxene granodiorite could have been derived, suggests that the Rubidoux granites were not the last batholithic rock types to be emplaced in the Riverside area.

Petrography and Mineralogy

The abundance of available analytical information on the mineralogy and chemistry of the Rubidoux granites has greatly aided the present study. Of particular value have been the works of Larsen (2) and Larsen and Draisin (4).

Several of their tables are reproduced in the following for continuity and clarity.

Primary samples were collected at the sites shown on Plate 1, which were chosen to provide the freshest possible material. The coarse granite sample, SCB-36, was obtained from the central portion of a large in situ boulder of disintegration that had been drilled and blasted to provide space for housing construction. The fine granite sample, SCB-102, was collected from a road cut partly blasted through the massive rock. Other smaller samples for thin section examination were collected from many places on Mt. Rubidoux.

The coarse-grained and fine-grained leucogranites. Hand specimens of the two leucogranites differ considerably in appearance. The coarse granite has a striking blue-green color, enhanced by an unusual degree of transparency of the feldspar crystals. Individual grains of feldspar and quartz range up to 1 cm. in length. The fine granite, on the other hand, has a light gray color; the feldspars are translucent to opaque; and individual grains range up to 3-4 mm. in length.

In thin section the rocks are more notable for their similarities than for their differences. Modal analyses are shown in Table 1. The most abundant minerals are quartz, microcline perthite, and plagioclase. Their proportions are such as to place both rocks in the class of quartz monzonites or adamellites. The fine granite has a variable but consistently higher ratio of potash feldspar to plagioclase than

Table 1

MOUNT RUBIDOUX GRANITES

MODAL ANALYSES

	A. Coarse	B. Coarse	C. Fine	D. Fine
Quartz	35.8	33	39.8	34
Plagioclase	30.5	34	21.6	26
Microcline	27.0	32	34.0	36
Myrmekite	2.5	Tr.	1.5	--
Biotite	2.5	2	2.1	2
Hornblende	1.4	1	0.4	Tr.
Opaques	0.1	-	0.3	0.7
Hypersthene	Tr.	0.5	--	n.r.
Fayalite	Tr.	n.r.	--	n.r.
Altn. minerals	0.2	n.r.	0.2	n.r.
Accessories	zircon allanite apatite thorite	zircon allanite sphene	zircon allanite apatite thorite	ziroon allanite sphene monazite
An in plag.	18	18	17	18

A. Coarse-grained leucogranite, SCB-36. Average of 12 thin sections, 20,000 points (L.T. Silver)

B. Coarse-grained leucogranite (Larsen, 2)

C. Fine-grained leucogranite, SCB-102. Average of 4 thin sections, 10,000 points

D. Fine-grained leucogranite (Larsen, 2)

the coarse granite. The gross texture of the rocks is equigranular, and there is no evidence of preferred orientation, cataclasis, or superimposed strain.

Plagioclase is generally somewhat smaller than the quartz or perthite and occurs as discrete, subhedral to euhedral grains. Apparently, therefore, it crystallized independently and at essentially the same time as the perthite; hence these rocks are of the two-feldspar or "subsolvus" type. Most of the plagioclase is albite-twinned unzoned oligoclase (An 18) but occasional grains show strong zoning, with cores as calcic as An 45 in which development of sericite, chlorite, calcite, and other alteration materials has taken place.

Microcline is highly perthitic in both rocks and displays stringers, small exsolved crystals, and rims of albitic plagioclase.

The granites contain an unusual suite of mafic minerals, consisting of hornblende, biotite, hypersthene, and fayalite. The presence of hypersthene was reported by Larsen, but fayalite has been unrecognized previously. It is noteworthy that this suite is present in both rocks, although the mineral separates show that the abundance of hypersthene and fayalite is smaller in the fine granite than in the coarse.

Hornblende and biotite are considerably more abundant than the anhydrous phases. Deep pleochroic colors in both minerals indicate high iron content. In general, they occur as scattered anhedral to subhedral grains. The biotite is

often skeletal or symplektic in form. Occasional euhedral faces of hornblende formed against biotite suggest that the hornblende crystallized somewhat earlier. In places, particularly on the southeast flank of Mt. Rubidoux, the biotite of the fine granite has been altered to a brown chlorite. Commonly associated with the mafic silicates are small opaque grains of both magnetite and ilmenite.

The fayalite and hypersthene are not readily detected in thin section, partly because of their low abundance and partly because they are often severely altered. Where unaltered grains can be seen, they are always anhedral and are texturally interstitial to the other minerals (Photographs 2 and 3, Appendix B). They are usually found in association with the biotite and hornblende, but show no evidence of being in reaction relationship. These features suggest that the anhydrous minerals formed relatively late in the crystallization sequence, and that they were either in equilibrium with the other mafic minerals or else formed out of equilibrium so rapidly that no reaction could occur.

It appears that the abundance of hypersthene and fayalite in the granites varies significantly with location. The samples in this study from which mineral separates were obtained yielded a fair amount of fayalite but almost no hypersthene. On the other hand, Larsen and Draisin (4) worked with a sample of the coarse granite that yielded sufficient hypersthene for a chemical analysis, but they did not report any fayalite. Primary variations in abundance

must be partly responsible for this, but the occurrence of the two minerals is also affected by their susceptibility to later alteration.

Alteration of the hypersthene and fayalite to yellow-orange or red-orange materials is a common feature, and in many instances no trace of the original mineral remains. Under crossed nicols the altered material shows a platy to fibrous, partly isotropic structure. For want of a better name it is here called "iddingsite." The origin of the iddingsite is somewhat uncertain. It could, of course, be produced by weathering, but samples which otherwise show no evidence of weathering, indicated especially by the clear blue-green color of the fresh coarse granite, also contain iddingsite. A second possibility is that the iddingsite was formed by late-stage deuteric activity. This hypothesis is supported by the presence of other deuteric materials.

Material which is interpreted to be truly deuteric in origin occurs as small grains having a slightly pleochroic brown to olive green color and occupying texturally interstitial positions (Photograph 4, Appendix B). Under crossed nicols the grains show a platy, partly isotropic structure somewhat like the iddingsite. Non-isotropic portions have a small negative 2V. A fracture pattern, best described as "shrinkage cracking", is characteristic. Magnetite is often associated with this material.

Extending outward from the grains of deuteric material are thin greenish colored filaments which fill fractures and

cleavage surfaces in the feldspar crystals. It is believed that the blue-green color of the coarse granite is caused by reflections from these filaments within the very clear feldspars. The color is not seen in the fine granite in part because the filaments are less abundant and in part because the feldspars are not as translucent as in the coarse granite.

Accessory minerals of both granites consist of magnetite and ilmenite, zircon, apatite, allanite, thorite and molybdenite. Magnetite and ilmenite usually occur in association with the mafic silicates and the deuteric material. Zircon is commonly present in thin sections and is often included in biotite, where it produces dense pleochroic haloes. Apatite is sparsely distributed as small crystals usually included in feldspar. Allanite occurs as subhedral to euhedral grains, both in isolated positions and associated with biotite and hornblende. It is often twinned. Thorite is very rarely seen in thin section and has been observed only as anhedral grains included in biotite (Photograph 5, Appendix B). Larsen identified sphene in the coarse granite and monazite in the fine granite. Neither of these minerals were seen in this study. A minute amount of molybdenite was obtained in the mineral separates from both granites.

The accumulated data on optical properties of the minerals in the granites are shown in Table 2. Indices of refraction for hornblende, biotite, and hypersthene from the

Table 2

MOUNT RUBIDOUX GRANITES

OPTICAL PROPERTIES OF MINERALS

Coarse-Grained Leucogranite

1.	Hornblende	α = 1.690	yellow brown
		β = 1.702	gray green
		γ = 1.711	olive green
		-2V = 55°	
		Z∧c = 15°	
		Sp. G. = 3.42	
2.	Biotite	α = 1.602	pale yellow-brown
		β = 1.670	dark brown
		γ = 1.673	dark red-brown
3.	Hypersthene	α = 1.752	pale pink
		β = 1.759	pale pinkish green
		γ = 1.765	pale green
		-2V = 78°	
4.	Fayalite	α = 1.807 ± 0.003	
		β = 1.838 ± 0.004	
		γ = 1.852 ± 0.003	
		-2V = 60° est.	
5.	"Iddingsite"	min. obs. index 1.594	
		max. obs. index 1.627	
		2V 50-75° (est.), pos. or neg.	
		Birefringence small, obscured by color of mineral	
6.	Allanite	α = 1.775	yellow brown
		β = 1.789	dark red-brown
		γ = 1.791	nearly opaque
		-2V= 35°+	

Fine-Grained Leucogranite

7.	Biotite	α = 1.610	pale brown
		β = 1.676	dark brown
		γ = 1.677	dark red-brown
8.	Allanite	α = 1.735	amber
		β = 1.750	dark red-brown
		γ = 1.752	nearly opaque
		-2V ca. 30°	

Table 2 (Cont'd)

9.	Monazite	α = 1.798 β = 1.800 γ = 1.848 +2V=5-10°
10.	Zircon (fresh)	N_o = 1.922 N_e = 1.967
11.	Zircon (partly altered)	N_o = 1.918 N_e = 1.968

1, 2, 3, 6, 7: Larsen and Draisin (4)

4,5: SCB-36, This study

8, 9, 10, 11: Larsen (2)

coarse granite, SCB-36, were checked and found to agree within the limits of error with the values reported by Larsen and Draisin. The figures for the mafic minerals indicate a high iron content, which is borne out by chemical analysis (next section). The iddingsite was found to have a considerable range of indices, suggesting that variable compositional factors such as degree of hydration significantly affect its optical properties. The indices are generally lower than for typical iddingsites (e.g. Gay and LeMaitre, 12). An attempt was made to determine more closely the nature of the iddingsite by means of x-ray diffraction, but no reflections could be obtained from the separated material.

Inclusions in the coarse granite can be divided into two types. The most common type is a dark gray to black, fine- to medium-grained equigranular material. A typical specimen contained about 48% plagioclase (An 15-17), 23% biotite, 27% hornblende, 1.5% fayalite, and 0.5% quartz. The mafic minerals have the same optical characteristics as those in the granite. The second type of inclusion has a blue-gray color and is composed of fine-grained, slightly inequigranular quartz and plagioclase in roughly equal amounts, with a relatively low abundance of biotite and hornblende and rare fayalite.

Miscellaneous granodiorite. This is a light gray, medium-grained, equigranular rock showing moderately abundant biotite and hornblende in hand specimen. A modal analysis gave the following results: 36% quartz, 31%

plagioclase (An 18), 22% microcline, 6% biotite, 3% hornblende, and 2% myrmekite. Opaque minerals are present in small amounts and zircon is a prominent accessory. No fayalite or hypersthene or their presumed alteration products were seen. Besides the lack of these minerals, the granodiorite differs from the fine-grained granite in three ways: it has a greater abundance of mafic minerals, it has a lower ratio of potash feldspar to plagioclase, and the microcline is less perthitic. The mafic minerals, however, have optical properties similar to those in the granites.

The miscellaneous granodiorite occurs in locations where nearby exposures of the fine granite show more variable characteristics than are typical of the central dike. In particular, the fine granite locally develops a higher proportion of dark minerals. While complete gradations between the fine granite and the granodiorite have not been found, it seems likely that the granodiorite is a minor development of the same magma which produced the two leucogranites.

Pyroxene-bearing granodiorite. The fresh rock has a medium-gray color, somewhat mottled by small clusters of dark minerals. It is medium- to medium-coarse grained, except near the contacts where it becomes fine-grained, and is roughly equigranular. Small, rounded, dark inclusions 2-3 cm. across are sparsely distributed. A modal analysis gave 45% plagioclase, 23% quartz, 20% potash feldspar, 7% biotite, 2% augite, 1% hypersthene, and 1% hornblende. The

plagioclase contains about 33% anorthite, but ranges to An 40 in the cores of zoned crystals. Opaque minerals and zircon are present.

Grain shape for all constituents is predominantly anhedral. Microcline occurs in an unusual form as large irregular grains interspersed among and surrounding smaller grains of quartz and plagioclase. Smaller grains of potash feldspar are also present and in some cases have a small optic angle like that of sanidine. Hornblende occurs as reaction rims on pyroxene.

A sample of quartz diorite was collected from a small quarry about 0.2 miles northeast of Little Rubidoux. No potash feldspar is present in this rock, but the composition of the plagioclase is very nearly the same as in the pyroxene granodiorite. Augite is present but is almost completely reacted to form uralitic hornblende. The addition of a small amount of potassium and a slightly different cooling history could readily produce from this quartz diorite the pyroxene granodiorite.

The petrographic data thus reinforce the earlier conclusion that batholithic rock types younger than the Rubidoux granites occur in the Riverside area. In addition, two important characteristics of the Rubidoux granites themselves are revealed:

1) They not only have very nearly the same major mineral content, but they both contain small amounts of

hypersthene, fayalite, and distinctive alteration products of these minerals, and both show a similar development of late-stage deuteric material. Therefore it seems most likely that they formed from the same melt and underwent practically identical cooling histories, and thus that they were emplaced at only slightly different times.

2) The occurrence of several iron-bearing phases: magnetite-ilmenite, hornblende, biotite, hypersthene, and fayalite; and the observation that the anhydrous mafic silicates appear to have crystallized late and are not in reaction relationship with biotite or hornblende, suggest that the cooling history was unusual, and that if crystallization occurred at equilibrium the temperature-pressure conditions must have been closely defined.

Chemistry

Chemical analyses of the coarse-grained and fine-grained granites, and the norms calculated therefrom, are shown in Table 3. The analysis of SCB-36 was obtained from L. T. Silver. The figures bring out the close similarity between the two rocks, and in particular demonstrate that they are fairly low in calcium relative to the alkalis, and that they are high in iron relative to magnesium.

Analyses of individual minerals are shown in Table 4 and confirm the iron-rich nature of the mafic phases. An x-ray diffraction pattern was obtained from the fayalite

using quartz as an internal standard, and compared with the determinative curve of Yoder and Sahama (13). A value equivalent to 93% fayalite molecule was found, which is in good agreement with the chemical data.

The analysis of potash feldspar indicates an upper limit for the calcium content of this mineral as it is difficult to completely separate the perthitic material from plagioclase. Larsen and Draisin (4) presented the following figures for potash feldspar:

	Coarse granite	Fine Granite
Na_2O	3.48	2.88
K_2O	10.62	12.36

As a check on the internal consistency of the data, a chemical composition for the coarse granite was calculated from the modal analysis of SCB-36 and is shown in column C of Table 3. The following assumptions were used: 1) biotite and hornblende have the compositions given by Larsen and Draisin; 2) plagioclase is pure $Ab_{80}An_{20}$; 3) myrmekite is 30% quartz and 70% albite; 4) potash feldspar is pure microcline; 5) opaques are pure magnetite; and 6) alteration minerals have the composition of iddingsite given by Winchell and Winchell (14). Agreement with the chemical analyses is quite good.

Table 3

MOUNT RUBIDOUX GRANITES

CHEMICAL AND NORMATIVE ANALYSES

	A. Coarse	B. Coarse	C. Coarse	D. Fine
SiO_2	75.01	73.60	75.60	75.38
TiO_2	0.19	0.18	0.18	0.11
Al_2O_3	13.08	13.84	12.79	12.90
Fe_2O_3	0.51	0.63	0.32	0.79
FeO	1.33	1.43	1.28	0.86
MgO	0.12	0.29	0.27	0.16
CaO	1.40	1.34	1.50	0.84
Na_2O	3.76	3.74	3.08	3.48
K_2O	4.43	4.27	4.69	4.95
H_2O+	0.19	0.17	0.07	0.23
H_2O-	0.10	0.06	0.02	0.02
P_2O_5	0.10	0.02	-	-
MnO	0.02	0.04	-	0.02
SO_3	n.d.	0.13	-	Tr.
BaO	n.d.	0.08	-	0.09
	100.24	99.82	99.80	99.83
q	32.40	31.20		33.72
or	26.20	25.38		29.47
ab	32.00	31.44		29.36
an	5.56	6.95		4.17
hy	1.42	2.55		1.19
mg	0.74	0.93		0.15
il	0.36	0.30		1.16
C	-	-		0.20
di	1.21	-		-
	99.89	98.75		99.42

A. Coarse-grained leucogranite, SCB-36 (W. Blake, analyst)

B. Coarse-grained leucogranite (Larsen, 2)

C. Coarse-grained leucogranite, calculated composition. For details, see text.

D. Fine-grained leucogranite (Larsen, 2)

Table 4

MOUNT RUBIDOUX GRANITES

MINERAL ANALYSES

	A. Potash feldspar	B. Fayalite	C. Hypersthene	D. Hornblende	E. Biotite	F. Biotite
SiO_2	66.79	30.60	44.52	39.56	35.96	37.17
TiO_2	0.02	0.26	1.39	1.46	5.32	3.14
Al_2O_3	18.15	-	4.76	12.18	14.36	14.60
Fe_2O_3	-	-	1.26	4.10	1.42	3.75
FeO	0.34	62.14	38.66	23.18	26.16	26.85
MnO	n.d.	2.08	0.28	0.09	0.04	0.06
MgO	-	2.44	6.59	4.43	5.59	4.23
CaO	0.55	-	1.40	9.98	0.54	0.17
Na_2O	3.22	n.d.	0.39	1.81	0.53	0.15
K_2O	10.23	n.d.	0.19	1.38	8.62	8.25
H_2O+	n.d.	n.d.	0.41	1.26	1.10	1.35
H_2O-	0.01	0.18	n.r.	n.r.	-	-
F	n.d.	n.d.	n.r.	1.20	0.21	0.85
	99.31	97.70	99.85	100.63	99.76	100.21
$\frac{Fe''}{(Fe''+Mg+Mn)}$ atom ratio		0.91	0.76	0.74	0.72	0.78

n.d. - not determined; n.r. - not reported

A, B Coarse-grained leucogranite. Analysis by A.D. Maynes. Total iron computed as FeO

C, D, E Coarse-grained leucogranite (Larsen and Draisin, 4)

F Fine-grained leucogranite (Larsen and Draisin, 4)

Comparison with Experimental Systems

Two experimental studies of silicate systems are particularly appropriate for estimating the physicochemical conditions that prevailed during crystallization of the Rubidoux granites. The first of these is the work of Tuttle and Bowen (9) on the system $NaAlSi_3O_8$-$KAlSi_3O_8$-SiO_2-H_2O and the second is the work of Eugster and Wones (15) on the stability relations of annite.

In general, the crystallization of iron-rich silicate melts is governed by four parameters: temperature, total pressure, partial pressure of water, and oxygen fugacity. For a given number of chemical components in the system, the values of these parameters are more rigidly specified as the number of coexisting phases in the crystallizing material increases. Thus the occurrence of four iron-bearing silicates plus magnetite in the Rubidoux granites represents an equilibrium assemblage only at restricted physicochemical conditions.

Approximate values for temperature and water pressure can be obtained by comparison with the "Residua" system studied by Tuttle and Bowen. Figure 3 is a projection on the anhydrous base of the four-component system of their study. The position of the quartz-feldspar boundary is shown for two values of water pressure, 1000 and 2000 bars, and the experimental minima are indicated by small ticks. The system is considered to appropriately describe rocks with at least

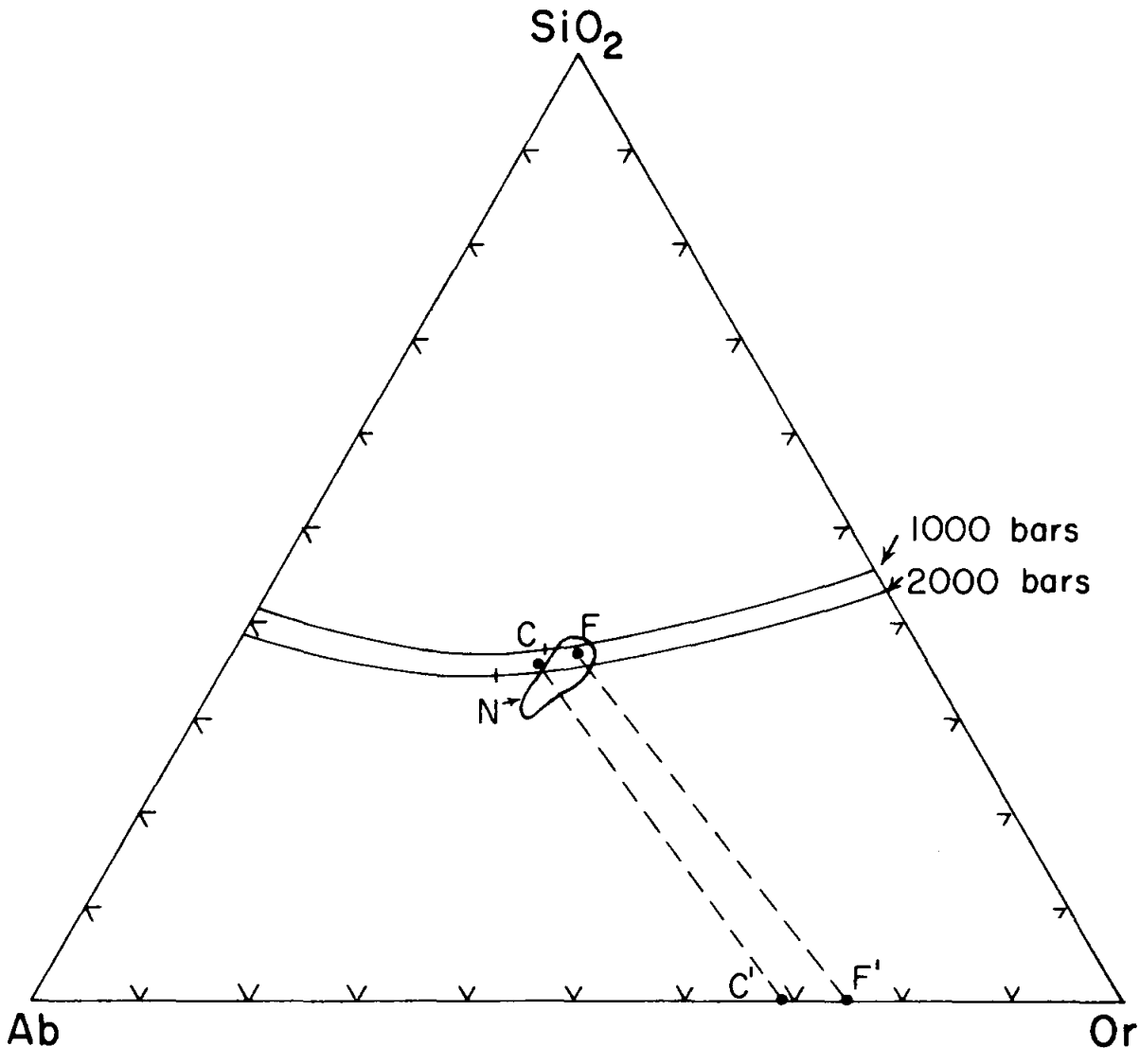

Figure 3. The System $KAlSi_3O_8$-$NaAlSi_3O_8$-SiO_2-H_2O

(Tuttle and Bowen, 9)

80% normative quartz, albite, and orthoclase. The majority of natural granites that fulfill this restriction plot within the area labelled N, which in effect determines the position of the minimum for natural systems.

The compositions of the Rubidoux granites are plotted on the diagram at points C (coarse) and F (fine), and the compositions of their respective potash feldspars are plotted at C' and F'. The trend with respect to the quartz-feldspar boundary and the natural minimum is quite satisfying and suggests 1) that the granites are closely related by a process of fractional crystallization, and 2) that the fine granite is compositionally at or very near a natural minimum.

Direct applicability of the experimental data to natural systems is limited primarily by two factors. The first is that the vapor pressure of water in natural systems may be less than the total pressure, and the second is that natural systems almost always contain some calcium.

Tuttle and Bowen suggested that the discrepancy between the natural and experimental minima reflects undersaturation of the natural systems with water. Based on evidence from extrusive rhyolites, they believe that natural magmas seldom contain more than about 2% water, which corresponds to a vapor pressure of about 500 bars. Lower water pressure, <u>per se</u>, causes the quartz-feldspar boundary to be shifted away from the Ab-Or sideline. At 500 bars water pressure (equal to total pressure) the experimental minimum is slightly

outside the region N, in the direction of the silica apex. If natural systems are indeed undersaturated, then the natural minimum has its observed location either because total pressure in excess of water pressure has the same order-of-magnitude effect as water pressure alone, or because the presence of other components such as calcium causes a shift of the quartz-feldspar boundary.

It seems unlikely that "dry" pressure has an effect equivalent to water pressure. A significant shift of the quartz-feldspar boundary would probably require a very large increase in total pressure, which does not agree with the relatively shallow depths at which many granites are thought to crystallize. The effect of calcium is difficult to assess. It is well known that a small amount of calcium causes the solidus to intersect the solvus in the three-feldspar system (e.g. Stewart and Roseboom, 16), and this phenomenon is responsible for the presence of two feldspars even in rocks with as little calcium as the Rubidoux granites. The shift of the natural minimum toward the Q-Or sideline is probably a result of calcium addition, but it is not known whether an apparent shift of the quartz-feldspar boundary also occurs.

It cannot be ruled out, of course, that natural magmas may be more nearly saturated than Tuttle and Bowen suggested. The environment in which rhyolites and obsidians form is different from that in which plutonic rocks form, and caution should therefore be exercised in making comparisons.

Whether the Rubidoux granites formed by partial melting of pre-existing metasediments or by fractional crystallization from a more basic magma, there is no compelling reason to assume undersaturation. It seems more reasonable that such processes would generate a magma which approached saturation, either by the assimilation of water from the country rock or by the concentration of water in the late magmatic stages.

In any case, the relationships are such that the experimental system probably indicates a maximum value for the water pressure in natural systems. Therefore, according to Fig. 3, the Rubidoux granites crystallized under a water vapor pressure not greater than 1500 bars. This corresponds to a depth emplacement of about 5 km., which is reasonable for such rocks. Since some undersaturation is possible the true pressure may have been as low as 1000 bars, but a much lower pressure seems unlikely.

The temperature of crystallization at the experimental minimum at 1500 bars is very nearly 700°C. As a general rule, the presence of other components in the system causes a lowering of this temperature. A smaller pressure of water, on the other hand, causes it to increase. In both cases the change is fairly slow, and therefore the competing effects largely cancel. The temperature of crystallization of the Rubidoux granites must thus have been very close to 700°C.

The above conclusions concerning the temperature and pressure at which the granites crystallized are partly confirmed by the study of Eugster and Wones (15) Figure 4 is a slightly simplified reproduction of their diagram showing the ranges of oxygen fugacity and temperature for which annite is stable in the presence of excess quartz at about 2000 bars water pressure (equal to total pressure).

The biotite of the coarse granite is 78% by weight annite. An x-ray diffraction analysis was made to compare this material with synthetic annite. Using silicon metal as a standard, cell dimensions were computed from the 003, 20$\bar{1}$-130, and 201 spacings to be:

$$a = 5.328\ \text{Å}$$

$$b = 9.153\ \text{Å}$$

$$c = 10.053\ \text{Å}$$

$$\beta = 98^\circ\ 43'$$

This is an unusually small cell for iron-rich biotite and corresponds more closely to the unit cell of phlogopite (e.g. Yoder and Eugster, 17). In addition, the 060 spacing of the Rubidoux biotite is 1.540 Å, whereas Wones (18) found that synthetized biotites of the same composition have d060 closer to 1.550 Å. The cause of the difference is not known but might result from substitutions in the hydroxyl positions as indicated by the chemical analysis.

The annite experimental system does not apply directly to the Rubidoux granites, both because the natural biotite

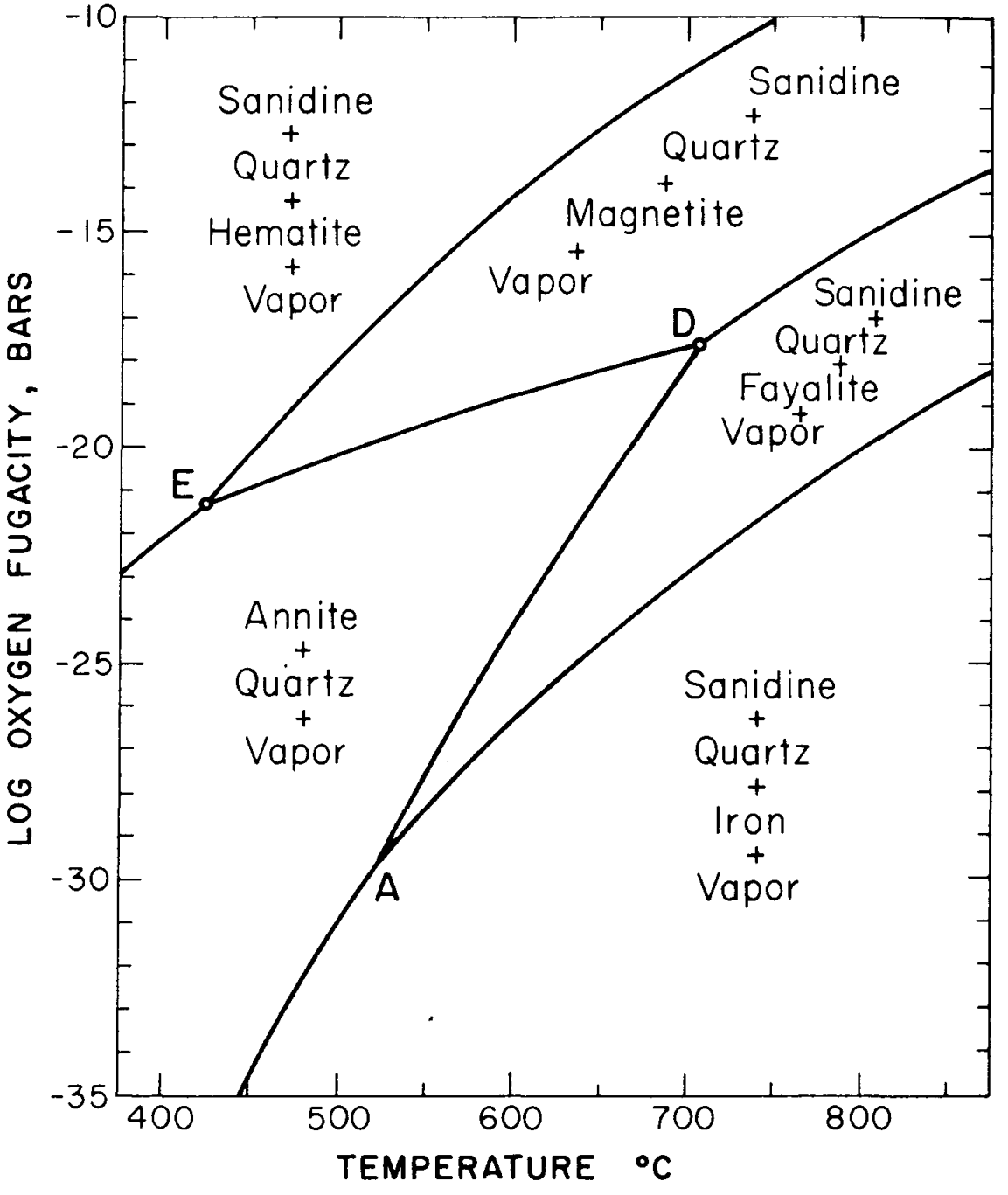

Figure 4. Phase relations of annite + quartz for total pressure equal to 2070 bars (Eugster and Wones, 1962)

contains the phlogopite end member and because it has fluorine in the hydroxyl positions. The effect of the fluorine is unknown at present and will be neglected. The presence of phlogopite in solid solution increases the temperature limit for which the biotite is stable. On the other hand, decreasing the water pressure lowers the upper temperature limit.

Fig. 4 shows that the upper temperature limit for annite at 2000 bars is about 700°C. Addition of 22% phlogopite increases this limit by not more than 100°, and probably more nearly 60°. It was shown previously that the water pressure prevailing during crystallization was not more than 1500 bars, and this lower pressure slightly offsets the effect of the additional phlogopite. Thus, as a first approximation, the biotite could not have been stable above about 760°C. Two lines of evidence therefore bracket the crystallization temperature of the Rubidoux granites between 700° and 760°C.

During most of the crystallization history biotite must have been formed in equilibrium with quartz, potash feldspar, and magnetite. The relation of oxygen fugacity to temperature would thus have been determined by the boundary DE in Fig. 4, appropriately displaced to account for the phlogopitic component and the difference in water pressure. If crystallization occurred by lowering of the temperature at constant pressure, the system would follow the curve from D toward E.

Textural evidence suggests that fayalite (and hypersthene) formed generally later than the biotite (and hornblende). But if the system cooled along the curve DE, the fayalite stability field would never be reached. Hence it is necessary to postulate a late secondary event which changed the conditions of crystallization. One way of reaching the fayalite stability field is by a decrease of oxygen fugacity at constant temperature and pressure. However, it is difficult to propose a mechanism which would accomplish this.

Another way, as suggested by Eugster and Wones, is by decreasing the water pressure at constant temperature. The behavior of oxygen fugacity during such a process would be a complex function of the composition of the system. Lowered pressure would result in lower temperature limits for the stability of the biotite, and hence if the temperature was not too low the system would enter the fayalite stability field.

In the general case, further crystallization should result in some sort of reaction between biotite and fayalite. Since no reaction relationships are seen in thin section, two alternatives are suggested. The first is that the system happened to reach the univariant curve (passing through point D in Fig. 4) at which the hydrous and anhydrous mafic silicates, quartz, feldspar, and magnetite were in equilibrium.. The observed texture in this case would be a true

equilibrium texture. However, the special circumstances required by this interpretation seem unlikely. The second, more likely alternative is that loss of water pressure caused the system to enter completely the field of fayalite stability, but that final crystallization was so rapid that the resulting disequilibrium between biotite and fayalite was "frozen in".

Loss of water pressure is a reasonable event, particularly in tectonically active areas such as southern California. It may well be a fairly common occurrence in crystallizing plutons, since in many cases no evidence would be preserved either because the system has an inappropriate composition or because the loss could occur at a stage where subsequent crystallization would completely react the anomalous phases.

The above discussion has dealt with the non-equilibrium formation of fayalite at the expense of biotite. Similar relationships must hold for the formation of hypersthene, although experimental data are lacking. The formation of one mineral or the other at any particular site is probably dependent on detailed variations in the composition of the residual fluids and the relative local abundance of hornblende or biotite.

Summary

The Mt. Rubidoux granites are leucocratic quartz monzonites containing an unusual assemblage of mafic minerals. Field work has shown that the coarse granite was the first to be emplaced. The similarities between the coarse and fine granites suggest that they underwent identical cooling histories and hence that the time lapse between the two intrusions was probably small. Both rocks were intruded by a pyroxene granodiorite dike possibly related to a plutonic body of quartz diorite northeast of Mt. Rubidoux. This is the only direct evidence for the relation of the granites to other rocks of the southern California batholith.

Chemical similarities between the granites and two experimentally studied systems permit an estimate to be made of the physicochemical conditions that prevailed during crystallization. Water vapor pressure may have been as high as 1500 bars if the melts were saturated. Although some undersaturation is possible, it is unlikely that the pressure was lower than about 1000 bars. The "Residua" system studied by Tuttle and Bowen indicates an approximate lower limit of 700°C. for the temperature of crystallization. Data from the work of Eugster and Wones, qualitatively adjusted for compositional effects, places an approximate upper limit of 760°C on the stability of biotite in the granites, which in turn must be an upper limit for the temperature of crystallization.

Fayalite and hypersthene were formed in both granites by a process which probably consisted of late-stage loss of water pressure. The lack of reaction relationships with biotite and hornblende suggests that final crystallization was so rapid that non-equilibrium assemblages were preserved.

Chapter 3

ISOTOPIC STUDIES

I. PRELIMINARY CONSIDERATIONS

Introduction

The general problem of the distribution of uranium, thorium and lead in igneous rocks has been under investigation for a number of years. Early autoradiographic studies (e.g. Picciotto, 19) established that the radioactive elements are heterogeneously distributed and are usually concentrated in discrete accessory minerals, with lesser amounts occurring in minute inclusions, unidentified interstitial materials, and the lattice structures of the major rock-forming minerals. Brown and Silver (1) discussed the distribution of uranium, thorium, and other trace elements in igneous rocks and their availability to acid leaching. They noted the importance of apatite, metamict allanite, thorite, bastnaesite, and a few other species as significant sources of the soluble radioactivity in granites and confirmed the general autoradiographic observations of Picciotto. The association of uranium and thorium with accessory minerals was studied further by Larsen, Keevil and Harrison (20) and Hurley and Fairbairn (21), using spectrographic and alpha-counting techniques. Whole rock concentrations of uranium and thorium have been investigated

by Whitfield, Rogers and Adams (7). Uranium concentrations in individual mineral separates as well as whole rock samples were measured by Larsen and Gottfried (3), who also conducted acid leaching experiments on their samples.

Isotopic studies, however, rarely have been undertaken. Tilton, Patterson, Brown, Inghram, Hayden, Hess and Larsen (22) have reported the only available work pertaining to the problem of the isotopic balance of uranium, thorium, and lead in a total rock system. They performed detailed analyses of major and accessory minerals from the Precambrian Essonville granite of Ontario and correlated the results with analyses of both fresh and acid-washed total rock material. They found that a material balance could not be achieved, and therefore concluded that significant amounts of uranium, thorium and lead resided in loosely bound, supposedly inter-crystalline positions. Moreover, because the radioactive minerals were isotopically discordant, they postulated that micro-transfer of uranium and lead, and possibly macro-transfer of thorium, had occurred within the rock.

The present study is similar in purpose to the Essonville work but differs in approach. Greater emphasis has been placed on the geological evaluation of the sample and on the determination of the isotopic systematics of individual accessory minerals. In addition, preliminary studies of weathered material have been undertaken.

Distribution of Radioactivity in the Mt. Rubidoux Granites

Two problems seriously limit the accuracy of direct material balance calculations of the distribution of trace elements in rocks: 1) mineralogical purity and 2) adequate sampling. These may be illustrated with particular pertinence to the present study by the results of two previous investigations.

Larsen and Gottfried (3) separated the minerals from the coarse-grained and fine-grained Rubidoux granites and determined the concentration of uranium in each species by fluorimetry. Their results for the coarse granite are shown in Table 5. Agreement between the calculated and measured values for the concentration of uranium in the whole rock is quite good. However, their data suggest that almost 90% of the uranium in the rock is situated in the three major minerals, quartz, potash feldspar, and plagioclase. A question arises as to whether this distribution reflects the properties of these particular minerals or whether it is related to the presence of impurities in the mineral concentrates, either as discrete material or as inclusions. If impurities were present the data have little significance as an indication of the true distribution of uranium in the rock.

A different method of investigating the same problem was undertaken by L. T. Silver, who made available to the writer the unpublished results of autoradiographic studies

Table 5

MOUNT RUBIDOUX COARSE-GRAINED LEUCOGRANITE

Uranium Analyses

(from Larsen and Gottfried, 3)

Mineral	Wt. %	U(ppm)	Contribution to Total U (ppm)
Quartz	33	3.5	1.2
Orthoclase	32	2.6	.83
Plagioclase	34	2.8	.95
Biotite	2	2.2	.04
Hornblende	1	19	.19
Hypersthene	0.5	9.0	.01
Muscovite	0.5	9.0	.01
Opaques	0.5	6.8	.03
Zircon	0.1	1,080	.11
Allanite	0.1	400	.04
			Sum 3.4 ppm
		Measured total	U: 3.2 ppm

of three thin sections from the coarse Rubidoux granite. Two independent observers examined the autoradiographs and found the distribution of radioactivity (as alpha tracks) to be roughly as follows: quartz and feldspar 8-12%, biotite 1%, hornblende 0.5%, apatite 2-3%, zircon 18-26%, allanite 34-46%, thorite 14%, and fractures, grain boundaries, and unidentified material 1-10%. These figures are clearly different than those of Larsen and Gottfried. Since autoradiography entails an observation of the actual source of each alpha track, there is some justification for believing these results to be more accurate. If so, a comparison between the two studies strongly indicates the need for establishing mineralogical purity when examining individual mineral separates for their content of trace elements.

Autoradiography, on the other hand, is limited by its statistical nature. The examination of a single thin section is time-consuming, and it often requires many sections to give an adequate sampling of accessory minerals. The extent of this problem may be indicated by anticipating the results of the present study. Uranothorite was known to be an accessory mineral in the Rubidoux granites at the time this work was undertaken. It has been found that the uranothorite contains about 9% uranium, whereas the coarse granite contains about 4 ppm uranium. It would thus require only 0.005% of uranothorite in the rock to account for <u>all</u>

of the observed uranium. Since other accessory minerals also contribute uranium to the rock the actual abundance of uranothorite must be still less than this.

Evaluation of the contribution of minerals of such low abundance as uranothorite is therefore a difficult matter in any attempt to construct a material balance for the whole rock, whether by autoradiography or by mineral separation procedures. For this reason a direct material balance calculation was not undertaken in the present study. Analytical work has been restricted to measuring the isotopic properties of the whole rock system. It is recognized that some of the sources of uranium (and lead) in the rock, such as interstitial material, have been neglected by doing this. However, it is believed that the net contribution of these sources is small relative to the contribution of the accessory minerals, at least in the Rubidoux granites.

Sample Descriptions

The objectives of the analytical work on the Rubidoux granites required the collection of samples of both fresh and weathered materials. Each site was examined to insure that dikes of the miscellaneous granodiorite or pyroxene granodiorite were not in close proximity. Samples of the coarse granite were selected to be as free as possible from inclusions. The blue-green color of the fresh coarse granite was used as a sensitive indicator of the freshness of the sample. Weathered rock samples were collected at sites which showed

no characteristics that could not be attributed to the modern weathering environment. Sample numbers and descriptions are listed below.

SCB-36. Fresh coarse granite. The location of this site is indicated on the geologic map (Plate 1) and its general appearance is shown in Photograph 6, Appendix B. As was described in the previous chapter, samples were obtained from the interior of a large *in situ* boulder of disintegration (Photograph 7, Appendix B) that had been drilled and blasted apart during the excavation of a shelf as a housing site on the lower southeastern slope of Mt. Rubidoux. Specimens collected here showed essentially no evidence of weathering. This boulder has been the primary source for whole rock samples and mineral separates of the fresh coarse granite.

SCB-105. Fresh coarse granite. A small sample was collected for total rock analysis from the large body of coarse granite included in the dike of fine granite at the north end of the mountain. The site is a cut made in the rock for the Mt. Rubidoux road. The color of the sample was distinctly modified by a brownish hue, indicating that some-oxidation of iron had taken place.

SCB-107. Fresh coarse granite. This site is located about 100 feet south of the SCB-36 and is also an *in situ* boulder of disintegration that had been drilled and blasted apart. A sample was collected here primarily to obtain a

zircon separate. It showed a slight degree of discoloration due to iron oxide staining and hence was not quite as fresh as SCB-36.

SCB-101. Weathered coarse granite. The site occurs about 30 feet south of SCB-36 (Photograph 6, Appendix B) and was chosen to provide a complete weathering profile over the coarse granite. Excavation of the shelf described above was responsible for making this site available.

From the lower part of the profile granularly disaggregated C-zone material was collected and labeled SCB-101C_3. This material was texturally identical to the coarse granite but could be easily crumbled by hand. The feldspar grains were opaque and white in color and the material was pervasively stained with yellow iron oxides.

A transition region 2-3 feet thick occurred between the C and B zones. A sample of the material was collected and labeled SCB-101C_1. It consisted of fragments of rock, retaining little textural identity, in a matrix of clays and red iron oxides.

The B zone consisted of about 2 feet of medium-brown, compact, blocky material containing very few fragments of the original rock but a noticeable amount of roots and other organic matter. A sample from here was labeled SCB-101B.

A fairly sharp boundary separated the B zone from the overlying A zone. The A-zone layer was about 8 inches thick and consisted of typical loose, friable material

containing abundant organic matter. Above this, and separated from it by a mat of decayed grass, was a layer of disturbed material evidently deposited mechanically when the excavation was made. A sample of the A-zone layer, labeled SCB-101A, was collected taking care that none of the overlying spurious material was included.

The relationships between the A, B, and transition C zones are shown in Photograph 8, Appendix B. As far as could be determined in the field, this profile represents typical residual soil development over the coarse granite. Some transported material may be present because the site is at the base of a steep-sided mountain, but there is no evidence, for example, that reworking or deposition in a fluviatile environment has occurred.

Before collecting the samples of this series, the outermost exposed portions were stripped off and discarded. In this way the possibility of contamination from the air or other extraneous sources was reduced.

SCB-108. Weathered coarse granite. The site is the same as SCB-107. A sample of weathered rind was collected from the boulder in order to compare its zircons with those of the fresh inner material. The rind was rather variable in its characteristics. Some individual layers were extensively weathered whereas others were similar to the fresh rock except for bleaching of the feldspars and oxidation of the iron.

SCB-102. Fresh fine granite. Samples were collected from a roadcut on the uphill portion of the Mt. Rubidoux road, just beyond the wooden crossover bridge. The location of this site is indicated on Plate 1. The fine granite was never found to have the unusual blue-green color of the fresh coarse granite and hence less sensitive criteria had to be used in selecting fresh samples. The outermost parts of the outcrop were discarded and only those specimens showing no observable evidence of iron oxide staining or bleaching of the feldspars were collected.

SCB-106. Weathered fine granite. No adequate soil profile over the fine granite was found. However, a sample of C-zone equivalent material was collected from a small exposure just to the west of the crestline of the mountain and about 100 yards south of the downhill portion of the Mt. Rubidoux road where it curves around the south end of the mountain. This material was not as thoroughly disaggregated as the C zone coarse granite sample.

Pyroxene granodiorite. A sample of this rock was obtained for the purpose of making an isotopic age determination on zircon. All accessible exposures were found to be somewhat weathered. The sample was collected from a boulder situated on the inside edge of the uphill portion of the Mt. Rubidoux road, about 400 feet from the crossover bridge.

The procedures which were employed to process the bulk samples and separate out the desired minerals for analysis are described in Appendix A. Feldspar and total rock

analyses were made on selected hand specimens from among the large number comprising the total collected sample at each site.

Chapter 4

ISOTOPIC SYSTEMS

II. RADIOACTIVE ACCESSORY MINERALS IN THE MT. RUBIDOUX GRANITES

Introduction

In the previous chapter the distribution of radioactivity in the coarse-grained Rubidoux granite was discussed with particular reference to autoradiographic studies. The early work had established that zircon, allanite, apatite, and uranothorite contribute significant amounts of radioactivity to the total rock system. For the present work it was necessary to determine whether other important sources of radioactivity occur in the rocks. Examinations were made of many thin sections and especially of the mineral separates. No other significant sources were found.

This chapter deals with uranium-lead isotopic analyses of zircon, allanite, and uranothorite. Apatite was not obtained in sufficient quantity for analysis, probably because its small abundance in the rock and its small grain size restrict the yield from the rock crushing procedure. Mineral concentrates were obtained chiefly from the fresh coarse granite, SCB-36, and the C-zone weathered coarse granite, SCB-101C_3. Additional zircon concentrates were obtained from another sample of the fresh coarse granite (SCB-107), from a related weathered rind (SCB-108), from

the upper part of the soil profile (SCB-101C_1, -101B, and -101A), and from the fresh and weathered fine granite (SCB-102 and SCB-106). Each mineral species was divided into two primary fractions of different grain size: -100+200 mesh (R200) and -200 mesh (P200). Further partitioning, where desired, was done either on the basis of variations in magnetic properties or by hand picking of selected material. The chemical procedures for dissolving the samples and extracting the lead and uranium are described in Appendix A.

Results of the isotopic studies have been interpreted under the assumption that the Rubidoux granites crystallized and their isotopic systems became closed, essentially contemporaneously and during an interval of time too short to discriminate by present methods. The detailed petrologic similarity between the two rocks suggests contemporaneity of crystallization and their mineralogy suggests emplacement at a moderately shallow depth where cooling should be fairly rapid. Larsen (23) has calculated that the entire southern California batholith could have cooled to a depth of 6 km. in 1 million years, assuming that it was emplaced in a single episode and had no internal source of heat such as radioactivity. Accepting this figure instead as a rough measure of the cooling time for an individual pluton, better than 1% precision would be needed to distinguish material which had crystallized early from that which had crystallized late, and this cannot be achieved with present techniques.

The analytical work has been designed to emphasize the variations in isotopic properties that occur within single mineral species. It should be noted that the analyzed samples do not represent the entire population of each species in the rock. At least three factors contribute to this: 1) the bulk processing procedure does not produce 100% yield, 2) grains larger than 100 mesh have been excluded arbitrarily, and 3) clean mineral separates were obtained either magnetically or by hand picking, which necessarily introduces bias into the sampling.

Data Reduction

The isotopic measurement of radiogenic lead requires a correction for common lead contamination, whether from the sample or from the laboratory. Lead composition analyses were corrected in the usual way by normalizing to Pb^{204}. Zircon samples were assumed to contain little or no original common lead and therefore the isotopic composition of lead in the borax flux was used as the correction (Appendix A). The composition of lead in the potash feldspar of the coarse granite (next chapter) was used to correct the analyses of allanite and uranothorite. In most cases the difference in using these two corrections is negligible.

Lead concentration analyses were corrected by a graphical procedure adapted by Silver (unpublished): a triangular diagram is constructed having the abundances of the three major isotopes (normalized to 100%) as coordinates.

Four points are plotted: the composition of radiogenic lead in the sample, the observed mixture of sample and spike leads, the composition of the spike lead, and the composition of the blank lead. A straight line is drawn connecting the radiogenic sample point and the spike composition, and another one connecting the blank lead and the sample-spike mixture. The intersection of the two lines is the corrected mixture of radiogenic sample lead and spike lead, and can be easily read to the nearest 0.05% atom abundance.

No corrections were made for the uranium analyses as the level of contamination is negligibly small.

In some cases it was necessary to correct the calculated lead concentration for a drift of the concentration of the spike. This effect is discussed in Appendix A. The magnitude of the correction was in most cases less than 1% and never more than 1.5%.

Zircon Analyses

Twelve zircon fractions from both fresh and weathered samples of the coarse- and fine-grained Mt. Rubidoux granites have been analyzed. Three other fractions from the upper soil profile (SCB-101 series) were also analyzed but were found to contain zircon from older material and are discussed separately.

The Mt. Rubidoux zircons have been rather extensively studied, not only because of their contribution to the total rock system, but also to evaluate their use in determining

the age of geologically young rocks. Previous investigations have shown that the southern California batholith is generally somewhat over 100 million years old. For example, Aldrich, Wetherill and Davis (24) found Sr^{87}/Rb^{87} ages of 106 and 114 million years for lepidolite from pegmatites at Pala, California; Reynolds (25) reported Ar^{40}/K^{40} ages of 92±2.5 million years for associated lepidolite and feldspars from pegmatites at the same locality; Silver (personal communication) found Pb^{206}/U^{238} ages of 115 million years for monazite and zircon from batholith rocks in Baja California; and Larsen, Gottfried, Jaffe and Waring (6) found lead-alpha ages of 98 and 99 million years for zircons from the Rubidoux granites. Since isotope dilution normally has a precision of about 1% the most severe limitation on age determinations by this method arises from the natural sample. In other words, it must be established whether the isotopic system being studied has been disturbed in any way during its lifetime.

Uranium-lead analyses of systems considerably older than 100 million years provide a built-in check on disturbance by the presence or lack of agreement among the Pb^{206}/U^{238}, Pb^{207}/U^{235}, and Pb^{207}/Pb^{206} ages. This test, however, is not sensitive in young systems and therefore some other criterion must be sought. It is believed that a criterion of general applicability has been illustrated by the zircon analyses of this study.

All zircon fractions were found to have essentially the same physical characteristics. Individual crystals range

from colorless to pale brown and the color of the whole sample is pale yellowish brown. Most crystals are transparent but the transparency decreases slightly as the degree of coloration increases. A few milky-white translucent to opaque grains are present and are in greater abundance in those fractions with higher radioactivity. The average length-to-width ratio for well-formed crystals was estimated to be between 2 and 3. The first-order prism and dipyramid are the most prominent forms; the second-order prism and the basal pinacoid are commonly present, and the ditetragonal dipyramid is more rare. Many crystals show very poor development of the interfacial edges which gives the grains a rounded appearance. Zoning occurs but is not typical. Inclusions consist of apatite, magnetite, and possibly in rare cases uranothorite. Some of these characteristics are shown in Photographs 9-15, Appendix B.

Each fraction was thoroughly washed in hot concentrated HNO_3 before analysis. A number of tests were made to determine reproducibility and are shown in Table 6. Three variables were considered: 1) the reproducibility of the bulk processing procedure, 2) the effect of the size of the sample put into solution, and 3) the effect of adding spike to the sample before or after fusion. Three different samples of the fresh coarse granite, SCB-36, were processed and splits of the R200 zircon fractions were analyzed. The lead composition was measured for only one of these and it was used for calculating the results for the other samples.

Table 6
MOUNT RUBIDOUX GRANITES
REPLICATE ZIRCON ISOTOPIC ANALYSES

Sample No.	Rock Specimen No.	Weight (gm)	Spike Used B: Before fusion A: After fusion	Observed Pb Atom Ratios $\frac{206}{204}$	$\frac{206}{207}$	$\frac{206}{208}$	Radiogenic Pb^r Composition, Atom Percent 206	207	208	Concentrations (ppm) Pb^r	U	Atom Ratios $\frac{206r}{238}$	$\frac{207r}{235}$	Apparent Age (m.y.) $\frac{206}{238}$	$\frac{207}{235}$
SCB-36 R200	3	0.3827	208A	1786	17.68	9.603	88.32	4.27	7.41	32.21*	1882	0.01759	0.1172	114±2	114±3
"	2	0.1234	207B							31.24	1792	0.01791	0.1193	116±1	116±2
"	2	0.3604	208A							30.97	1772	0.01797	0.1197	116±1	116±2
"	1	0.0410	208B							32.96	1853	0.01829	0.1218	118±1	118±2
"	1	0.4045	208A							32.64*	1862	0.01802	0.1200	116±2	117±3
SCB-102 R200	1	0.3514	208B	355.1	31.68	69.62	87.51	4.19	8.30	44.29	2639	0.01709	0.1127	110±1	110±2
"	1	0.1711	207B							43.18	2691*	0.01637	0.1080	106±2	106±3

*Concentrations corrected for drift of spike concentration

A similar procedure was followed for a single sample of the fresh fine granite, SCB-102. The data of Table 6 lead to the following conclusions: 1) the reproducibility (measured in terms of Pb and U concentrations) for splits of a zircon fraction from a single portion of rock is usually between one and two percent; 2) there are small but measurable differences between samples obtained from different portions of rock, which probably reflect differences in processing yield; and 3) the accuracy of analysis is not in general affected by the size of the sample or by the spiking procedure. The only serious discrepancy is between the two analyses of SCB-102 R200. It is believed that the analysis with the lower Pb^{206}/U^{238} ratio is incorrect due in part to additive errors from the calibration of the 207 spike and a correction that was required for drift in the concentration of the uranium spike. (This was the only sample so corrected.)

Analytical results for the twelve zircon fractions are shown in Table 7. Each fraction was separated as described above except SCB-101C_3 P200 (4°M), which was a more highly magnetic fraction obtained by recycling the total P200 fraction through the magnetic separator at 4° side tilt instead of the normal 10° tilt. All analyses were sufficiently radiogenic that errors due to the common lead correction were small. Other sources of error and the precision of the mass spectrometry are discussed in Chapter 6 and in Appendix A.

The age of the Rubidoux granites is such that only the Pb^{206}/U^{238} ratio can be used as a precise measure of the

Table 7

MOUNT RUBIDOUX GRANITES

ZIRCON ISOTOPIC ANALYSES

Sample No.	Weight (gm)	Observed Pb Atom ratios $\frac{206}{204}$	$\frac{206}{207}$	$\frac{206}{208}$	Radiogenic Pb^r Composition, Atom Percent 206	207	208	Concentrations (ppm) Pb^r	U	Atom Ratios $\frac{206r}{238}$	$\frac{207r}{235}$	$\frac{207r}{206r}$	Apparent Ages (m.y.) $\frac{206}{238}$	$\frac{207}{235}$
SCB-36 R200	0.3827	1786	17.68	9.603	88.32	4.27	7.41	32.21*	1882	0.01759	0.1172	0.04831	114±2	114±3
SCB-36 P200	a)0.7327 b)0.5524	1414	17.05	9.895	88.99	4.29	6.71	38.97	2370 2307	0.01749	0.1163	0.4825	113±1	113±2
SCB-102 R200	a)0.3514 b)0.1962	355.1	11.19	5.101	87.51	4.19	8.30	44.29	2610 2639	0.01709	0.1127	0.04783	110±1	110±2
SCB-102 P200	a)0.5720 b)0.2577	892.1	15.40	8.532	88.88	4.31	6.81	48.28	3010 3000	0.01665	0.1113	0.04849	108±1	109±2
SCB-107 R200	0.4517	1826	17.74	10.10	88.26	4.26	7.48	29.33	1765	0.01706	0.1137	0.04832	110±1	110±2
SCB-101C$_3$ R200	a)0.4538 b)0.1425	1367	16.72	8.595	87.79	4.31	7.90	30.80*	1937	0.01624	0.1099	0.04907	105±2	107±3
SCB-101C$_3$ P200	0.4518	1653	17.49	9.793	88.61	4.28	7.11	37.52*	2415	0.01602	0.1066	0.04828	103±2	104±3
SCB-101C$_3$ P200 (40M)	0.1663	Comp. assumed same as SCB-101C$_3$ P200						48.85*	3279	0.01536	0.1023	-	99±2	100±3
SCB-108 R200	0.5024	1711	17.52	10.12	88.80	4.31	6.89	28.74	1771	0.01677	0.1123	0.04850	108±1	109±2
SCB-108 P200	0.4630	2036	17.85	10.11	88.50	4.32	7.18	36.33	2253	0.01660	0.1118	0.04881	107±1	109±2
SCB-106 R200	0.4265	1194	16.22	8.898	88.38	4.36	7.26	43.74	2676	0.01681	0.1144	0.04937	108±2	111±3
SCB-106 P200	0.2951	1230	16.39	7.997	87.34	4.29	8.37	49.20	2990	0.01672	0.1127	0.04908	108±1	110±2
Precision		±1.8%	±0.30%	±0.35%				±1%	±1%					

*Concentrations corrected for drift of spike concentration

Common Lead Correction	$\frac{206}{204}$	$\frac{207}{204}$	$\frac{208}{204}$
	17.83	15.55	37.62

apparent age of each sample. The Pb^{207}/Pb^{206} apparent age is highly sensitive to errors both in the mass spectrometry and in the accepted decay constant of U^{235}. The Pb^{207}/U^{235} apparent age is intermediate in precision. The general agreement between the two Pb/U apparent ages for each analysis indicates 1) that the analyses are internally consistent, 2) that these zircons have not inherited a significantly older radiogenic lead, and 3) that the accepted half-life of U^{235}, relative to U^{238}, is not greatly in error. An evaluation of this last problem is presented in Chapter 6.

For the purposes of this chapter, the most significant aspect of the data in Table 7 is that the various samples show a scatter of apparent ages that is outside of analytical error. For each sample group the apparent age decreases with increasing uranium concentration. The regularity of this phenomenon is brought out in Figure 5.

It is clear that the zircons in the Mt. Rubidoux granites have not been closed isotopic systems throughout their lifetimes, and it is equally clear that the radioactivity of each sample has had a fundamental influence in determining its degree of disturbance. Relationships of this sort have been observed for other, older zircon systems (e.g. Silver and Deutsch, 26), but it was not expected to occur in a young system. It should be noted that the analysis of a single zircon fraction from these rocks would not indicate the existence of a disturbance. Therefore the phenomenon

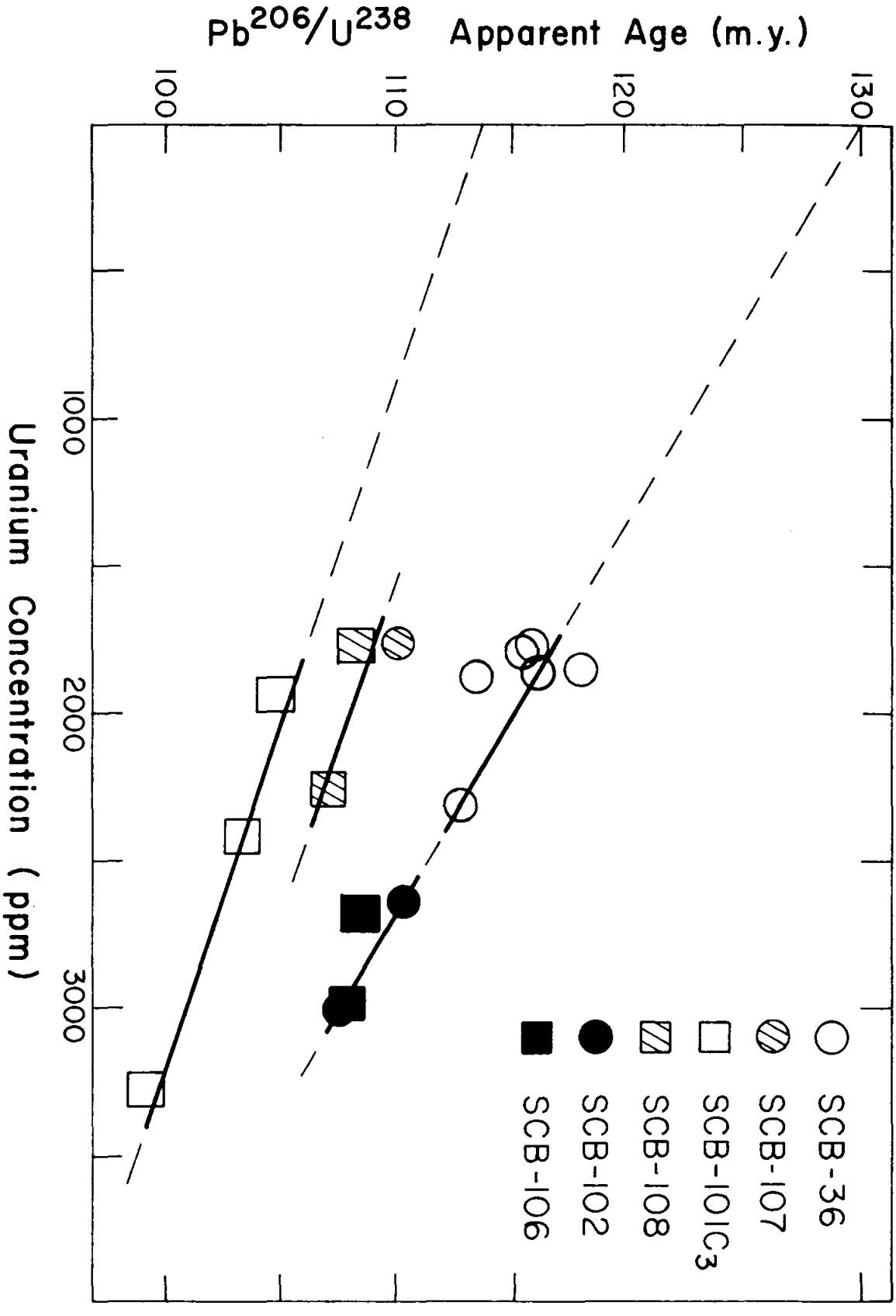

Figure 5. Mt. Rubidoux Granites, Zircon Isotopic Analyses

has been called a "cogenetic discordance" to emphasize the need for two or more analyses of a cogenetic suite.

Any interpretation of the cause of this discordance must account for the fact that samples obtained from different localities show different apparent ages for comparable radioactivities. For example, a difference of up to 10% in apparent age exists for comparable fractions from the fresh coarse granite, SCB-36, and the weathered coarse granite, SCB-101C_3; yet these samples were collected only 30 feet apart. The exceptionally low ages for fractions from SCB-101C_3 could conceivably be caused by contamination with younger material, but no evidence for younger dikes or other material was seen at the site, and moreover it is unlikely that contamination would produce the consistent relationships observed. It was initially thought that recent weathering might have caused loss of lead but the data do not bear this out: samples from the weathered fine granite give results identical to those from the fresh rock; and samples of weathered rind (SCB-108) from the coarse granite agree with the single fraction from the interior of the same boulder (SCB-107).

Three possible causes of discordance have been proposed in the literature: 1) episodic loss of lead and/or uranium and thorium (Wetherill, **27**), 2) continuous diffusion loss of lead (Nicolaysen, **28**; Tilton, **29**; Wasserburg, **30**), and 3) intermediate daughter loss (e.g. Kulp, Bate and Broecker, **31**). The isotopic data do

not permit a choice between these alternatives. However, other parameters can be measured. For example, if continuous diffusion of either lead or intermediate daughters has been the primary cause of discordance it might be expected that the different degrees of disturbance shown by the various sample groups reflects some sort of difference in internal properties.

In order to test for the existence of different internal properties among the various zircon fractions, from SCB-36 and SCB-101C_3, in particular, x-ray diffraction and zirconium/hafnium measurements were made. The results are shown in Table 8. The (200) reflection was measured by continuous scanning at $\frac{1}{4}^{o}$ per minute using CuK_{α} radiation and Si metal as an internal standard. The average value of a_o among the samples is 6.626 Å and the individual samples do not differ from this outside of the uncertainty of the method. Holland and Gottfried (32) found a_o for undamaged zircon from Ceylon to be 6.602 Å. The slightly larger value for the Rubidoux zircons may indicate some radiation damage, but it is not known what the undamaged cell dimensions of these zircons should be.

Zirconium/hafnium ratios were determined by x-ray fluorescence using techniques developed by L. T. Silver and A. A. Chodos. Mixtures of the metal oxides were used as standards and therefore the analytical results may have a slight but consistent bias. The results demonstrate that the Zr/Hf ratio and the uranium content of the samples are

Table 8

MOUNT RUBIDOUX GRANITE ZIRCONS

X-RAY DIFFRACTION AND ZIRCONIUM/HAFNIUM MEASUREMENTS

Sample	U(ppm)	Normalized (200)	a_o	Zr/Hf
SCB-36 R200	1880	26.92±0.01	6.624±0.003	-
SCB-36 P200	2340	26.92	6.624	17.3±0.3
SCB-102 R200	2620	26.90	6.629	16.4
SCB-102 P200	3005	26.92	6.624	13.3
SCB-101C_3 R200	1940	26.92	6.624	-
SCB-101C_3 P200	2415	-	-	17.1
SCB-101C_3 P200 (4°M)	3280	26.90	6.629	-

related. However, no difference between corresponding zircon fractions from the two localities was found.

The lack of any measurable differences among the sample groups suggests that the observed discordance may not be simply related to an internally controlled mechanism such as diffusion. The data do not exclude the possibility of diffusion loss of lead or of intermediate daughters in part because the tests have not been exhaustive and in part because the different degrees of disturbance among the sample groups may reflect internal differences which are not resolvable by the techniques used.

It is possible that an external episodic event could have caused the apparent losses of lead. Such an event might be locally variable in its "intensity". Since the lowest zircon age that has been measured is 99 million years, the hypothetical episode would have occurred not more than 99 million years ago. As a check on this possibility a Rb:Sr analysis was made on a biotite separate from the coarse granite sample SCB-36. G. J. Wasserburg and M. A. Lanphere generously permitted the use of their facilities and assisted the writer on this determination. Using a decay constant of $1.39 \times 10^{-11}/yr^{-1}$ an apparent age of 100 ± 3 million years was found. The sample contained about 90% radiogenic Sr^{87}. If it is assumed that zircon and biotite became closed isotopic systems at essentially the same time, this result seems to support the hypothesis of a younger episodic event.

The intrusion of pyroxene granodiorite dikes into the granite was investigated as a possible event. Zircons from the granodiorite (see below) indicate that its age is about 108 million years and hence that it is too old to have caused the entire disturbance seen in the Rubidoux zircons. The late Mesozoic and Tertiary history of the general southern California area has been rather complex in terms of plutonic, volcanic, and tectonic activity, but it is difficult to relate any other specific event to the Mt. Rubidoux locality. Therefore there is no compelling evidence to choose between external or internal causes of the discordance, although the available data seem to favor more strongly an episodic event of variable local intensity.

The isotopic results indicate that the true age of the Rubidoux granites must be at least 116 million years. A simple interpretation of the observed systematics is that the relation between apparent age and radioactivity is truly linear for all values of radioactivity within a single group of samples. An extrapolation to zero concentration based on the data of SCB-36 and SCB-102 suggests an upper limit of 130 million years for the true age of the rocks (Fig. 5). It seems remarkable, and must be in part fortuitous, that these two sample groups plot on the same line. The extrapolated age is considered to be a maximum because it is believed that the sensitivity to disturbance decreases more rapidly than decreasing radioactivity as zero concentration is approached.

Data from older cogenetic zircon suites (Silver, personal communication) bear this out. Therefore the true age of the Rubidoux granites is thought to be probably on the order of 120 million years.

In order to evaluate preliminarily some of the geochronological problems posed by the discordance in the Rubidoux zircons, zircons from three other rocks were analyzed; the pyroxene granodiorite, the Crestmore quartz monzonite porphyry (Burnham, 11), and the Woodson Mtn. granodiorite (Larsen, 2). The pyroxene granodiorite sample was described previously. L. T. Silver and the writer visited the Commercial Quarry at Crestmore and collected a sample of the quartz monzonite porphyry from a large block of fresh rock lying at the base of the upper face of the quarry. The sample of Woodson Mountain granodiorite was provided by Silver, who obtained it from an exposure south of Temecula, California.

Analytical results are shown in Table 9 and the data are plotted in Figure 6. The composition of feldspar lead from the coarse Rubidoux granite was used to correct the analyses. Within the limits of error, none of these zircon suites shows evidence of being discordant. Therefore it is interpreted that the apparent ages of the rocks are very nearly the true ages. Although these data are preliminary they demonstrate that plutonic activity related to the southern California batholith must have occurred during at least a 15 million year interval and probably longer. The

Table 9

OTHER BATHOLITH ROCKS

ZIRCON ISOTOPIC ANALYSES

Sample		Weight (gm)	Observed Pb Atom Ratios $\frac{206}{204}$	$\frac{206}{207}$	$\frac{206}{208}$	Radiogenic Pb^r Composition, Atom Percent 206	207	208	Concentrations (ppm) Pb^r	U	Atom Ratios $\frac{206r}{238}$	$\frac{207r}{235}$	$\frac{207r}{206r}$	Apparent Age (m.y.) $\frac{206}{238}$	$\frac{207}{235}$
Pyroxene granodiorite	R200	0.4481	812.0	14.92	5.406	83.99	4.11	11.90	14.0	823	0.01665	0.1124	0.04894	108±1	110±2
Pyroxene granodiorite	P200	0.9313	1174	16.53	6.467	85.29	4.09	10.62	18.5	1100	0.01674	0.1107	0.04800	108±1	108±2
Crestmore qtz. monz. porphyry R200*		0.5224	n.obs.	n.obs.	n.obs.	85.71	4.12	10.17	a)10.1	609	0.01646	0.1091	-	106±2	107±3
									b) 9.97	609	0.01633	0.1082	-	105±2	106±3
Crestmore qtz. monz. porphyry P200	a)	0.8081	324.1	10.67	4.209	85.14	4.12	10.74							
	b)	0.0217							20	1215	0.01626	0.1085	0.04838	105±1	106±2
Woodson Mtn. granodiorite R200		0.4500	325.8	10.69	4.435	85.85	4.16	9.99	20.0	1080	0.01842	0.1231	0.04846	119±1	120±2
Woodson Mtn. granodiorite P200		0.2639	231.2	8.884	3.588	85.12	4.18	10.70	23.5	1265	0.01841	0.1246	0.04910	119±1	121±2

*Lead composition derived by comparing two differently spiked aliquots:

a) Pb^{208} spike;

b) Pb^{207} spike

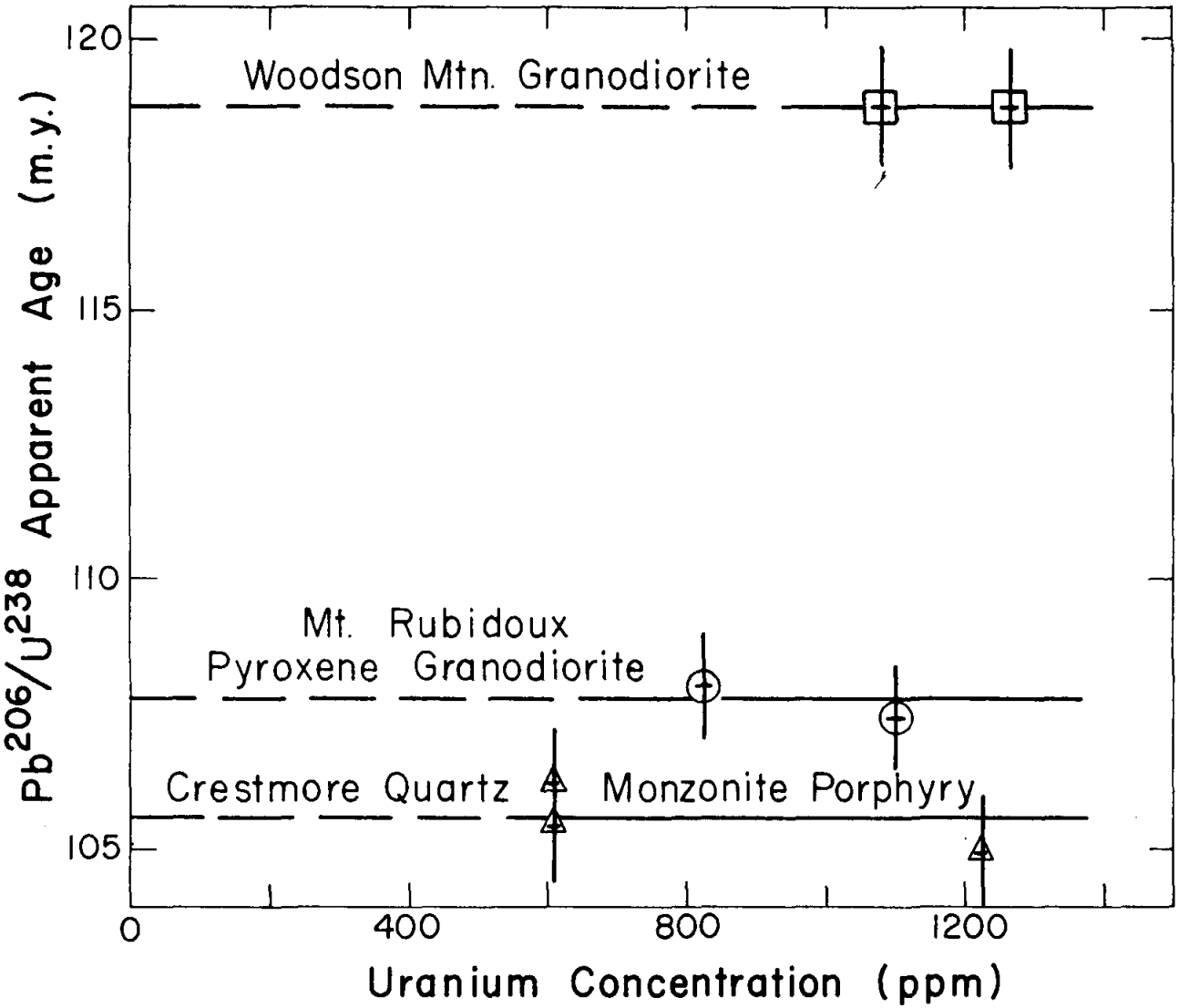
120
115
110
105
Woodson Mtn. Granodiorite
Mt. Rubidoux
Pyroxene Granodiorite
Crestmore Quartz Monzonite Porphyry
Pb206/U238 Apparent Age (m.y.)
0
400
800
1200
Uranium Concentration (ppm)

Figure 6

apparent age of the Woodson Mountain granodiorite lends support to the interpretation that the Rubidoux granites may be about 120 million years old. It is possible that the granites are older than the granodiorite, but this can not be proven at present.

The following conclusions have resulted from the isotopic analyses of zircon fractions performed in this study:

1) It is possible to obtain and analyze zircons from rocks whose age is on the order of 100 million years, and to achieve analytical results with a precision approaching 1%.

2) Discordance in young zircons can be recognized by analyzing more than one fraction of a cogenetic suite, provided that the fractions differ significantly in radioactivity.

3) The pattern of discordance in zircon fractions from the Mt. Rubidoux granites and the Sr^{87}/Rb^{87} apparent age of a biotite sample from the coarse granite suggest that the radioactive systems were disturbed by an episodic event of locally variable intensity. If so, the event must have occurred more recently than 99 million years. The intrusion of dikes of pyroxene granodiorite at about 108 million years is not adequate to account for all of the disturbance.

4) Mt. Rubidoux granites are at least 116 million years old, and may be as old as 130 million years. It is believed likely that their true age is more nearly 120 million years.

5) Plutonic activity related to the batholith of southern California has been shown to have occurred during at least a 15 million year interval.

Zircons from the Upper Soil Profile

Zircons from the upper soil profile, SCB-101C_1, -101B, and -101A, were analyzed initially to investigate further the possibility of weathering as a cause of discordance in the Rubidoux zircons. It was found that a significant amount of much older zircons was present in the mineral separates. The analyses are shown in Table 10. The lead composition analysis for SCB-101C_1 was characterized by poor ion beam intensity and only the Pb^{206}/Pb^{207} and Pb^{206}/Pb^{208} ratios could be measured. The approximate corrected lead composition was obtained by assuming that the radiogenic Pb^{207}/Pb^{206} ratio should be very nearly 0.0485 and determining the amount of lead having the composition of the borax flux blank that would have to be subtracted from the observed sample-plus-common lead to give this figure. A graphical method was used, similar to the one employed to correct lead concentration analyses.

The data have been interpreted by assuming that the samples consist of varying proportions of two different populations, one having the average age of the Rubidoux zircons and the other having a single older age. The value of the older age was derived by means of a concordia plot

Table 10

MOUNT RUBIDOUX UPPER SOIL PROFILE,

ZIRCON ISOTOPIC ANALYSES

Sample No.	Weight (gm)	Observed Pb Atom Ratios $\frac{206}{204}$	$\frac{206}{207}$	$\frac{206}{208}$	Radiogenic Pb Composition, Atom Percent 206	207	208	Concentrations (ppm) Pb^r	U	$\frac{206r}{238}$	Atom Ratios $\frac{207r}{235}$	$\frac{207r}{206r}$	Apparent Age (m.y.) $\frac{206}{238}$	$\frac{207}{235}$	$\frac{207}{206}$
SCB-101C$_1$ P200	0.5390	not obs.	12.98	7.332	89.80	4.33	5.87	34.5	1790	0.02010	-	-	130•5	-	-
SCB-101B R200	0.5923	1284	12.96	8.911	86.96	5.73	7.31	31.2*	1374	0.02293	0.2085	0.06594	148•2	195•2	821•10
SCB-101A P200	0.4852	229.7	6.692	4.214	85.59	7.59	6.82	40.6	783	0.05165	0.6316	0.08863	321•3	503•5	1420•40
				$\frac{206}{204}$	$\frac{207}{204}$	$\frac{208}{204}$									
		Common lead correction:		17.83	15.55	37.62									

* Concentration corrected for drift of spike concentration

(Wetherill, 33), which is shown in Figure 7. The upper intersection indicates an age of about 1730 million years for the older component. It is probable that the older component is discordant and/or that it consists of a mixture of zircons of different ages. If so, then at least some of the zircons may be even older than 1730 million years.

The presence of the older zircons is striking both because of their great age and because of their retention in a soil where no other evidence of the parent rock could be found. The fraction of zircons having the largest proportion of older material, SCB-101A P200, was examined under a microscope. Two populations could be distinguished. One of these, averaging slightly coarser in size, had characteristics typical of the Rubidoux zircons: light yellowish-brown color, generally transparent, with rather poor development of crystal faces. The second population was colorless and transparent to white and opaque. Some grains were entirely opaque whereas others showed opaque cores or zones. Individual grains were commonly distinctly rounded with slightly pitted surfaces, but where crystal faces were preserved they were better developed than the average of the Rubidoux zircons. The second-order prism and ditetragonal dipyramid were commonly present. Most grains showed very few inclusions.

The characteristics of the second population suggest that at least some of the grains have experienced a sedimentary environment. The most likely interpretation is that

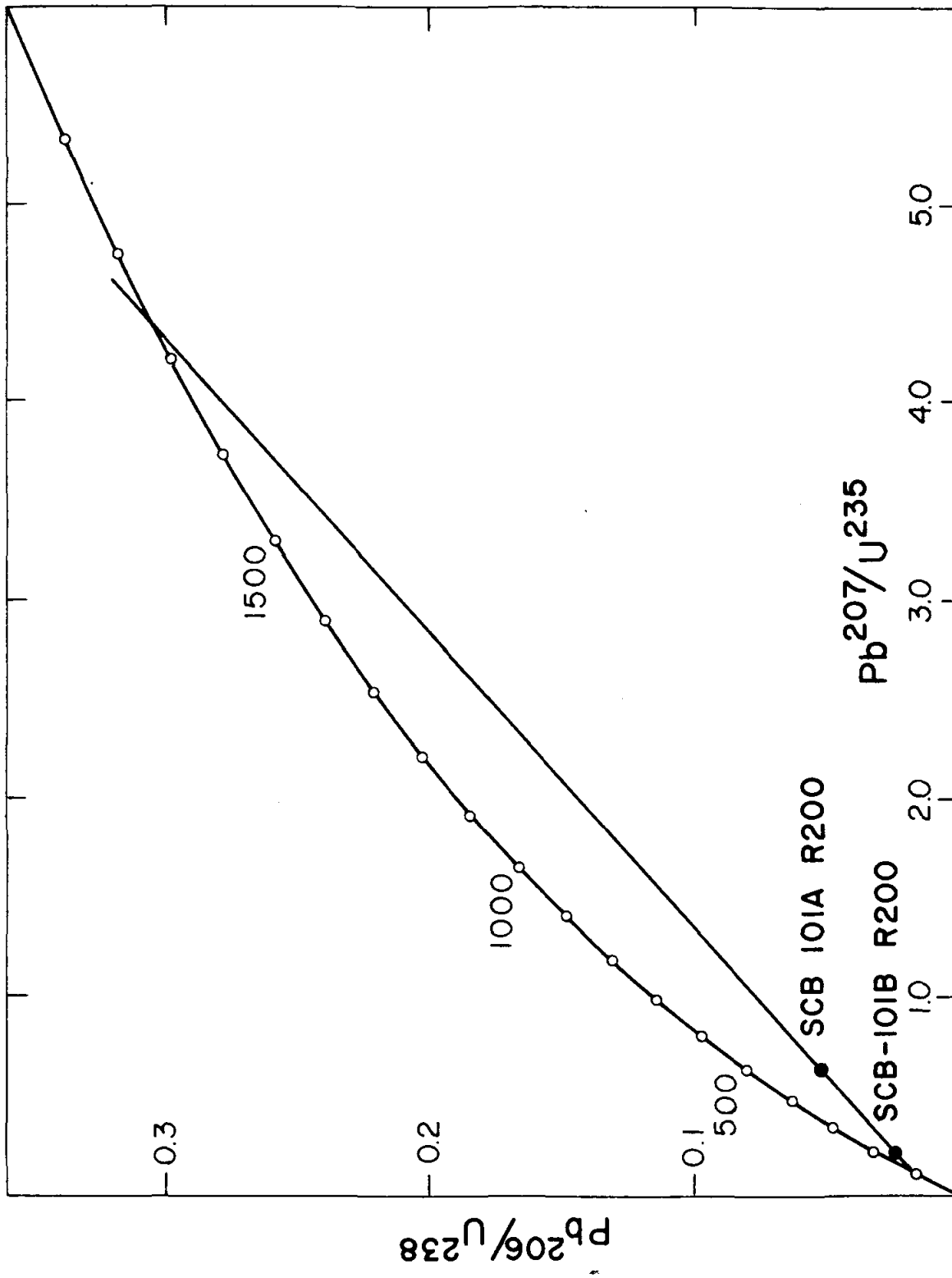

Figure 7. Zircons from Upper Soil Profile, Mt. Rubidoux

they are derived from the metasedimentary rocks into which the granites are intruded. It is possible that they have come from a xenolithic mass, but their relatively large abundance in the soil indicates that a fairly large amount of material must have been weathered. No evidence for the presence of wall rock was found either at the site or higher on the slope, although elsewhere near the base of the mountain a few small masses possibly related to the wall rock do occur. The collection site seemed to be a normal, largely residual, weathering profile. Yet the older zircons were found even in the transition C-zone layer. The mechanism by which this has come about is not understood.

The apparent age of 1730 million years is the oldest yet indicated in southern California. Since the physical characteristics of the older zircons reflect a sedimentary origin it is probable that their age is that of the source(s) from which they were originally derived and is not the age of metamorphism. The oldest age that has been measured for basement rocks in southern California is 1450 million years, obtained by Silver, McKinney, Deutsch and Bolinger (34) for zircons from the Mendenhall gneiss in the San Gabriel Mountains.

Because of the presence of older zircons in the upper soil profile, studies of the effects of weathering on the Mt. Rubidoux granites were not extended beyond the lower C-zone material.

Allanite Analyses

Three fractions of allanite were analyzed. SCB-36 R200 and SCB-101C_3 R200 were splits of their entire size fractions. SCB-36 P200 was passed through the magnetic separator adjusted so as to partition the sample roughly in half. The less magnetic portion was analyzed.

Allanite separates from the fresh coarse granite consist of dark coffee-colored grains commonly showing conchoidal fracture surfaces and no crystal faces. The grains are rather free of internal inhomogeneities (Photograph 16, Appendix B) although in thin section they are often twinned or zoned. Separates from the weathered coarse granite show the same general characteristics but the color of the grains is modified by the external development of yellow to red oxides of iron and rare earths (?).

Analytical results are shown in Table 11. The lead composition analysis for SCB-36 P200 was affected by poor ion beam intensity and therefore the radiogenic component was derived by the graphical procedure outlined in the previous section. The allanites have a much higher Th/U ratio than the zircons as indicated by the radiogenic Pb^{206}/Pb^{208} ratio. The ratio of uranium to any common lead either in the sample or introduced during analysis is unfavorably low for obtaining a significant Pb^{207}/U^{235} determination.

All allanite fractions have yielded Pb^{206}/U^{238}

Table 11

MOUNT RUBIDOUX GRANITES

ALLANITE AND URANOTHORITE ISOTOPIC ANALYSES

Sample	Weight (gm)	Observed Pb Atom Ratios $\frac{206}{204}$	$\frac{206}{207}$	$\frac{206}{208}$	Radiogenic Pb^r Composition, Atom Percent 206	207	208	Concentrations (ppm) Pb^r	U	Atom Ratios $\frac{206r}{238}$	$\frac{207r}{235}$	$\frac{207r}{206r}$	Apparent Age (m.y.) $\frac{206}{238}$	$\frac{207}{235}$
SCB-36 R200 Allanite	0.3375	102.8	5.310	0.1777	13.36	0.60	86.04	62.5	501	0.01923	0.1191	0.04459	124±2	116±6
SCB-36 P200 Allanite	0.3571	n.obs.	3.419	0.1812	12.30	0.60	87.10	69.1	409	0.02397	-	-	154±3	-
SCB-101C_3 R200 Allanite	0.6323	38.73	2.284	0.7820	61.58	4.17	34.25	50.9	320	0.03469	-	-	222±10	-
SCB-36 R200 Urano-Thorite composite	0.0083	1634	17.54	0.7002	40.50	1.94	57.56	2605	81,615	0.01497	0.09883	0.04801	97±2	97±3
SCB-36 P200 Urano-Thorite composite	0.0038	1037	15.95	0.7581	42.48	2.06	55.46	2480	80,950	0.01507	0.1008	0.04852	97±2	99±3
SCB-36 R200 Urano-Thorite A	0.0041	623.9	14.02	0.6529	39.02	1.87	59.11	3200*	108,130	0.01339	0.08850	0.04797	87±2	87±3
SCB-36 R200 Urano-Thorite B	0.0057	498.4	12.65	0.6413	38.63	1.92	59.45	3780*	98,205	0.01723	0.1181	0.04962	111±2	115±3
SCB-101C_3 R200 Urano-Thorite A	0.0108	n.obs.	3.075	0.6573	43.68	2.15	54.17	137.4*	36,490	0.00191	-	-	12±2	-
SCB-101C_3 R200 Urano-Thorite B	0.0056	n.obs.	14.48	0.8115	44.25	2.15	53.60	2535*	96,550	0.01346	-	-	87±2	-
Precision		±1.8%	±0.30%	±0.35%				±1.0%	±1.0%					

*Concentrations corrected for drift of spike concentration

	$\frac{206}{204}$	$\frac{207}{204}$	$\frac{208}{204}$
Lead correction	18.95	15.62	38.52

apparent ages that are higher than any obtained from the zircon fractions. The radiogenic quality of the zircon analyses and their internal consistency suggest that the true age of the Rubidoux granites is not greater than 130 million years. Therefore it appears that the allanites are discordant in the reverse sense from the zircons. The results of Gottfried, Jaffe and Sentfle (35), who analyzed several allanite samples by the lead-alpha method, suggest that this may be a general situation. It is interesting that some monazites, which are also high in thorium relative to uranium, have been found to be discordant in this reverse sense (Tilton and Nicolaysen, 36).

Discordance in allanites is probably a complex phenomenon involving mobilization of both uranium and lead. It is noteworthy that there is an inverse correlation between the apparent age of each sample and its uranium content. The weathered sample is particularly interesting. It is distinctly different than the fresh rock samples in that it has a higher content of common lead and a significantly different radiogenic Pb^{206}/Pb^{208} ratio. The common lead may be associated with the oxide alteration which could serve as a trap for lead released from the feldspars during weathering. The different radiogenic lead composition is more difficult to interpret. In part it may be due to a different Th/U ratio acquired at the time of crystallization. The yield of accessory minerals from a weathered rock is generally

different than from the equivalent fresh rock. Therefore a great deal of caution should be exercised in making direct comparisons. However, the fresh rock allanites show consistently high proportions of Pb^{208}. If it is assumed that the allanite fraction from SCB-101C_3 was originally more like the allanite from SCB-36, then the data indicate that Pb^{208} has been selectively removed from this sample. The possibility of such an event would depend in detail on how the thorium and uranium were originally distributed in the crystal lattice. This matter deserves further investigation.

Uranothorite Analyses

Uranothorites from the Rubidoux granites show a wide range of physical characteristics. Two composite fractions from the fresh coarse granite were analyzed. From the composites, individual grains exhibiting particularly uniform characteristics were hand picked and analyzed. SCB-36 Uranothorite A consisted of lemon-yellow, translucent to transparent grains, showing no visible crystal forms. Opaque inclusions are commonly present. In the composite fraction all gradations occur from the clear lemon-yellow variety to practically opaque brownish-black material. Individual grains show a heterogeneous distribution of clear and opaque portions. The hand-picked specimens were placed in immersion oils and found to be variably isotropic to weakly birefringent. The index of refraction is somewhat variable and averages about 1.70. Photograph 17, Appendix B, is a

photomicrograph of this material.

SCB-36 Uranothorite B consisted of gray-green opaque grains showing conchoidal fracture surfaces but no crystal forms. In transmitted light thin flakes have a uniform gray-brown color. It is isotropic with an index of refraction about 1.85, and occurs as discrete grains, as cores within the lemon-yellow variety, and as cores surrounded by black metamict material.

Uranothorite separates from the weathered coarse granite contained a higher proportion of grains with well developed crystal forms, which are tetragonal prismatic much like zircon. The occurrence of these grains suggests that weathering releases them in gentler fashion than the rock crushing procedure in the laboratory.

SCB-101C_3 Uranothorite A consisted of orange translucent grains which are thought to be equivalent to the yellow variety from the fresh granite. The orange material shows similar gradations to brownish-black opaque material, and the presence of gray-green cores. The average index of refraction is 1.68.

SCB-101C_3 Uranothorite B was equivalent in every way to the gray-green material from the fresh rock, except for the presence of occasional well developed crystal forms and minor amounts of orange oxide materials coating the surfaces of the grains.

X-ray powder photographs were made of each of the hand-picked fractions. In all four cases diffuse but strong

reflections were observed corresponding to the (200), (011), (112), (312), and (121) reflections reported for thorite by Frondel, Riska and Frondel (37).

The results of the isotopic analyses are shown in Table 11. The data show that, on the average, uranothorite in the Rubidoux granites is somewhat more highly disturbed than the zircons and in the same direction. The uranothorites are more than 40 times as radioactive as the zircons and the diffuse nature of the x-ray reflections indicates that they have suffered significant radiation damage. Yet the degree of discordance is not very much greater than for zircon. These results demonstrate that the correlation between radioactivity and degree of disturbance is a complex phenomenon and must be treated in relation to specific minerals. The behavior of the Rubidoux uranothorites departs from the behavior of other uranothorites that have been analyzed. Silver and Deutsch (26) and Silver (personal communication) have found that in older rocks uranothorites may be much more highly disturbed than zircons from the same rock.

The hand-picked fractions from the fresh rock are not a representative selection of the composite inasmuch as they both have higher uranium concentrations and lower Pb^{206}/Pb^{208} ratios than the composite. On the other hand, their apparent ages bracket the apparent age of the composite quite well.

The representative nature of the fractions from the weathered rock is particularly open to question. Selection

of material requires the ability to recognize it and thus it is possible that very badly weathered uranothorites are not at all represented by these fractions. However, the trends of weathering effects are clearly demonstrated. SCB-101C_3 Uranothorite A has apparently been drastically affected and has lost nearly two-thirds of its uranium and almost 95% of its lead. These figures may be incorrect to the extent that this fraction was not originally equivalent to SCB-36 Uranothorite A, but the effect of weathering on the Pb/U ratio is pronounced and must be real. By contrast, SCB-101C_3 Uranothorite B shows relatively little effect due to weathering. Assuming that this sample was originally equivalent to SCB-36 Uranothorite B, weathering appears to have removed a measurable portion of the lead but almost none of the uranium.

This study has shown: 1) that uranothorites with a distinct range of physical and isotopic properties occur in the coarse-grained Rubidoux granite, 2) that individual uranothorites differ significantly in their response to weathering, and 3) that weathering causes loss of lead more readily than loss of uranium. It is apparent that the behavior of uranothorites in the natural environment is a very complex phenomenon and is sensitively dependent on factors not having to do merely with their high thorium and uranium content.

Summary

The data presented in this chapter illustrate various uranium-lead isotopic properties of zircon, allanite, and uranothorite in the Mt. Rubidoux granites. The uranium and radiogenic lead in the whole rock must be located primarily in these minerals. The only other radioactive accessory mineral that has been observed in the rocks is apatite, which was not obtained in sufficient quantity for analysis. The abundance and activity of apatite indicated in thin sections and autoradiographs are low enough that its contribution is probably small relative to the minerals that have been analyzed.

The properties of the whole rock system are expected to reflect the properties of these minerals. The important characteristics are listed below:

1) Each of the three minerals has a distinctive Th/U ratio which is reflected in the isotopic composition of its radiogenic lead. Zircon contains Pb^{206}-rich lead whereas allanite contains Pb^{208}-rich lead. Uranothorite contains lead of intermediate isotopic composition.

2) The concentration of radioactive elements, and hence of radiogenic lead, in each species varies in a significant way. Zircon and allanite may be considered roughly equivalent, but oranothorite is markedly enriched. For equal weights of mineral, uranothorite contäins 45 times more uranium and 100 times more total radiogenic lead than zircon,

and 200 times more uranium and 60 times more radiogenic lead than allanite.

3) All of the radioactive minerals have been isotopically disturbed during their lifetimes, even in the freshest rock obtainable. Discordance in zircon and uranothorite reflects loss of lead relative to uranium, whereas in allanite it reflects loss of uranium relative to lead. The degree of discordance for minerals from the fresh rock averages about 10% in the case of zircon and 20% in the case of uranothorite, if the true age of the rock is about 120 million years. The average degree of discordance for allanite is not certain but appears also to be 10-20%.

4) The systematics of discordance are more regular for zircon than for uranothorites or allanites. The results of this study suggest that young uranothorites or allanites may be useful for geochronological work. Analyses of uranothorites should indicate minimum ages whereas analyses of allanite should indicate maximum ages.

5) The mobility of uranium and radiogenic lead during weathering is complex. Weathering appears to have no effect on zircon. The data suggest that weathering of allanite may result in preferential loss of thorium and Pb^{208} although this is not certain. The presence of oxide coatings appears to provide a trap for mobilized common lead. Individual types of uranothorite differ considerably in their response to weathering but in general lose lead more readily than uranium.

Chapter 5

ISOTOPIC STUDIES

III. COMMON LEAD AND THE TOTAL ROCK SYSTEM

Introduction

The total rock uranium-lead system includes, in addition to uranium and radiogenic lead, the original lead that was taken up at the time the rock crystallized. The isotopic composition of this original or common lead must be known in order to evaluate isotopic balance in the total system. In the present study it has been assumed that there is only one common lead in each of the Mt. Rubidoux granites, although not necessarily the same in both. This implies that the originally acquired lead was homogeneous in composition throughout each rock and that there has been no exchange of common leads with the surroundings. The petrologic homogeneity of the granites and the lack of any visible secondary alteration support this assumption.

The composition of the common lead was determined by several analyses of lead isolated from potash feldspar. Following this, the isotopic composition of the lead and the concentration of lead and uranium in samples of total rock were measured. Finally, acid leaches of whole rock material were analyzed. These data, coupled with the information on the accessory minerals discussed in the previous chapter,

permit a close evaluation to be made of the balance of lead and uranium in the rocks, and in addition illustrate some factors concerning the mobility of these elements during weathering.

Common Lead Analyses

Feldspar separates were obtained from two different hand specimens of the fresh coarse granite, SCB-36, and from one hand specimen of the fine granite, SCB-102. Each hand specimen was pulverized in a carefully cleaned, hardened steel "diamond" mortar to -30 mesh. Aliquots for feldspar analyses were passed through Nylon bolting cloth screens and the desired size fractions placed in a mixture of tetrabromoethane and acetone adjusted to a specific gravity of about 2.60. The floats, containing primarily potassium feldspar, were rinsed with acetone, dried, and passed through the Frantz magnetic separator operated at full current. All magnetic material was discarded.

From one hand specimen of the coarse granite the P200-R400 mesh concentrate of potash feldspar was split into two parts, one of which was put directly into solution and the other acid washed for one hour in hot concentrated HNO_3 before being put into solution. These were labeled SCB-36 FsIA and FsIB, respectively. A similar procedure was followed for the P100-R200 mesh concentrate from the second hand specimen, and the samples were correspondingly labeled

SCB-36 FsIIA and FsIIB. A third fraction, SCB-36 FsIIC, was further pulverized in a "Diamonite" mortar to -325 mesh and then acid washed. The very finest particles from this sample were lost during rinsing.

From the hand specimen of the fine granite the P200-R400 mesh concentrate was put directly into solution, whereas the P100-R200 fraction was acid washed before being dissolved. These samples were labeled SCB-102 FsIA and FsIB, respectively. The procedures employed to dissolve the samples and extract uranium and lead are described in Appendix A.

Results of the isotopic analyses are shown in Table 12. Five feldspar and nine total rock lead composition analyses were statistically evaluated to determine the precision of the mass spectrometry. The measured 206/207 and 206/208 ratios were found to have standard deviations of 0.25% and 0.30%. The measured 206/204 ratio was found to have an average standard deviation of 0.3%. However, somewhat greater deviations of this ratio occasionally occurred for unaccountable reasons. Moreover, the relatively low intensity of the mass 204 signal makes possible a consistent bias in reading the chart. To account for these uncertainties the precision has, somewhat arbitrarily, been decreased from 0.3% to 0.5%.

The data in Table 12 are displayed graphically in Figures 8, 9, and 10. Figures 8 and 9 are conventional plots

Table 12

MOUNT RUBIDOUX GRANITES

FELDSPAR ISOTOPIC ANALYSES

	Sample No.	Mesh Size	Weight (gm)	Observed Pb Atom Ratios $\frac{206}{204}$	$\frac{206}{207}$	$\frac{206}{208}$	$\frac{207}{204}$	$\frac{208}{204}$	Atom Percent 204	206	207	208	Concentrations (ppm) Pb	U	$\frac{Pb}{U}$
Coarse Granite SCB-36															
Not acid washed	Fs I A	P200 R400	1.052	19.09	1.2215	0.49240	15.63	38.76	1.343	25.63	20.98	52.05	12.1	0.57	21.2
	Fs II A	P100 R100	1.875	19.48	1.2444	0.50078	15.65	38.89	1.333	25.96	20.86	51.84	24.6	0.47	52.4
Acid washed	Fs I B	P200 R400	1.978	18.95	1.2130	0.49206	15.62	38.52	1.350	25.58	21.09	51.98	12.3	0.11	111
	Fs II B	P100 R200	1.913	18.95	1.2123	0.48735	15.63	38.89	1.343	25.45	20.99	52.22	25.3	0.21	120
	Fs II C	P325	1.396	20.01	1.2721	0.81602	15.73	38.78	1.324	26.50	20.83	51.35	17.1	0.11	155
Pine Granite SCB-102															
Not acid washed	FsI A	P200 R400	0.9920	19.26	1.2280	0.49442	15.68	38.95	1.335	25.72	20.94	52.01	9.7	1.44	6.73
Acid washed	Fs I B	P100 R200	1.640	19.18	1.2268	0.49630	15.63	38.65	1.343	25.76	21.00	51.90	20.7	0.17	122
	Precision			±0.5%	±0.25%	±0.30%							± 1%	± 5%	

Mt. Rubidoux Granites, Feldspar
Lead Isotopic Compositions
15.72
15.68
15.64
15.60
Pb^{207}/Pb^{204}
19.0
19.2
19.4
19.6
19.8
20.0
Pb^{206}/Pb^{204}
COARSE GRANITE
FINE GRANITE

Figure 8

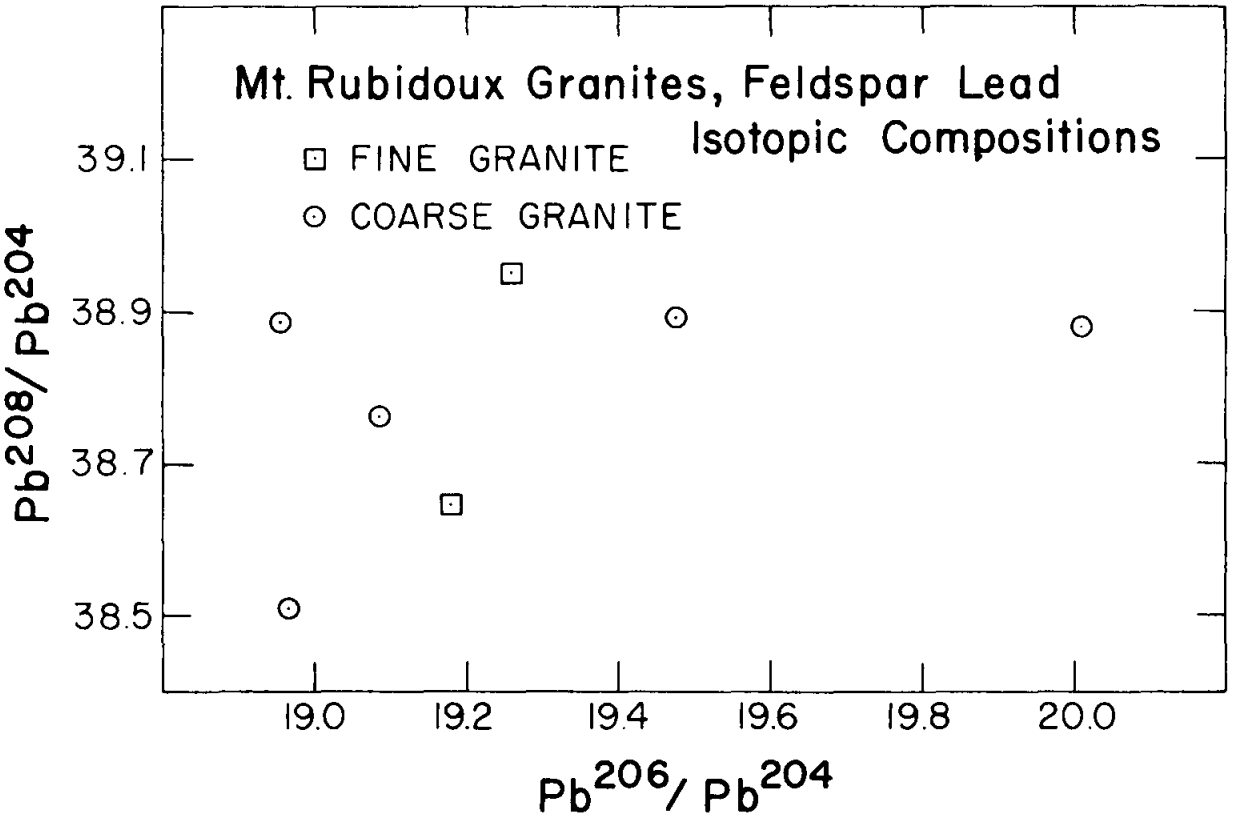
Mt. Rubidoux Granites, Feldspar Lead Isotopic Compositions
FINE GRANITE
COARSE GRANITE
39.1
38.9
38.7
38.5
Pb^{208}/Pb^{204}
19.0
19.2
19.4
19.6
19.8
20.0
Pb^{206}/Pb^{204}

Figure 9

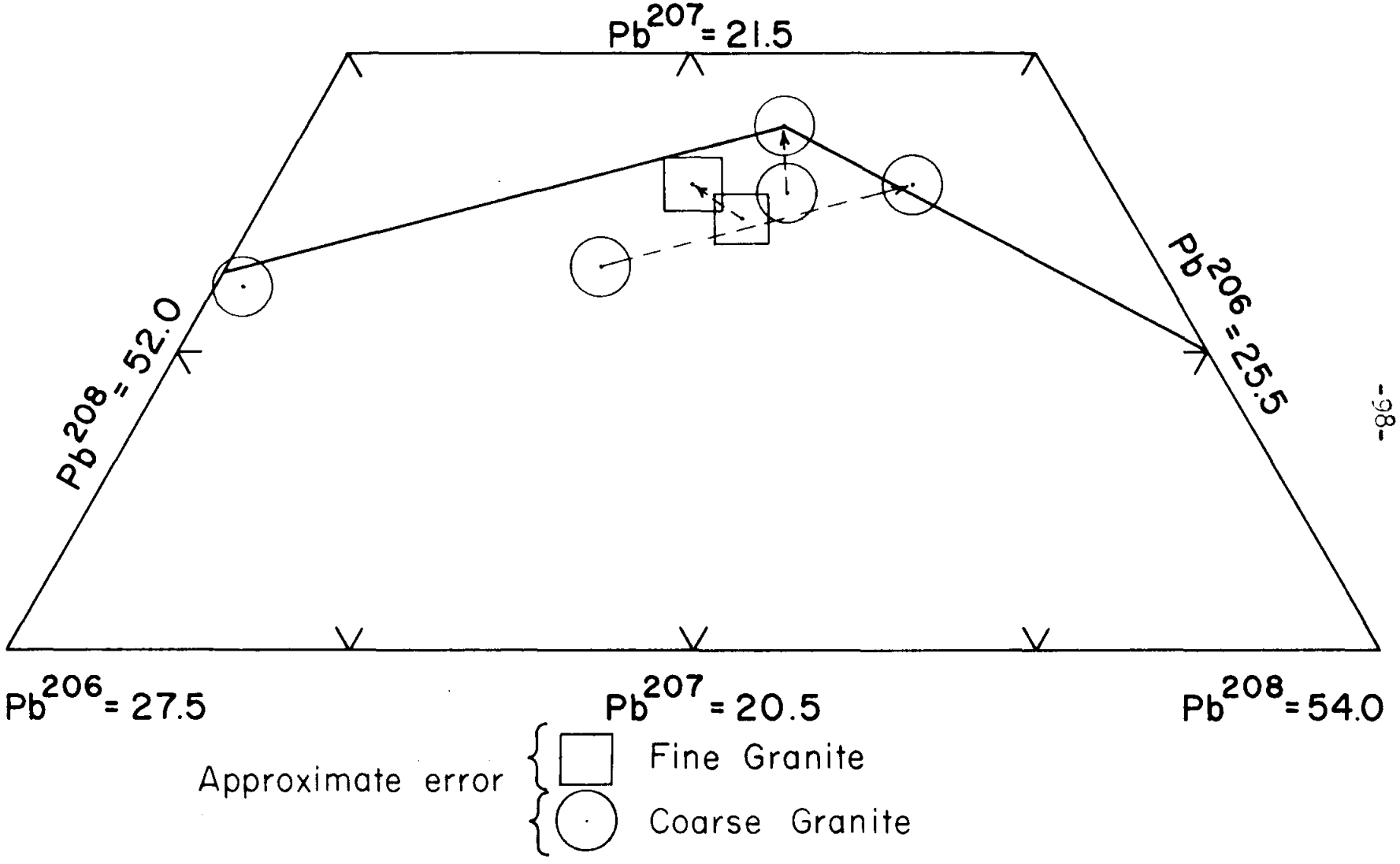

Figure 10. Mt. Rubidoux Granites, Feldspar Lead Isotopic Compositions

of 207/204 vs. 206/204 and 208/204 vs. 206/204. The symbols on these diagrams do not indicate error limits. Figure 10 is the less conventional triangular method of plotting the data and has the virtue that the relatively large error in determining the Pb^{204} isotope is eliminated from consideration when comparing several analyses. The two solid lines shown in this figure are, in one case, the locus of compositions that would result from adding pure thorium-derived lead to SCB-36 FsIB, and in the other case, the locus of compositions that would result from adding pure uranium-derived lead of about 120 m.y. age to SCB-36 FsIB. The single line shown in Fig. 8 is likewise the locus of compositions resulting from mixtures of 120 m.y. uranium-derived lead and SCB-36 FsIB.

One of the major problems in determining the composition of common leads is sample purity. If small inclusions of radioactive materials are present or if surfaces and fractures within the sample hold extraneous leads, then the measured composition is different than the desired true composition. The acid washing experiments were designed to test the possible magnitude of this problem. During the work, however, it was found that unusual contamination appeared occasionally from the laboratory procedure, and this has partly obscured the effects of impurities in the sample and also introduced a greater degree of uncertainty in specifying the true common lead composition. Nevertheless it is believed that the analyses indicate very nearly

the correct composition of the common lead in the coarse granite.

The analyses have not been corrected for possible radiogenic lead associated with the observed uranium in the samples, partly in order to emphasize the differences in observed lead composition and partly because the acid washed samples have such low concentrations of uranium that the correction is well within mass spectrometric errors. In addition, no correction has been made for laboratory blank lead. The compositions of leads from three laboratory sources are shown in Appendix A. The most likely source in the case of the feldspar analyses is the ammonium citrate. Relatively large quantities of this reagent were required for the lead extractions, which were done using the double dithizone technique. In a single analysis about 0.1-0.2 μg of lead would have been contributed by the citrate, which corresponds to up to 2% of the total lead extracted. The citrate lead is so nearly like the observed leads that, again, the correction is within mass spectrometric errors. Moreover, the presence of citrate lead would tend to cancel the presence of lead derived from the uranium in the sample.

The effect of acid washing for the three sample sets, excluding SCB-36 FsIIC, is shown by the dashed arrows in Fig. 10. It appears that the result in each case was to remove a small amount of radiogenic lead from the sample. Another way of evaluating the effect is by noting the Pb/U

ratio for each set; in particular the group composed of SCB-36 FsIIA, FsIIB, and FsIIC. This group shows a progression of values for the Pb/U ratio, with FsIIC having the highest value. These results are readily interpreted to mean that acid washing has a definite influence in reducing the amount of radioactivity in the sample, and that the proportion of such impurities available to acid attack is increased by pulverizing the sample to finer grain size as was done for FsIIC. The somewhat lower lead concentration measured for this sample is possibly a result of flotation of very fine potash feldspar particles during acid washing. Particles of plagioclase released from perthitic lamellae would be less likely to float and therefore the sample would be artificially diluted.

However, the composition of the lead from SCB-36 FsIIC is considerably more radiogenic than the other two samples of this set. No explanation could be found for such a result until repeated analyses of a single solution of total rock sample (next section) showed that occasional contamination with uranium-derived radiogenic lead occurred. It is not understood how the contamination came about nor why it should have been of essentially pure uranium-derived lead. Most of the samples that are analyzed in the laboratory do contain primarily this sort of lead, but for each such analysis, Pb^{208}-rich lead is used as a spike for determining lead concentrations. One would expect, therefore, that arbitrary contamination would be a mixture of

206-rich and 208-rich lead. The amount of radiogenic contamination indicated by FsIIC is about 1% or 0.1 μg. It is believed that FsIIA may in part be contaminated in the same way as FsIIC.

The relationship between the lead compositions from SCB-36 FsIA and FsIB is exactly what would be expected if the non acid washed fraction contained small inclusions or particles of uranothorite or apatite, or surficial sources of uranium, thorium, and radiogenic lead. The composition of SCB-36 FsIIB is open to question. It is possible that both this sample and SCB-36 FsIIA were slightly contaminated by Pb^{208}-rich lead from a spike. However, it is also possible that this sample, being of coarser grain size than the FsI set, contained a higher proportion of inclusions or internal surfaces that were inaccessible to acid washing. The presence of a small amount of allanite in the sample, for example, would have sufficed to produce the observed enrichment of Pb^{208} relative to SCB-36 FsIB.

The above discussion has implicitly assumed that SCB-36 FsIB is most nearly the true common lead of the coarse granite, and this is the interpretation proposed here. It appears that significant contamination arises either from impurities in the natural sample or from anomalous contamination in the laboratory. Both sources yield leads of radiogenic character. Therefore the sample which shows the least radiogenic character should be most nearly the correct common lead.

In addition, it is believed that the measured abundance of Pb^{204} in the analysis of SCB-36 FsIB is very nearly the "correct" abundance, in the sense that random errors have largely cancelled out. There may be a consistent bias introduced either by the peculiarities of the mass spectrometer or by the method of reading the charts, but this bias will be common to all samples analyzed in this study and will not detract from the relative values of the measurements. Fig. 8 shows the overall consistency of the data. Five of the seven feldspar analyses lie very close to a single line, which, as drawn, passes through the point corresponding to SCB-36 FsIB and has a slope (Pb^{207}/Pb^{206}) equal to 0.0484. The fit is much better than analytical precision requires, and therefore it appears that in the majority of cases random errors tend to cancel. The two points with the greatest departure are both anomalous. One is SCB-36 FsIIC, which is anomalously radiogenic, and the other is SCB-102 FsIA, which has an anomalously high uranium concentration.

The observed relationship for the samples from the fine granite are more difficult to interpret since similar size fractions were not analyzed. The coarser size fraction, which was acid washed, yielded a slightly less radiogenic lead than the finer size fraction. The extreme discrepancy between the uranium contents of these two samples does not agree with the small shift in isotopic composition. It is possible that both samples were slightly contaminated with

anomalous radiogenic lead in the laboratory.

However, the consistency of the data (Fig. 10) suggests that the fine granite may have a common lead which is naturally richer in uranium-derived lead than is the common lead of the coarse granite. From geological evidence the two rocks are essentially contemporaneous, and therefore one would not expect to be able to see any evolution of the common lead in the magma reservoir. A possible interpretation of the discrepancy, if it is real, arises from the fact that the coarse granite contains numerous inclusions whereas the fine granite contains none. Thus the common lead of the coarse granite may be slightly more primitive by virtue of having assimilated an older lead from the wall rock.

The concentrations of lead in the various feldspar samples show a correlation with size fraction. Grain mounts of the samples from the coarse granite were examined. It was found that the P200-R400 fraction contains a considerably larger proportion of plagioclase than the P100-R200 fraction, which is probably a result of the relative efficiency of the flotation procedure in each case. This leads to the conclusion that the potash feldspar in the coarse granite contains a minimum of 25 ppm lead, and in the fine granite a minimum of 21 ppm lead. A probable maximum is 30 ppm for both rocks.

The important results of this section are summarized below:

1) Sample purity is measurably improved by acid

washing. Pulverizing of the sample to fine grain size appears to make accessible to acid solution a larger proportion of the included uranium and radiogenic lead.

2) The observed isotopic composition of lead from SCB-36 FsIB is probably very nearly the composition of the common lead in the coarse-grained Rubidoux granite. For reference it is reproduced here:

	206/204	207/204	208/204
Best Value Mt. Rubidoux Coarse Granite Common Lead	18.95	15.62	38.52

3) The isotopic composition of common lead in the fine granite is uncertain, but may be slightly more radiogenic than in the coarse granite. If so, this probably reflects contamination of the coarse granite system with a more primitive lead rather than enrichment of the fine granite system by the decay of uranium.

Total Rock Analyses

Total rock samples were obtained as splits of the powders from which potassium feldspar concentrates were also obtained (previous section). In each case, between 100 and 200 grams of rock were pulverized before being split. The total rock aliquots from the two hand specimens of the fresh coarse granite were labeled SCB-36 TRI and TRII. In order to provide a qualitative check on areal variability in the coarse granite a third sample, SCB-105 TRI, was also prepared (see Chapter 3). The sample of fresh fine granite

was labeled SCB-102 TRI. Samples of C-zone and B-zone weathered coarse granite were prepared in the same way as the fresh rock samples and were labeled SCB-101C_3 TRI and SCB-101B TRI, respectively.

The total rock samples were not treated in any way before being put into solution. The procedures followed for dissolving the samples and extracting lead and uranium are described in Appendix A. Inasmuch as it was not desirable to acid wash the samples a check was made of the possible isotopic composition of foreign lead that might have been introduced in the natural environment, especially from the air since Mt. Rubidoux is located in a portion of southern California which has a high concentration of lead in the atmosphere due to smog. Leads from two sources were analyzed. One source was a rusted iron chain surrounding a viewpoint on Mt. Rubidoux. The chain was rinsed with dilute HCl and the rinsings were collected directly in a clean polyethylene bottle. The other source consisted of several strips of wood taken from the traveled surface of the crossover bridge on the Mt. Rubidoux road. These were soaked for about one hour in dilute HCl and the acid was stored temporarily in a second clean polyethylene bottle. The following compositions were found:

Source	206/204	207/204	208/204
Chain	18.16	15.53	37.87
Bridge	18.35	15.43	37.83

These compositions are not grossly different than the Rubidoux leads and would not affect the measurement unless they comprised about 5% or more of the observed lead. Since all samples, especially the weathered ones, were collected only after the exposed portions were discarded, it seems unlikely that such large proportions of contamination lead were present. Therefore it is believed that the analyses have not been affected by this source of error.

The results of the total rock isotopic analyses are shown in Table 13. In most cases a rather large weight of sample was put into solution in order to insure proper representation of trace constituents such as uranothorite. The resulting large amount of solution permitted repeat analyses to be made. Where this was done it is indicated by a subscript after the sample number; e.g. SCB-36 $TRII_1$ and $TRII_2$. The data in Table 13 are shown graphically in Figures 11, 12, and 13. The composition of the coarse granite feldspar lead, SCB-36 FsIB, is shown for reference, and the solid lines in Figs. 11 and 13 correspond to the lines shown previously in Figs. 8 and 10. Also shown in Fig. 13 is the average composition of the two contamination leads discussed above. None of the analyses has been corrected for laboratory blank lead since the effect is within mass spectrometric errors.

In Fig. 13, the repeat analyses of single sample solutions are connected by dashed lines. It is obvious that in both cases one of the analyses was considerably more

Table 13

MT. RUBIDOUX GRANITES

TOTAL ROCK ISOTOPIC ANALYSES

Sample No.		Weight (gm)	Observed Pb Atom Ratios $\frac{206}{204}$	$\frac{206}{207}$	$\frac{206}{208}$	$\frac{207}{204}$	$\frac{208}{204}$	Atom Percent 204	206	207	208	Concentrations (ppm) Pb	U	$\frac{U^{238}}{Pb^{204}}$
Coarse Granite SCB-36	TRI	1.672	20.07	1.2791	0.51353	15.69	39.08	1.318	26.46	20.69	51.53	11.6	3.65	20.6
	$TRII_1$	12.68	19.78	1.2663	0.50675	15.62	39.04	1.325	26.22	20.71	51.74	11.1	4.65	27.4
	$TRII_2$	"	19.47	1.2403	0.49600	15.70	39.26	1.326	25.81	20.81	52.05	"	"	"
Coarse Granite SCB-105	TRI_1	17.84	19.60	1.2523	0.50303	15.65	38.96	1.330	26.06	20.81	51.80	11.4	2.50	14.3
	TRI_2	"	19.16	1.2262	0.49221	15.63	38.93	1.338	25.65	20.91	52.10	"	"	"
	TRI_3	"	19.07	1.2229	0.49137	15.60	38.81	1.343	25.61	20.94	52.11	"	"	"
Weathered Pine Coarse Granite SCB-102	TRI	2.382	19.62	1.2536	0.50196	15.65	39.08	1.327	26.04	20.77	51.87	9.2	3.20	22.7
Weathered Coarse Granite SCB-101C	TRI	11.92	19.23	1.2313	0.49385	15.62	38.93	1.337	25.71	20.88	52.07	11.6	4.08	22.7
Weathered Coarse Granite SCB-101B	TRI	2.563	19.35	1.2324	0.49126	15.70	39.38	1.326	25.65	20.81	52.21	15.5	3.44	14.5
	Precision		±0.5%	±0.25%	±0.30%							±1%	±2%	

Figures 11 and 12 (following two pages). Mt. Rubidoux Granites, Total Rock Lead Isotopic Compositions. Plots of Pb^{207}/Pb^{204} vs. Pb^{206}/Pb^{204} and Pb^{208}/Pb^{204} vs. Pb^{206}/Pb^{204}, respectively.

Mt. Rubidoux Granites, Total Rock Lead
Isotopic Compositions
COARSE GRANITE
FINE GRANITE
WEATHERED COARSE GRANITE, C-ZONE
WEATHERED COARSE GRANITE, B-ZONE
SCB-36 FsIB
15.72
15.68
15.64
15.60
Pb207/Pb204
19.0
19.2
19.4
19.6
19.8
20.0
Pb206/Pb204

Figure 11

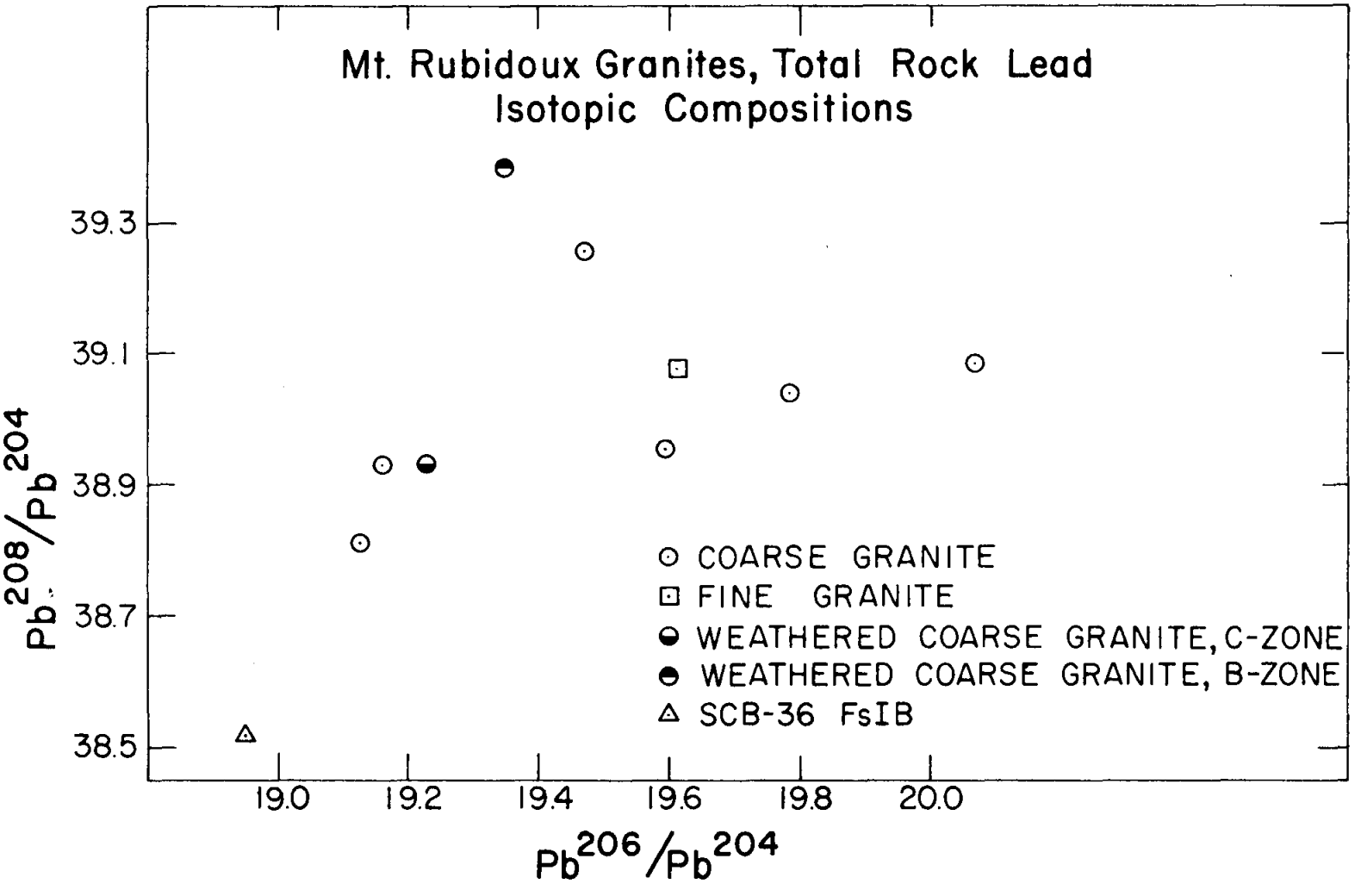
Mt. Rubidoux Granites, Total Rock Lead
Isotopic Compositions
39.3
39.1
38.9
38.7
38.5
Pb^{208}/Pb^{204}
19.0
19.2
19.4
19.6
19.8
20.0
Pb^{206}/Pb^{204}
COARSE GRANITE
FINE GRANITE
WEATHERED COARSE GRANITE, C-ZONE
WEATHERED COARSE GRANITE, B-ZONE
SCB-36 FsIB

Figure 12

Figure 13 (next page). Mt. Rubidoux Granites, Total Rock Lead Isotopic Compositions. Triangular Diagram.

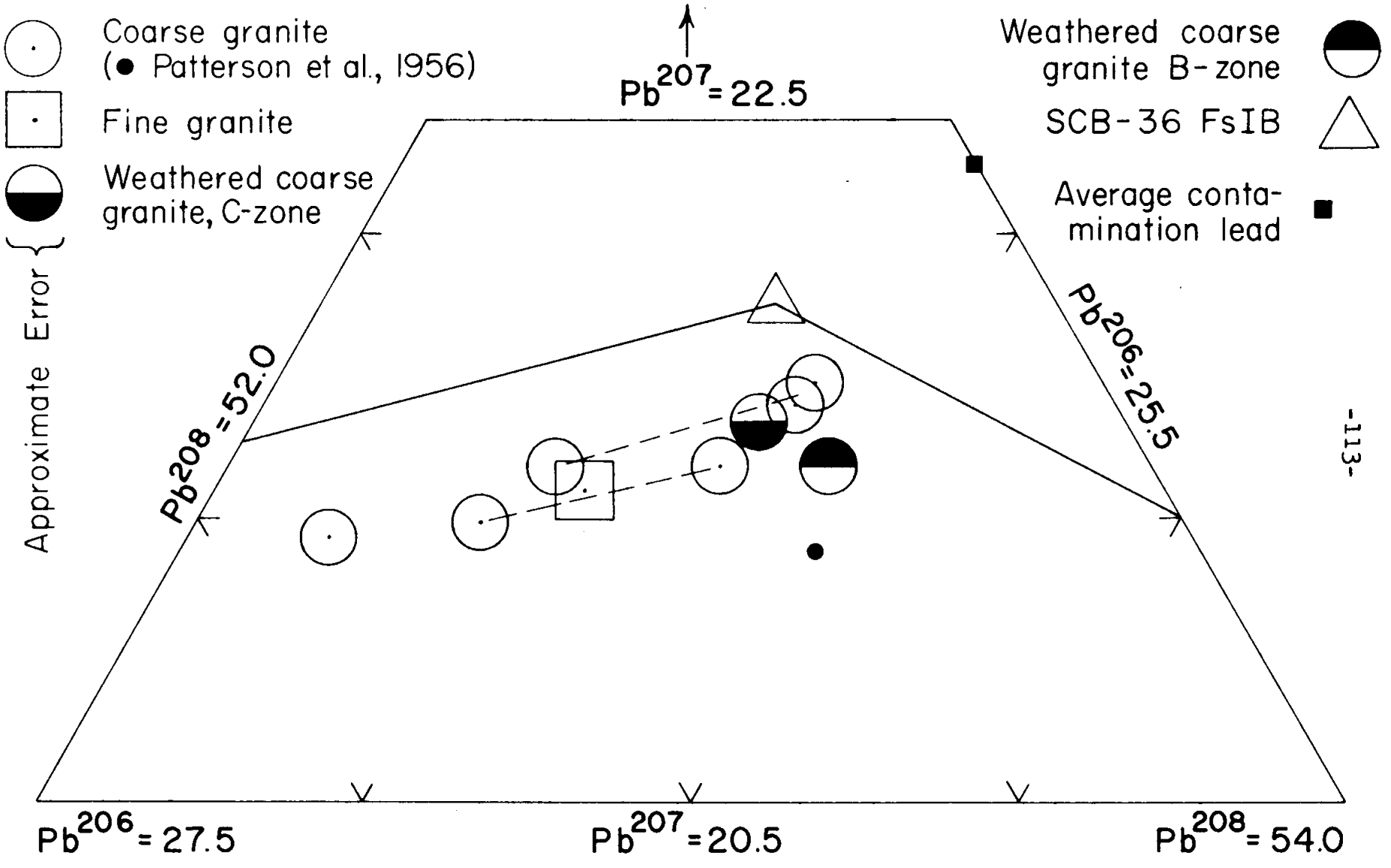

Figure 13. Mt. Rubidoux Granites, Total Rock Lead Isotopic Compositions

radiogenic in composition than the other. The clustering of five analyses very closely below the point corresponding to SCB-36 FsIB, and the fact that SCB-105 TRI_2 and TRI_3 were identical within the limits of error, are believed to indicate that these particular analyses are essentially uncontaminated. The analyses of SCB-36 $TRII_1$ and SCB-105 TRI_1 must therefore be contaminated with uranium-derived radiogenic lead. It is believed that SCB-36 TRI is very likely also contaminated. As was discussed in the previous section it is not understood how this particular sort of contamination came about.

As a possible check on the uncontaminated character of five of the analyses, a point is shown in Fig. 13 corresponding to the composition of lead from the coarse Rubidoux granite which was measured considerably earlier by Patterson, Silver and McKinney (5). Their work was done in the same laboratory using the same mass spectrometer as the present study, and their analysis is as follows:

	206/204	207/204	208/204
Patterson et al. (5) Mt. Rubidoux Coarse Granite	19.44	15.61	39.48

In terms of the major isotopes the early analysis agrees reasonably well with the five believed to be

uncontaminated. It is shifted in the direction of higher content of radiogenic lead, which agrees with the observed 7 ppm U in Patterson's sample compared to about 4 ppm for samples of this study.

The analysis of SCB-101B TRI is very difficult to interpret. As was discussed in Chapter 4, a significant amount of older zircon was present in the mineral separates from this sample. The amount of older material other than zircon is not known. It seems likely that the observed lead composition represents a mixture of lead from the Rubidoux granites with a lead from some other rock source. For this reason the sample will not be considered further.

It is not certain whether or not the sample of fresh fine-grained granite, SCB-102 TRI, is contaminated. Its composition is nearly like the contaminated leads from the coarse granite. However, the data shown in the previous section suggest that the fine granite has a common lead of more radiogenic character than the coarse granite. If so, the observed total rock composition may be correct. There is sufficient uncertainty on this matter that the question should remain open.

Isotopic Balance in the Total Rock System

It is possible now to examine the question of the overall uranium-lead isotopic balance in the total rock systems. In order to do so, however, it is necessary to eliminate any relative errors in the determination of the

abundance of Pb^{204} for the various samples. The assumption involved in doing this is that the observed lead in each total rock sample should be a mixture of the known common lead plus some amount of radiogenic lead which has a Pb^{207}/Pb^{206} ratio corresponding to the known age of the rock. The correction can be made quite easily by a graphical technique based on Fig. 11. The common lead composition is assumed to be correct. A line is drawn as shown through the point corresponding to the common lead analysis which, in this case, has a slope (207/206) equal to 0.0484. Then, through each point corresponding to a total rock analysis, a line is drawn that has a slope equal to the observed 207/206 ratio for that sample. The intersection of this line and the first one gives the corrected, or normalized, ratios 206/204 and 207/204. The normalized 208/204 ratio is determined by multiplying the normalized 206/204 ratio by the observed 208/206 ratio for the sample.

The isotopic balance in each sample is estimated by subtracting the common lead (indexed to Pb^{204}) from the total rock lead (also indexed to Pb^{204}) and computing the concentration of the residual radiogenic lead in the total rock sample. The final step is to compute the atom ratio of each radiogenic lead isotope to its parent uranium isotope, which in effect gives the apparent age of the total rock uranium-lead system. Only the 206/238 ratio is significant in this regard.

The results of performing the above calculations are shown in Table 14. A correction for thorium-derived radiogenic lead was made for SCB-102 TRI by using the data of Whitfield, Rogers and Adams (7), who found 10.0±0.2 ppm Th by gamma spectrometry in a sample of the fine granite from Victoria Hill. The data in Table 14, especially with respect to the coarse granite, are very interesting and are discussed below.

1) All samples of the coarse granite have apparent ages that are considerably lower than the true age of the rocks as presently interpreted. The accuracy of the apparent age depends on errors in mass spectrometry and on the possibility of extraneous lead contamination. Errors in mass spectrometry and isotope dilution, if cumulative, could change the apparent age by 5 million years or perhaps slightly more. Extraneous contamination could have a significant effect even if present in small amounts. However, the consistency of the total rock data and the arguments developed previously for the accuracy of SCB-36 FsIB suggest that the apparent ages have not been influenced by the presence of contamination. Therefore it is believed that the indicated total rock apparent ages are analytically valid and are on the low side of the true age.

2) The degree of apparent discordance in the two samples of fresh coarse granite is on the average greater than would be expected for zircon and is in the wrong direction for allanite. On the other hand it is roughly

Table 14

MOUNT RUBIDOUX GRANITES

TOTAL ROCK APPARENT AGES

Sample No.	Normalized Pb Composition $\frac{206}{204}$	$\frac{207}{204}$	$\frac{208}{204}$	Apparent Age (m.y.) $\frac{206}{238}$	$\frac{208}{232}$
SCB-36 FsIB	18.95	15.62	38.52	-	-
SCB-36 $TRII_2$	19.41	15.65	39.13	108	-
SCB-105 TRI_2 / SCB-105 TRI_3	19.15	15.63	38.93	91	-
SCB-101C_3 TRI	19.26	15.64	39.00	88	-
SCB-102 FsIB	19.18	15.63	38.65	-	-
SCB-102 TRI	19.63	15.66	39.10	127	126

equivalent to the discordance that has been found for uranothorite. The possible influence of uranothorite is also suggested by the relationships in Fig. 13. It can be seen that as the amount of uranium increases in the various samples, the isotopic composition of the lead is shifted primarily toward an intermediate composition like that of uranothorite. This is not a conclusive demonstration because a roughly equal increase in both zircon and allanite would have a similar effect. However, as was pointed out in Chapter 3, the amount of uranothorite needed to produce a measurable change in the concentration of uranium in the total rock is very small relative to the amount of zircon or allanite needed to produce the same change. These considerations suggest that uranothorite may be of fundamental importance in determining the behavior of the total rock uranium-lead system.

3) The isotopic data do not permit a unique interpretation of the total rock discordance. There are two possibilities: a) Lead has migrated out of the radioactive minerals and into the feldspar. The total rock is not truly discordant in this case. b) Lead has migrated out of the radioactive minerals and also out of the rock. In this case the total rock is discordant in the same way that the minerals are. The first possibility does not seem likely because of the freshness and lack of secondary alteration in the coarse granite. The second hypothesis seems reasonable, especially if the radioactive minerals lost their lead during an

episodic event. If such an event removed lead from the minerals it would probably also have removed it from the rock. Where this lead would go is not known. It may be redistributed in the rock mass on a more grossly heterogeneous scale than the sampling volume, or it may have moved entirely out of the system. A similar result is possible if the minerals lost lead by continuous diffusion. In this case the diffused lead would possibly accumulate in interstitial positions where even minor secondary events could remove it.

4) The degree of apparent discordance for the sample of weathered coarse granite is not greater than for the fresh rock samples, yet a portion of the uranothorite in this sample (Chapter 4) had lost almost all of its lead and about two-thirds of its uranium. If the lead from the weathered uranothorite had also been lost from the rock, a measurable effect should have been produced. The lack of any apparent effect may be due in part to analytical errors; however, it also suggests that much of the lead and uranium lost from the individual minerals during the early stages of weathering are not lost from the whole rock. This means that on the average the lead and uranium released from the minerals by weathering must move only a short distance before finding new sites. Adsorption on clays and oxides may be perhaps an important factor. The detailed relationships and mechanisms are probably a function of the environment of the sample. In the present case the sample

was collected at the base of a well drained slope in an arid climate. It would be unwise to extrapolate the observed behavior of these samples to areas of significantly different climate, topography, or geology.

5) The sample of fine-grained granite is apparently not discordant either with respect to the uranium-lead system or the thorium-lead system. However, the uncertainty in determining whether or not the lead analyses for this sample and for its common lead were contaminated tends to cast doubt on the validity of the apparent concordance. It is especially fortuitous that the thorium-lead system shows no apparent discordance, since the thorium determination was made by other workers using a different technique on an entirely different sample. More work needs to be done to fix the isotopic composition of common and total rock leads for this sample.

Leach Analyses

Leaching experiments were performed on powders of whole rock material obtained as described in the section on common lead analyses. About 50 grams of powder were placed in a centrifuge bottle and cold 1N HNO_3 was added to cover the sample, which was then agitated and stirred for approximately one half hour. The solid matter was centrifuged out and the supernatant liquid was split into two fractions: one for the determination of lead composition and the other

for the determination of concentrations. The extraction techniques are described in Appendix A.

The isotopic analyses are shown in Table 15. The analysis of SCB-36 LI was provided by L. T. Silver. This particular leaching experiment was performed on the sample used by Patterson, Silver and McKinney (5) to determine the isotopic composition of lead in the coarse granite. The last column in Table 15 shows the "apparent age" of the uranium and radiogenic lead system in the leach. The calculations were performed in the same way as for the total rock analyses described in the previous section. A rather large correction was required to normalize the isotopic composition of SCB-36 LI, and therefore a greater degree of uncertainty is attached to the apparent age for this sample.

The leach analyses show several significant features which are discussed below:

1) The percentage of total lead leached from the fresh rock is small. However, in each case about 20% of the uranium and 20% of the radiogenic lead were leached. The fact that the uranium and radiogenic lead were leached in essentially equilibrium proportions suggests that they may have been derived from acid solution of particular mineral species. The high percentage of acid soluble radiogenic

Table 15

MOUNT RUBIDOUX GRANITES

LEACH ISOTOPIC ANALYSES

Sample No.	Time (min.)	$\frac{206}{204}$	$\frac{206}{207}$	$\frac{206}{208}$	$\frac{207}{204}$	$\frac{208}{204}$
SCB-36 LI	30	32.95	2.051	0.5696	16.06	57.85
SCB-36 LII	40	29.73	1.851	0.5585	16.06	53.23
SCB-101C$_3$ LI	25	22.29	1.407	0.4994	15.85	44.64

Sample No.	Atom Percent				Amt. Leached (μg/100 gm. of rock)		% Leached		* $\frac{206}{238}$
	204	206	207	208	Pb	U	Pb	U	
SCB-36 LI	1.022	23.45	16.41	55.32	17.8	139.0	1.6	20	126
SCB-36 LII	0.9998	29.72	16.06	53.22	13.0	107.2	1.2	23	99
SCB-101C$_3$ LI	1.194	26.61	18.92	53.28	25.3	67.9	2.2	17	108

*Apparent Age of Leached System (m.y.)

lead also suggests that in some cases it may be possible for natural processes to selectively remove radiogenic lead from these rocks.

2) The isotopic compositions of the leads leached from the fresh rock samples are shown in Figure 14. It is clear that these leads are weighted strongly in the direction of the composition of lead from uranothorite. This is the most direct available indication that uranium and radiogenic lead in the Mt. Rubidoux granites are contributed to a very significant degree by uranothorite. According to the figures in the preceding paragraph, it appears that uranothorite must account for a minimum of 20% of these elements, and probably considerably more.

3) The isotopic composition of lead leached from the weathered granite (not shown in Fig. 14) is enriched in both common lead and Pb^{208} relative to the fresh rock leaches. The higher proportion of common lead and the greater percentage of total lead leached from this sample probably reflect weathering of the feldspars and consequent release of common lead to acid soluble sites. The enrichment of Pb^{208} must indicate breakdown of allanite during weathering.

4) The fact that uranium and radiogenic lead are leached in approximately equilibrium proportions from the weathered granite agrees with the total rock analysis of this sample and indicates that the whole rock system is apparently not made more discordant by selective removal of

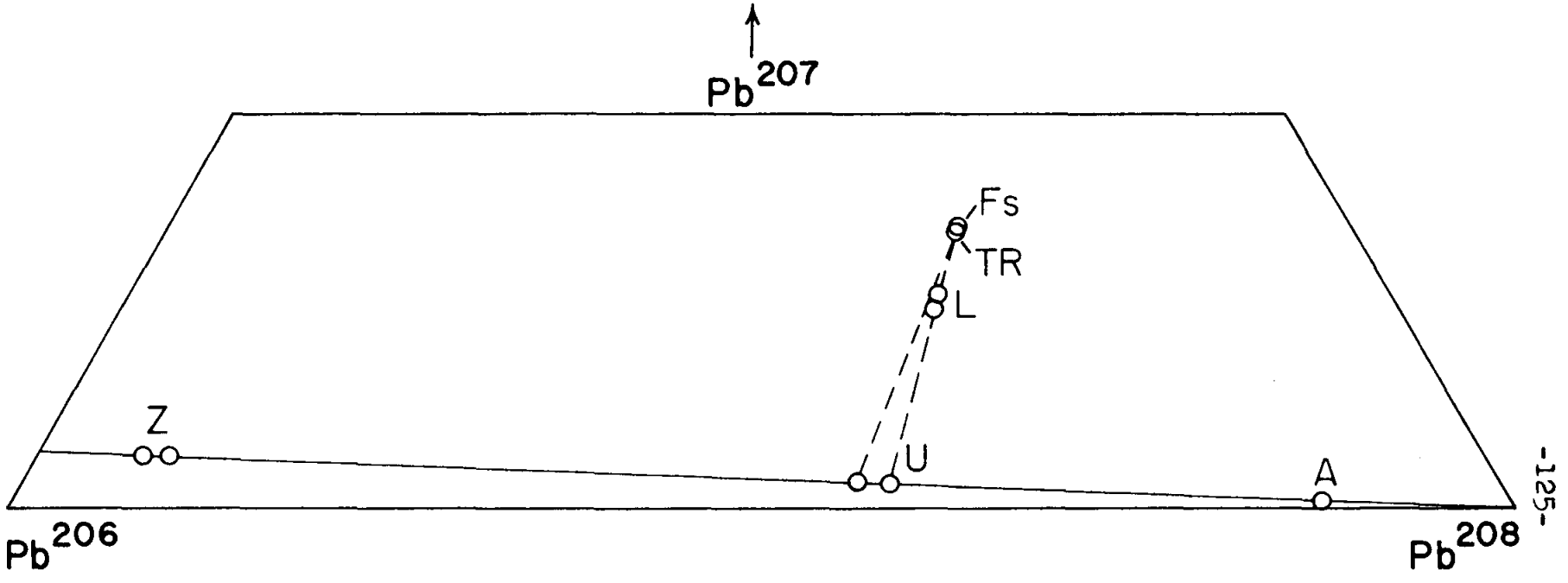

Fs = Feldspar L = Leach U = Uranothorite
TR = Total Rock A = Allanite Z = Zircon

Figure 14. Isotopic Composition of Leads from Various Sources in the Mt. Rubidoux Granites

either uranium or lead during initial weathering. This is in distinct contrast to the observed behavior of at least part of the uranothorite in the weathered specimen, which shows preferential loss of lead. The uranium and lead released from weathering of the uranothorite must be fixed in sites which are accessible to acid attack in a manner equivalent to the original uranothorite.

Conclusions

This study has attempted to obtain information which can be used to evaluate the isotopic balance in the uranium-lead systems of the Mt. Rubidoux granites. Most of the work has been concentrated on the coarse-grained granite and therefore the conclusions are applicable specifically to that rock. Isotopic studies of this sort do not always give a unique or conclusive answer. Nevertheless, the results suggest that four fundamental conclusions are valid:

1) The significant sources of uranium and radiogenic lead in the Mt. Rubidoux granites are discrete accessory minerals including zircon, apatite, allanite, and uranothorite. No evidence has been found to suggest that other possible sources contribute comparable amounts of uranium and radiogenic lead.

2) One of the most important contributors to the total rock system is the mineral uranothorite, which occurs in less than 0.005% abundance. The characteristics of this mineral control the availability of acid leachable uranium

and lead and strongly influence the isotopic balance or uranium and lead in the rock.

3) Isotopic discordance in the accessory minerals results in at least local isotopic discordance in the whole rock; that is, on the scale of sampling employed here, the lead and/or uranium lost by the individual minerals (exclusive of weathering effects) also appear to have been lost by the rock.

4) Initial weathering of the coarse granite to C-zone material has resulted in greater availability of common lead and Pb^{208}-rich lead from the breakdown of potash feldspar and allanite. Except for this, initial weathering appears to have little effect on the overall balance of uranium and radiogenic lead in the rock, within the detection limits of the techniques used.

These conclusions apply to the Mt. Rubidoux granites. Whether or not they are of general validity requires further investigation.

Table 16

MOUNT RUBIDOUX GRANITES

SUMMARY OF URANIUM AND LEAD CONCENTRATION MEASUREMENTS

	Coarse Granite		Fine Granite	
	U(ppm)	Pb(ppm)	U(ppm)	Pb(ppm)
Patterson et al. (5)	7.1 f	10.8 i	-	-
Whitfield et al. (7)	3.2 g	-	-	-
Larsen and Gottfried (3)	3.2, 4.1 f	-	5.2 f	-
This study, SCB-36 TRII	4.65 i	11.1 i	-	-
This study, SCB-105 TRI	2.50 i	11.4 i	-	-
This study, SCB-102 TRI	-	-	3.20 i	9.2 i

f = fluorimetry

g = gamma spectrometry

i = isotope dilution

Chapter 6

THE DECAY CONSTANT OF U^{235}

Introduction

The isotopic analyses of young radiogenic leads that have been accumulated in this study permit an evaluation of the decay constant of U^{235}, relative to the accepted decay constant of U^{238}, to be made with significantly greater precision than has existed previously. This is possible because the age of the Rubidoux granites is almost an order of magnitude less than the half-life of either uranium isotope and therefore the decay of each isotope has been nearly linear during the time span involved.

Because natural uranium-lead systems appear to be almost always isotopically disturbed, it is not possible to calculate the decay constant of U^{235} with confidence from the isotope ratios measured in a system whose age is of the same order of magnitude as the half-life (i.e. 10^9 years). The reason is that the differential effect of a disturbance on the apparent ages derived from the Pb^{206}/U^{238} and $Pb^{207}/U/^{235}$ ratios cannot be distinguished from the effect that an error in the assumed value of the decay constant would introduce. However, in young systems, with ages on the order of 10^8 years, the differential effect of a disturbance becomes small relative to the effect of a decay constant error. An important consequence of this fact is that the radiogenic

Pb^{207}/Pb^{206} ratio is more sensitively dependent on the relative half-life of U^{235} than it is on the age of the system. This may be illustrated in the following way: for a system of a given age, a 1% change in the half-life of U^{235} would require a 1% change in the 207/206 ratio corresponding to that age. However, at 120 million years, for example, it would require a change in the true age of 24 million years to produce a similar 1% change in the 207/206 ratio. Thus if the true age of the system can be fixed to within 24 million years (at 120 million years), and assuming that analytical errors are negligible, it should be possible to determine the half-life of U^{235}, relative to U^{238}, to within 1% by measuring the 207/206 ratio of the system.

Analytical errors, of course, are not negligible, and therefore in order to achieve a 1% evaluation of the decay constant it is necessary to know the true age to better than 24 million years. The present study has determined that the true age of the Mt. Rubidoux granites, based on the Pb^{206}/U^{238} ratio, is greater than 116 million years and is most likely less than 130 million years. The age is thus bracketed much better than is required to calculate the decay constant to 1%. The purpose of this chapter is to evaluate the sources of analytical error that may affect the determination of the Pb^{207}/Pb^{206} ratio and to synthesize the accumulated data on radiogenic leads from the Mt. Rubidoux granites.

The standard reference for the half-life of U^{235} has been the excellent work of Fleming, Ghiorso, and Cunningham (**38**). They obtained the value $t_{\frac{1}{2}}=(7.13\pm0.16) \times 10^8$ years by alpha counting of the isotopically enriched oxide, U_3O_8, in a specially designed ionization chamber. A correction for the presence of U^{234} was made on the basis of pulse analysis. The 2.2% error assignment included consideration of counting statistics, geometric factors, pulse analysis, chemical purity, and solution concentration.

Fleming *et al.* also discussed the half-life of U^{238} and concluded that $t_{\frac{1}{2}} = 4.51 \times 10^9$ years is the "best" value. It is generally accepted that this figure is correct to 0.2%.

The decay constants as evaluated by the above workers have been incorporated more recently in a table of isotope ratios *vs.* age, obtained by digital computation and published by Stieff, Stern, Oshiro, and Senftle (**39**). All measurements in the discussion to follow have been based on the ratios in this table, corrected slightly for a different value of the isotopic composition of uranium. For convenience, the critical values are here reproduced:

$$\lambda_{238} = {}^{1.53}_{69} \times 10^{-10}\,\text{yr.}^{-1}$$

$$\lambda_{235} = {}^{9.72}_{16} \times 10^{-10}\,\text{yr.}^{-1}$$

$$U^{238}/U^{235} = 137.8$$

An error of 0.2% has been assigned to the isotopic composition of natural uranium (Boardman and Meservey, **40**).

The only restrictive assumption made in the present evaluation is that the accepted values for λ_{238} and the

ratio U^{238}/U^{235} are "correct", i.e. that they are known to a very high degree of precision. The decay constant of U^{235} is to be indexed against these numbers, and to the extent that they are in error the error assignment for U^{235} will be correspondingly increased.

Fifteen samples have been isotopically analyzed that have yielded reasonably radiogenic lead compositions. Eleven of these are zircon fractions and four are uranothorite fractions. They are an excellent suite for the present purpose for four reasons:

1) They are cogenetic. All specimens were obtained from the two leucogranites of Mt. Rubidoux and there can be no doubt that they originated as radioactive clocks within a very short interval of time compared to their total age.

2) The true age of the system is most likely between 116 and 130 million years, and probably close to 120 million years. The reasons for choosing these figures have been discussed in Chapter 4. The true age lies in the range where the radiogenic Pb^{207}/Pb^{206} ratio is insensitive to small uncertainties in the true age, and moreover the actual uncertainty is such as to introduce not more than 0.5% uncertainty in the decay constant of U^{235} if it were the only factor to be considered.

3) Although the samples are discordant, they are not grossly so. Since the amount of discordance is known within reasonable limits, a qualitative correction can be made for this situation.

4) The samples have a wide range of Pb^{206}/Pb^{204} values; i.e. the proportion of common lead varies from sample to sample. Therefore it is not only possible to examine the individual analyses, but the aggregate can be used to derive a radiogenic Pb^{207}/Pb^{206} ratio independent of the common lead correction assumed.

The first step in evaluation is to consider the individual analyses and the possible sources of error. Data for the zircon samples have been presented in Table 7, and for the uranothorite samples in Table 11. The radiogenic Pb^{207}/Pb^{206} ratios shown in these tables were obtained using two different common lead corrections. For the zircons the correction is the composition of lead in a blank of the borax flux used to put the samples in solution, whereas for the uranothorites it is the composition of lead in the feldspar of the coarse-grained Rubidoux granite. It makes little difference which of these two corrections is used because their own ratios are related in such a way as to minimize the difference.

The total spread in the corrected ratios is 3.7%. This however is a misleading estimate of analytical uncertainty because the sources of error must be taken into account. Sources of error can be conveniently grouped into three broad categories: 1) True analytical errors, 2) errors due to contamination, and 3) natural "errors", or departure of the measured ratio from the expected ratio due to processes in the natural environment of the samples.

Analytical Errors in Mass Spectrometry

Mass spectrometric analyses are affected by several sources of uncertainty, including mass discrimination in the collector, departure of the shunt resistors on the recorder from their nominal values, insufficient ion beam intensity and/or instability, and statistical errors. The mass spectrometer used in this study is equipped with an electron multiplier and a dual-pen strip chart recorder, and thus must be calibrated for discrimination as well as recorder shunts. Discrimination factors have been recently determined for this particular machine by McKinney (**41**). Using isotopes of Rb, Ag, Tl, and U, he found that in the Tl-U mass region the discrimination is slightly different than the theoretical square root of the mass value. During this work he also re-measured the shunt resistors, indexed to the 100 mv shunt. The correction factors based on his results are shown in Table 17. All these corrections, with the exception of the 2 mv. shunt resistor, are less than 1%. A reasonable estimate of the possible error introduced through these corrections is 0.25% or less, which is an uncertainty in the measured ratios and cannot be equated directly to an uncertainty in the radiogenic Pb^{207}/Pb^{206} ratio.

Statistical errors and errors due to ion beam intensity or instability are related. Chow and McKinney (**42**) have determined the overall reproducibility characteristics of the machine used here. An attempt to evaluate statistical

Table 17

MASS SPECTROMETRY CORRECTION FACTORS

I. Corrections for shunt resistors

Shunt (Full Scale in mv)	Correction
2	1.0236
5	1.0078
10	1.0025
20	1.0006
50	1.0004
100	1.0000
200	0.9998
500	1.0002
1000	0.9999

II. Corrections for discrimination

Isotope Ratio	Correction
Pb^{206}/Pb^{204}	1.0050
Pb^{206}/Pb^{207}	0.9975
Pb^{206}/Pb^{208}	0.9950
U^{238}/U^{235}	1.0056

errors for the analyses of this study is shown in Table 18. For each sample, the minimum and maximum intensity of each isotope is shown in millivolts, where the input current is measured across a 2×10^9 ohm resistor. Isotope ratios were measured by scanning once up-mass and once down-mass and averaging the peak heights for each such set. The number of ratios so obtained is shown and the average deviation from the mean is indicated. As a rule of thumb it was considered desirable to obtain at least ten sets of ratios, although this goal was not always attained. Instability did not seem to be a problem except for those samples where the average deviation of the Pb^{206}/Pb^{207} ratio was significantly greater than 0.3%.

The data shown in Table 18 would lead one to assign a conservative uncertainty of 2% to the measured Pb^{206}/Pb^{204} ratio and 0.3% to the measured Pb^{206}/Pb^{207} ratio. The largest analytical uncertainty thus lies in the measured Pb^{206}/Pb^{204} ratio.

It is interesting to see what effect an error of 2% would have on the corrected radiogenic Pb^{207}/Pb^{206} ratio. Clearly it will depend on the proportion of common lead to radiogenic lead. Suppose that the only source of error is in the Pb^{206}/Pb^{204} ratio, and that the magnitude of the error is 2%. Figure 15 shows the percent effect that this would have on the radiogenic lead-lead ratio, as a function of the magnitude of the Pb^{206}/Pb^{204} ratio. This diagram, of course, applies in particular only to the leads that have

Table 18

STATISTICS OF RADIOGENIC LEAD COMPOSITION ANALYSES

Sample No.	Date of Analysis	Pb^{204} Intensity (mv) Min.	Pb^{204} Intensity (mv) Max.	Pb^{206} Intensity (mv) Min.	Pb^{206} Intensity (mv) Max.	Pb^{207} Intensity (mv) Min.	Pb^{207} Intensity (mv) Max.	Pb^{206}/Pb^{204} No. of Ratios	Pb^{206}/Pb^{204} Avg. Dev. from Mean(%)	Pb^{206}/Pb^{207} No. of Ratios	Pb^{206}/Pb^{207} Avg. Dev. from Mean(%)
SCB-36 R200 Zircon	2-26-62	0.070	0.156	33.6	285.0	1.89	9.16	9	1.1	22	0.22
SCB-36 P200 Zircon	1-12-61	1.19	5.55	171.0	1926.0	9.96	500.0	15	0.4	17	0.25
SCB-102 R200 Zircon	4-29-61	0.134	0.176	21.5	63.7	1.92	4.94	13	1.3	14	0.28
SCB-102 P200 Zircon	3-19-61	0.082	0.358	23.6	294.0	1.52	7.14	20	1.9	18	0.86
SCB-101C_3 R200 Zircon	6-29-62	0.068	0.120	30.1	166.4	1.79	2.20	9	1.6	16	0.54
SCB-101C_3 P200 Zircon	6- 6-62	0.032	0.072	24.8	124.0	1.41	4.74	8	6.8	17	0.29
SCB-106 R200 Zircon	11-15-62	0.040	0.048	49.1	57.2	3.05	3.40	10	2.7	9	0.16
SCB-106 P200 Zircon	1- 5-63	0.93*	1.25*	27.2	31.6	1.64	1.91	10	1.0	18	0.31
SCB-108 R200 Zircon	4- 3-63	0.164	0.260	93.6	462.5	5.32	26.3	8	0.8	17	0.18
SCB-108 P200 Zircon	4-12-63	0.074	0.174	96.4	370.0	5.39	7.68	13	1.2	10	0.27
SCB-107 P200 Zircon	4-25-63	0.094	0.166	55.1	312.5	3.08	8.50	15	1.4	15	0.19
SCB-36 R200 Urano-Thorite composite	11-18-61	0.232	0.268	25.1	445.5	2.84	21.1	4	0.4	16	0.35
SCB-36 P200 Urano-Thorite composite	11-30-61	0.124	0.138	32.2	144.2	2.00	2.16	6	1.3	14	0.22
SCB-36 R200 Urano-Thorite A	8-17-62	0.076	0.100	20.2	64.7	1.43	2.30	10	1.6	21	0.21
SCB-36 R200 Urano-Thorite B	8-23-62	0.196	0.234	30.5	120.0	2.42	8.96	10	0.8	15	0.25

* Measured across 10" ohm input resistor

Figure 15. Effect of 2% Error in Measured Pb^{206}/Pb^{204} for Leads of this Study

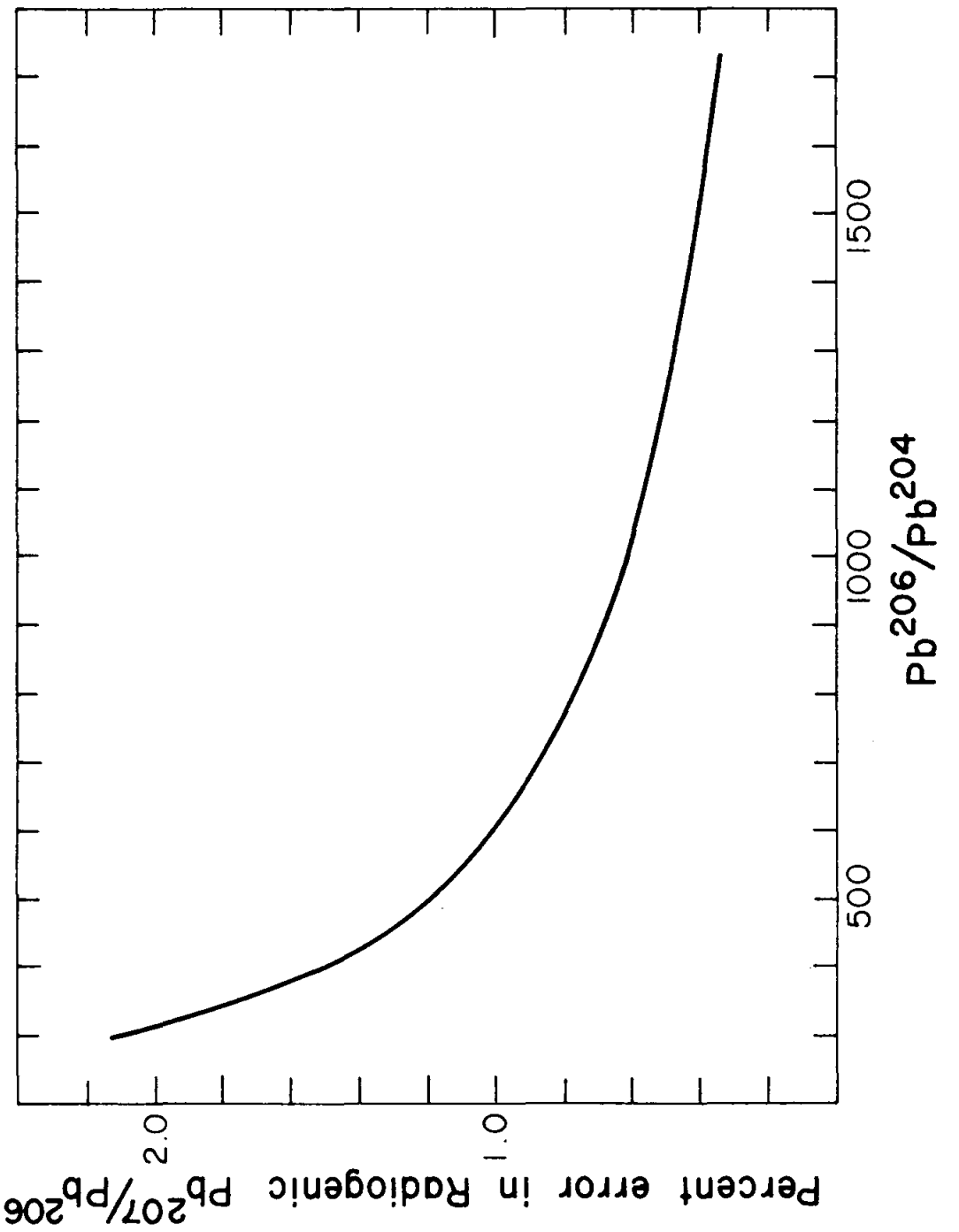

been analyzed in the present study, although the general relationship holds for leads of any age. It is a striking fact that the effect becomes less than 1% when the Pb^{206}/Pb^{204} ratio is 600 or larger. It can therefore be concluded that the large possible error in measurement of the Pb^{206}/Pb^{204} ratio introduces an uncertainty in the radiogenic lead-lead ratio which, for samples sufficiently radiogenic, is not significantly greater than the uncertainty introduced by possible errors in measurement of the Pb^{206}/Pb^{207} ratio.

Considering the possible statistical errors alone, it seems reasonable to assign a maximum uncertainty of 1% to the corrected radiogenic lead-lead ratio for an individual sample whose measured 206/204 ratio is greater than 600. The more radiogenic the sample is, the lower is the value of the uncertainty, until a limit of about 0.3% is reached. The average value of the corrected ratio for the eleven zircon samples is 0.04857. It can be seen from Table 18 that only two analyses differ from this figure by significantly more than 1%, and one of these has a measured 206/204 ratio considerably less than 600. However, this is an uncritical evaluation of the data because it neglects other sources of error. With the exception of the most "common" sample, the zircon analyses fall into two discrete groups. One group, containing 6 members, have corrected lead-lead ratios that range from 0.04825 to 0.04850. The other group, containing 4 members, have corrected ratios that are higher than 0.04880

and range up to 0.04937. It can be interpreted that the latter group are slightly contaminated with anomalous lead. This possibility is discussed below.

Contamination

Included under the heading of contamination is the common lead correction that is required for all samples. Other possible sources of contamination in the laboratory can occur in the form of minute amounts of radiogenic leads of a different age or of isotopically enriched spike leads. Both latter sources of contamination are especially serious in the analysis of "young" leads in which the amount of radiogenic Pb^{207} is quite small relative to the amount of Pb^{206}. It is an important observation that all possible sources of anomalous lead of this type in the C.I.T. laboratory have significantly higher 207/206 ratios than the radiogenic leads analyzed in this study.

Sample weights are listed in the tables of analytical data. Usually about two-thirds of the total weight was aliquoted for the determination of lead composition. In the case of zircons, this corresponded to 5-6 μg. of lead and in the case of uranothorites was 2-3 times higher, ranging up to 15 μg. A zircon sample having a Pb^{206}/Pb^{204} ratio of 1200 would contain about 5%, or 0.25-0.30 μg, of common lead. Some of this lead undoubtedly comes from the sample itself, some comes from the reagents, and some is probably random in origin.

The composition of original lead in the sample is known by means of analysis of feldspar lead in the rock (Chapter 5) and the compositions of the major sources of reagent lead have been measured several times by Dr. Silver and co-workers (Appendix A). The composition of random common lead is of course not known, but cannot depart widely from the other compositions, and moreover is probably only a small percentage of the total common lead observed.

Although the feldspar lead is somewhat more radiogenic than the reagent lead, it happens that both Pb^{206} and Pb^{207} are enriched in roughly the same proportion as exists for the radiogenic leads of the samples, and consequently it makes little difference which common lead is used for the correction. If the choice of the common lead correction was significantly in error, one would expect to see a more-or-less consistent shift in the radiogenic lead-lead ratio with increasing content of common lead in the sample. Inasmuch as this is not observed, it is concluded that errors introduced by the particular choice of common lead in this study are negligible.

A much more serious situation arises if the samples can be contaminated with leads that have widely diverse 207/206 ratios. All the samples of this study have been analyzed in a single laboratory. Most of the lead work in the laboratory involves radiogenic samples having considerably older ages and therefore higher lead-lead ratios than

the Rubidoux samples. In addition, all spiking is done with leads having relatively high 207/206 ratios. It is not understood completely how contamination from these leads can occur, although it is believed to be due in part to memory in the glassware. Until the latter part of this work no distinction was made between equipment used for the older samples and for the younger samples, and in particular no distinction was made between glassware used for extraction of spiked aliquots and glassware used for extraction of lead composition aliquots. The glassware was therefore in contact with leads of widely variable composition. It was believed that a two-stage hot nitric acid bath was sufficient to remove all memory of previous samples from the glassware. However, recent checks on procedure blanks have shown random occurrences of anomalous isotopic compositions, which are generally weighted toward the composition of the Pb^{208} spike used for the majority of concentration determinations.

It seems likely that the anomalous compositions are mixture of radiogenic sample leads and spike leads, in addition to common lead. From the standpoint of the present evaluation the worst possible case arises from contamination by Pb^{207} spike (see Appendix A). However, this spike is rarely used. The next most serious contamination arises from the Pb^{208} spike, which has a 206/207 ratio of about 0.43. It would require an extremely small amount of this lead to measurably affect the lead-lead ratio of the samples in this study. To the extent that the anomalous compositions

are mixtures of other leads in addition to the spike lead, it would require a greater amount of contamination to correspondingly affect the radiogenic lead-lead ratio.

As was pointed out above, four zircon analyses have higher lead-lead ratios than the others. One uranothorite analysis, SCB-36 R200 Uranothorite B, has a similarly high lead-lead ratio. It is believed that these five samples are slightly contaminated with an anomalous lead. The uranothorite sample is somewhat open to question because of its low Pb^{206}/Pb^{204} ratio. However, it serves to illustrate a limiting case. About 15 μg of lead were obtained from this sample for the determination of its isotopic composition. If the average radiogenic lead-lead ratio of the three other uranothorites is assumed to be the correct ratio, an order of magnitude calculation shows that 0.1-0.2 μg of Pb^{208} spike lead are required to produce the observed ratio for this sample.

Contamination from a characteristic lead such as the Pb^{208} spike might be expected to show an effect on the observed 206/208 ratio of the sample. However, the individual samples have sufficiently variable values of this ratio that the possible influence of a small amount of contamination cannot be detected.

The suggestion of Pb^{208} spike contamination conflicts with the data of Chapter 5, which indicate the occurrence of contamination by a 206-rich lead. All measurements of common

leads were completed prior to the time that the anomalous ratios appeared in the radiogenic leads. It may be that laboratory conditions changed in some unknown fashion. The radiogenic leads, of course, are less sensitive to contamination by other radiogenic leads than they are to spike leads.

Natural Causes of Deviation

The observed radiogenic Pb^{207}/Pb^{206} ratio of uranium-lead system which has been disturbed during its lifetime will be in general somewhat different than the ratio for the true age of the system. The extent of the deviation depends on the mechanism of the disturbance and the time it took place, if it was episodic. Data from older systems than the Mt. Rubidoux granites indicate that disturbance mechanisms usually operate in zircons and uranothorites in such a way as to lower the 207/206 ratio (Silver and Deutsch, 26).

Both the zircons and the uranothorites of this study have been found to be disturbed. There is thus an uncertainty in estimating what the actual 207/206 ratio of these samples should be, in contrast to what it would be if the samples were undisturbed. The magnitude of the uncertainty may be illustrated by postulating that the disturbance consisted of an episodic loss of lead. If the episodic loss took place at the present time there would be no effect on the lead-lead ratios. On the other hand, if it took place, say, 90 million years ago, the individual samples would have

lead-lead ratios corresponding to apparent ages distributed between about 90 million years and the true age of the rock.

No data are available to indicate what this effect is in the case of the Rubidoux samples. The amount of lead generated in the zircons 90 million years ago, and the amount of radiation damage accumulated at that time, would have been relatively small. One can argue qualitatively that the susceptibility to an episodic event would likewise be small. If so, the time of disturbance would likely be considerably younger than 90 million years. It is also possible that the systems have been disturbed by continuous diffusion loss of lead. In either case, the effect on the lead-lead ratio is much smaller than for an older episodic disturbance. It is suggested that the average lead-lead ratio for the zircon samples may have been reduced below the value corresponding to the true age of the rocks (assumed to be 120 million years) by an amount equivalent to perhaps a 10 million year reduction in apparent age. Since the uranothorites are, on the average, slightly more disturbed than the zircons, their average lead-lead ratio may have been reduced somewhat more; corresponding to perhaps a 15 million year reduction in apparent age.

Synthesis of Data

The conclusions of the above paragraphs are summarized below:

1) Analytical errors from machine corrections and

statistical fluctuations may introduce a maximum uncertainty of 1% in the radiogenic Pb^{207}/Pb^{206} ratio of a single sample, if the Pb^{206}/Pb^{204} ratio is 600 or greater. The largest source of error is in the measurement of the 206/204 ratio. Therefore, as the amount of common lead in the sample is reduced, the uncertainty in the corrected 207/206 ratio is reduced.

2) The appropriate common lead correction is well enough known in this study that it introduces a negligible error.

3) Frequent checks of laboratory contamination, and the availability of a large number of sample analyses, have made it possible to identify samples which may be contaminated with leads of anomalous composition.

4) The true age of the samples is believed to be known to within a 15 million year interval at 120 million years. The samples are known to be isotopically disturbed. Because of this the radiogenic lead-lead ratio of the samples may be 0.4-0.6% less than the value corresponding to the true age.

The analytical results may be treated by plotting the measured Pb^{207}/Pb^{204} ratio against the measured Pb^{206}/Pb^{204} ratio. In doing so, it is assumed that the samples have the same radiogenic lead-lead ratio and that the common lead correction is the same for all samples. A straight line of best fit through the data points will then have a slope corresponding to the radiogenic Pb^{207}/Pb^{206} ratio of

the samples.

This procedure has been done separately for the zircon samples in Figure 16 and for the uranothorite samples in Figure 17. The lines shown have been fitted by least quares analysis and as indicated have the slopes 0.04849 for the zircons and 0.04761 for the uranothorites.

Figure 16 shows also that the four zircon samples suspected of being contaminated depart slightly but consistently from the rest of data, in the direction of apparent enrichment in Pb^{207}. It is believed that there is sufficient justification for removing them from consideration. A line of best fit through the remaining seven zircon values has a slope of 0.04841. It is of interest to consider a "worst possible case" for the error in slope of this line. If the most radiogenic sample contained a 2% error in the measured 206/204 ratio, and the least radiogenic sample likewise contained a 2% error in this ratio, but in the opposite direction, the slope of the line as determined by these points alone would change by only about 1%. Since the line is actually determined by several points the uncertainty in its slope must be less than 1%.

The line drawn through the uranothorite values is biased in part by inclusion of the sample which is not only the least radiogenic but is also possibly contaminated. If this sample is left out of consideration the slope of the line is increased to 0.04792, or somewhat over 1% less than the value for the best zircon data. However, the statistics

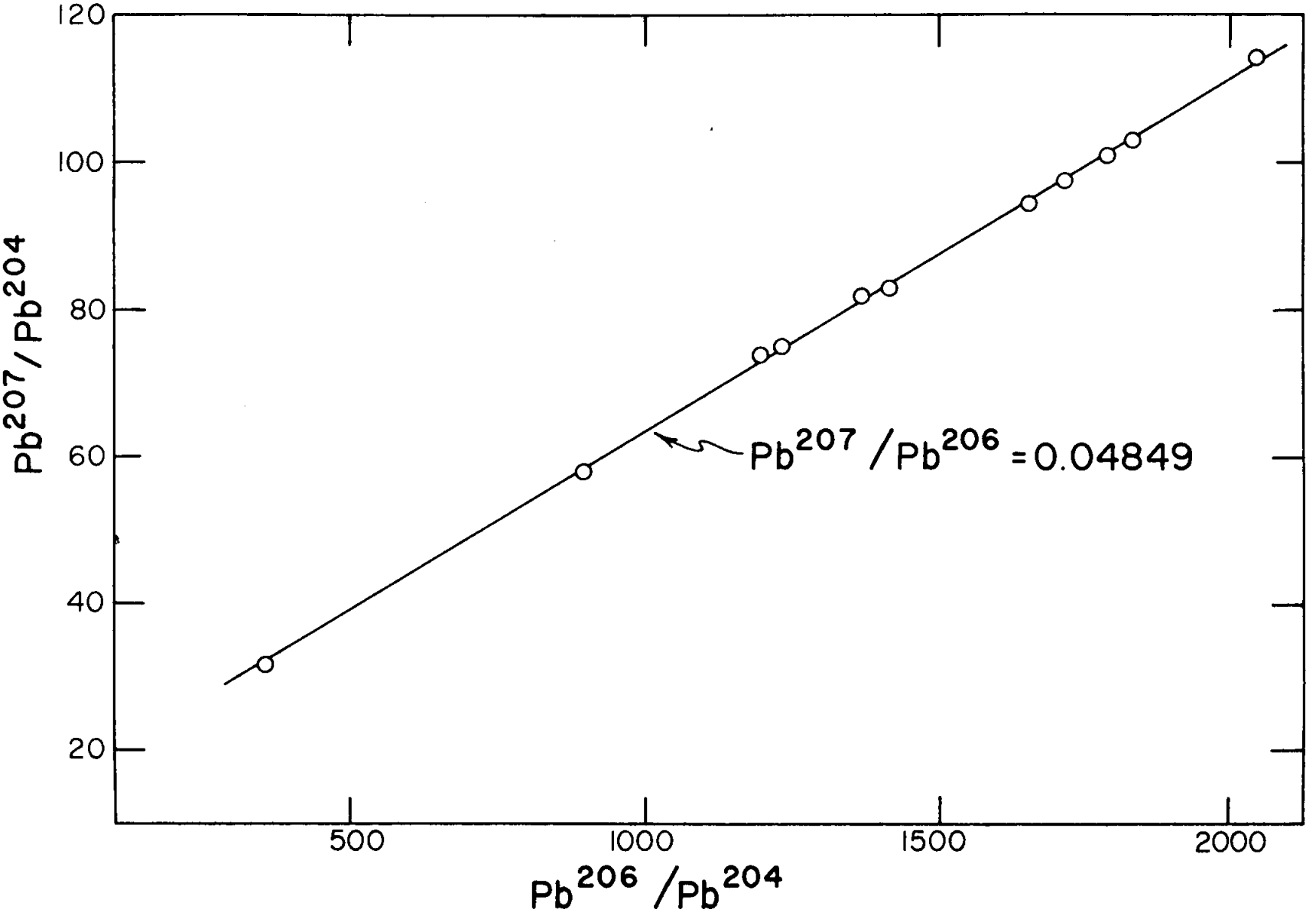

Figure 16. Zircon Analyses, Observed Lead Isotopic Compositions

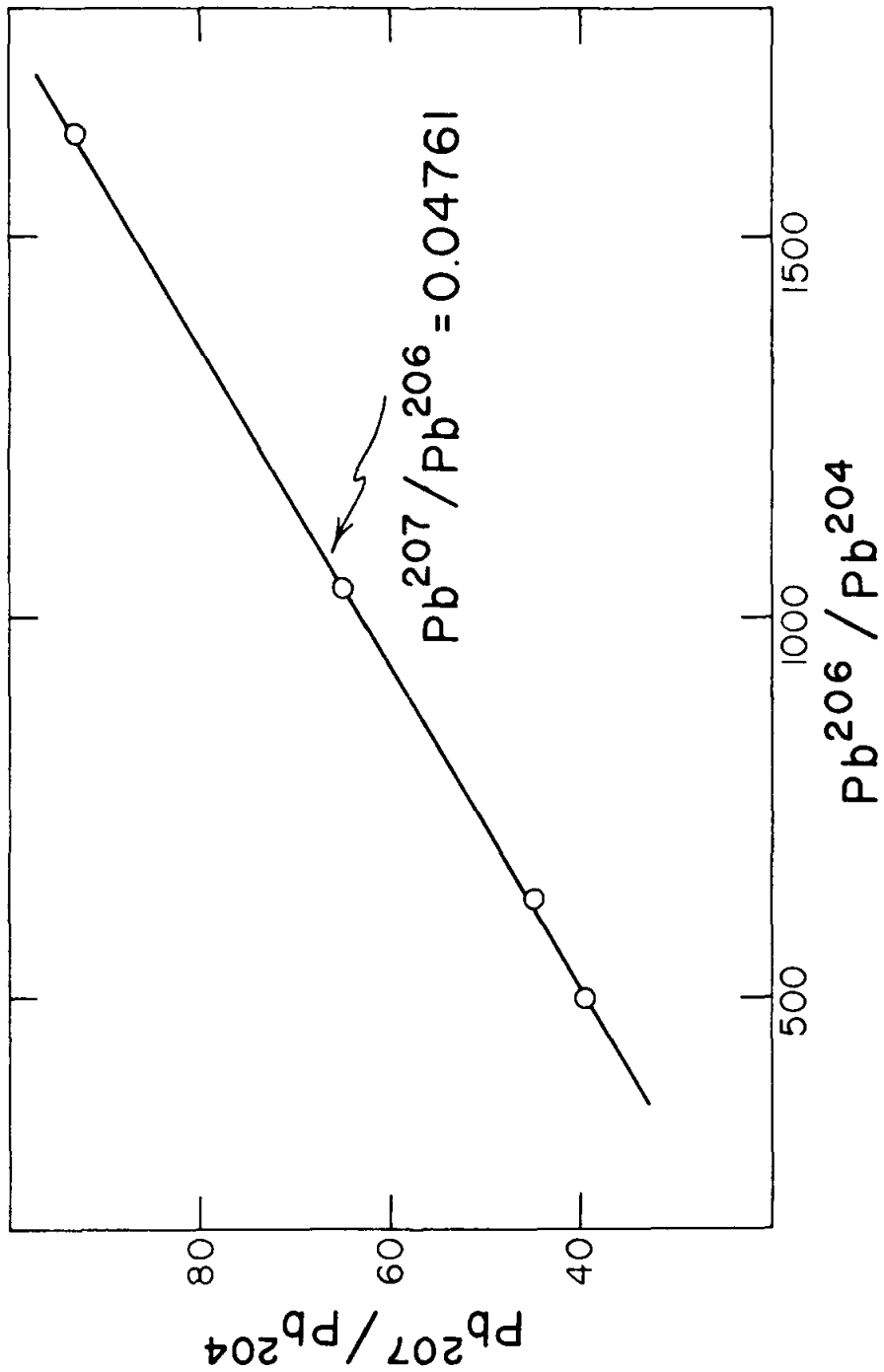

Figure 17. Uranothorite Analyses, Observed Lead Isotopic Compositions

are poorer in the case of the uranothorites.

The complete body of data is thus considered to consist of three subsets. The first of these is the group of four zircons and one uranothorite which are probably contaminated with anomalous lead. The second is the group of six zircons having a small net uncertainty in the radiogenic lead-lead ratio. The third consists of the three uncontaminated uranothorite samples, which have a smaller mean radiogenic ratio than the best zircons, but have a larger net uncertainty. If the presently accepted decay constant of U^{235} is applied to these data, the results are as follows:

Sample	Radiogenic Pb^{207}/Pb^{206}	Apparent Age (m.y.)
Zircons (7)	0.0484 ± 0.0002	128±10
Uranothorites (3)	0.0479 ± 0.0004	103±20

The apparent ages are within the limits of uncertainty arising from the uncertainty in the true age and from the uncertainty in the effect of later isotopic disturbance of the systems. Inasmuch as the uranothorite samples are more strongly disturbed than the zircons, the downward shift in apparent age is reasonable, although the magnitude of the shift seems unduly large. However, these effects are within the limits of error.

It can be concluded that the presently accepted decay constant of U^{235}, relative to U^{238}, is correct to within the precision of the data. Accepting the zircon

group as statistically most reliable, the uncertainty is within 1%. The half-life of U^{235} is therefore proposed to be:

$$t_{\frac{1}{2}} = (7.13 \pm 0.07) \times 10^{8} \text{ years}$$

Addendum: More recent work on the isotopic composition of natural uranium by Greene, Kienberger and Meservey (**43**) has given a value of 137.96 for the ratio U^{238}/U^{235}, with an uncertainty slightly less than 0.1%. Application of this figure to the results of the present work would increase the apparent ages in the above table (previous page) by about 4 million years. The zircons therefore would have a composite lead-lead apparent age of 132 ± 10 m.y., which begins to suggest that the accepted half-life of U^{235} may be slightly too large. Most geochronological work, however, has been based on the earlier value of 137.8 for the composition of natural uranium. Thus it appears that in earlier investigations a small possible error in the assumed half-life has been compensated by a small error in the assumed isotopic composition of uranium.

Chapter 7

INTERMEDIATE DAUGHTER LOSS

The purpose of this chapter is to investigate, by means of model calculations, the possibility that loss of intermediate daughters from the uranium decay chains may be a mechanism for producing patterns of discordance similar to those which have been observed for natural uranium-lead systems. In particular, it is desired to determine what limitations must be placed on such loss in order that it result in what is here called the zircon type of discordance.

It is convenient to refer the analytical data from discordant systems to the concordia diagram of Wetherill (33). Wetherill devised this graphical method of displaying the results in order to explain the discordance pattern of various pitchblende and uraninite specimens. However, it was not certain that all the specimens he plotted were of exactly the same age. The diagram was first used for samples known to be cogenetic by Silver and Deutsch (26), who analyzed several zircon fractions from the Johnny Lyon granodiorite of Arizona. The term "zircon type of discordance" is thus used because the first truly cogenetic samples to display this pattern were zircons.

However, the term is not meant to imply that there is a unique explanation for the observed patterns. There are, in fact, at least three possible explanations, and it is only in exceptional cases that uranium-lead isotopic data alone

will permit a choice to be made among these explanations. What is implied is that the analytical data, for cogenetic systems, have a characteristic pattern when plotted on the concordia diagram.

The zircon type of discordance has the fundamental characteristic that the analytical results form, within certain limits, a linear array on the concordia diagram. A straight line drawn through this array will intersect the concordia curve at two places. The upper intersection, according to currently conceived models, corresponds to the "true" age of the system. The lower intersection is of uncertain significance and depends on the model chosen to explain the results.

The lower intersection has so far never been observed to fall below the origin. Russell and Ahrens (**44**) presented data which suggested that the lower intersection might increase with increasing age of the system. More recent results do not substantiate this. For example, zircon suites from the Johnny Lyon granodiorite mentioned above yielded an upper intersection corresponding to 1660 million years and a lower intersection of about 90 million years, whereas zircons from the Marble Mountains, California (Silver and McKinney, **45**), yielded an upper intersection of 1450 million years and a lower intersection of 180 million years.

The zircon type of discordance can be interpreted in gross terms as an apparent loss of the stable daughter (lead). Wetherill (**27**) first discussed the possibility that an

episodic loss of lead, at a time corresponding to the lower intersection, could produce the observed pattern. Nicolaysen (28), Tilton (29), and Wasserburg (30) have discussed continuous loss of lead by diffusion as an alternative explanation. Wasserburg's treatment is very general and shows that a time-dependent diffusion coefficient can always be found to fit a given set of data. However, the choice of any particular time dependence requires physical justification.

A third possibility, which has received little treatment, is loss of intermediate daughters. It has generally been assumed that such loss would probably occur only for Rn^{222} from the U^{238} chain (Holmes, 46; Kulp, Bate and Broecker, 31). If this were the case, a suite of cogenetic samples with varying degrees of disturbance would form a linear array parallel to the Pb^{206}/U^{238} axis of the concordia diagram. A pattern such as this has never been observed for a natural system.

However, if it is assumed that intermediate daughters can be lost from both chains simultaneously, then it is possible to derive a wider variety of relationships, and if the losses from various samples of a cogenetic suite are related in a simple way, a linear pattern of discordance can be generated. The following development is intended to demonstrate this. No assumptions are made here about the daughter species that are lost, and in particular, no assumption is made about the process whereby loss may occur because it

appears from available data that it may be highly complicated in detail. The possibility of generating linear relationships was mentioned by Russell and Ahrens (44) and Aldrich and Wetherill (47), but they did not elaborate on the matter.

The growth of lead (e.g. Pb^{206}) from the decay of its parent uranium isotope is given by the equation

$$\frac{dN_{206}}{dt} = N^{o}_{238} \lambda_{238} e^{-\lambda_{238}t} \qquad (1)$$

where N^{206} is the number of lead atoms at time t, N^{o}_{238} is the initial number of U^{238} atoms, and λ is the decay constant. Since secular equilibrium is practically established within one million years of the time the decay system becomes closed, transient effects can be neglected. Suppose that some intermediate daughter is lost continuously according to some function of time. The growth of Pb^{206} therefore occurs at a smaller rate than given by equation (1). This can be represented by rewriting the equation

$$\frac{dN_{206}}{dt} = N^{o}_{238} \lambda_{238} h(t) e^{-\lambda_{238}t} \qquad (2)$$

where h(t) is such that at any instant of time it has a magnitude between 0 and 1. Suppose further that h(t) can be represented in the form

$$h(t) = \rho\, g(t) \tag{3}$$

It is assumed that g(t) is the same function for all samples of a suite, but that ρ, a constant, is a characteristic of each particular sample. Equation (2) then becomes

$$\frac{dN_{206}}{dt} = N^{o}_{238}\ \lambda_{238}\ \rho\, g(t) e^{-\lambda_{238} t} \tag{4}$$

The integral of this equation has the form

$$N_{206} = \rho\, N^{o}_{238}\, G(\lambda_{238}, t) \tag{5}$$

or equivalently

$$Y = \frac{N_{206}}{N_{238}} = \rho\, e^{\lambda_{238} t}\, G(\lambda_{238}, t) \tag{6}$$

It is now assumed that for whatever intermediate daughter element is lost from the U^{238} chain, an equivalent intermediate daughter is lost from the U^{235} chain. This is a permissible assumption because most of the intermediate daughter elements of significant abundance occur in both chains. Granting the assumption, it seems reasonable that the time dependence for loss would be the same for both chains, although the coefficients may be different. Thus, corresponding to equation (6) we have

$$X = \frac{N_{207}}{N_{235}} = \omega\, e^{\lambda_{235} t}\, G(\lambda_{235}, t) \tag{7}$$

It is next assumed that though ρ and ω may be characteristic of the individual sample, their ratio is independent of the sample; i.e. $\omega/\rho = k$. From the foregoing equations it follows immediately that any two samples from a cogenetic suite of age T_o will have ratios X, Y and X', Y' such that

$$X-X' = k(\rho-\rho')e^{\lambda_{235}T_o} G(\lambda_{235}, T_o) \qquad (8)$$

$$Y-Y' = (\rho-\rho')e^{\lambda_{238}T_o} G(\lambda_{238}, T_o) \qquad (9)$$

Hence

$$Y-Y' = \frac{e^{\lambda_{238}T_o} G(\lambda_{238}, T_o)}{ke^{\lambda_{235}T_o} G(\lambda_{235}, T_o)} (X-X') \qquad (10)$$

Equation (10) yields a linear relationship on the concordia diagram, as was to be shown.

Before considering specific forms of intermediate daughter loss it is well to examine the validity of the assumptions involved in setting up the model. The calculations above do not specify the manner in which the material is lost. It might be by diffusion in the crystal lattice, by diffusion along grain boundaries or "microfractures", or by recoil. Whatever the particular mechanism may be, it can have a strong influence on the relative values of ρ and ω, depending on the relative half-lives of the daughter isotopes

in each decay chain. That is, if the rate constant of the loss mechanism is much longer than the half-life of one of the daughter isotopes, but not the other, then the latter may be lost in significant amounts whereas the former will hardly be lost at all.

It has long been recognized that radioactive minerals lose a fraction of their emanation gases. Because this phenomenon has been studied to some extent, it will be used as an example. Analogous arguments could be presented for any intermediate daughters which occur in both chains provided one can find a physical explanation for their loss. It happens that for those daughters of significance, the half-life of the isotope occurring in the U^{238} chain is almost always considerably longer than the half-life of the corresponding isotope in the U^{235} chain. Therefore the rate problem in particular is analogous to emanation loss for the majority of cases.

Emanation loss was studied by Giletti and Kulp (**48**), who assumed that significant loss occurs only for radon (Rn^{222}) and employed an experimental procedure that in fact discriminated against actinon (Rn^{219}) and thoron (Rn^{220}) by permitting these isotopes of very short half-life to decay away before analysis. Nevertheless they found measurable emanation losses from pitchblende, uraninite, samarskite, and zircon. At about the same time Russian workers were investigating the isotopic character of emanation loss. According to Cherdyntsev (**49**), it was found

that the percentage losses of radon and actinon were about equal for samples of primary minerals. On the other hand, he quotes Starik et al. (50) who found that for uraninite the percentage loss of actinon was lower than that of radon. The loss of thoron appeared to be unrelated to the other isotopes, which is not surprising since the distribution of thorium in the mineral may be unrelated to the distribution of uranium.

Contrary to the assumption of Giletti and Kulp, it appears that significant loss of emanation from both decay chains can occur. As Cherdyntsev points out, this strongly supports the idea that loss occurs along microfractures of some sort rather than by diffusion through the lattice, which would have a rate constant too long to permit loss of actinon. Recoil energetics presumably play a part in the process. The recoil energies involved in the U^{238} chain are not greatly different than in the U^{235} chain. For the case of emanation, actinon has a slightly greater recoil energy than radon and therefore may be more likely to enter the microfractures, which might compensate for its shorter half-life.

The magnitude of emanation loss, according to the various studies that have been made, is normally quite low. Typical values range from a few tenths of a percent to a few percent. If such values represent the average loss for the lifetime of the mineral, one would not expect intermediate daughter loss to be a significant cause of discordance.

On the other hand, there is no information presently available to indicate whether or not emanation loss has remained low throughout the history of the mineral. Moreover, samples have been found which are only slightly discordant, and in these cases it is tempting to propose intermediate daughter loss as the cause of discordance.

The information available suggests that the coefficients ρ and ω should be assigned small values, at least for minerals such as zircon. There is presently no way of justifying the assumption that $g(t)$ is the same for both decay chains. If the mechanism of loss is the same throughout the life of the mineral, the assumption seems plausible. One could imagine, however, that loss is governed initially by, say, diffusion in the lattice, and that as radiation damage of the structure increases the loss takes place by diffusion through microfractures. In this case the isotope of shorter half-life would not be lost initially. Nevertheless, it is believed that the assumption proposed is reasonable within the limits of present knowledge.

In a similar way, current information indicates that the value of the constant k is 1 or less. But it is not known whether k is truly the same for all samples of a suite. Inasmuch as the term "sample suite" means here a set of samples of a single mineral species that are cogenetic and have shared identical external environments, any deviation of k from its average value would be expected to be small. However, the assumption must remain unjustified for the present.

Although it is not possible to verify the assumptions, it is worthwhile to investigate some specific forms for intermediate daughter loss. The intent here is to show that a variety of linear relationships can be generated by such loss, and thereby to show that intermediate daughter loss should be considered as a possible explanation for discordance in some instances.

Three situations will be considered which demonstrate some of the limiting characteristics of intermediate daughter loss according to the model framework developed above. They are: 1) constant rate of loss, 2) rate of loss as a function of the concentration, and 3) rate of loss as a function of radiation damage. For convenience it will be assumed that k has the value 1 in each case.

1. Constant rate of loss. In this case, equation (3) has the simple form

$$h(t) = \rho \tag{11}$$

The necessary integrations are easily performed, and equation (10) becomes

$$Y-Y' = \frac{e^{\lambda_{238}T_o} - 1}{e^{\lambda_{235}T_o} - 1}(X-X') \tag{12}$$

This is the equation of a straight line from the origin to the point on concordia corresponding to the true age of the sample, T_o. In other words, constant rate of loss of intermediate daughters has the same effect on the Pb/U ratios as

does modern episodic loss of lead.

A constant rate of loss is plausible for young systems and for systems which are not highly radioactive. Since the amount of any intermediate daughter is proportional to the uranium concentration, its own concentration changes slowly with time and always decreases. The decrease in concentration may be compensated to some extent by increasing radiation damage. This model could provide an explanation for cases where the data trend toward the origin and no modern disturbance can be discovered.

Equation (12) was developed assuming that $k = 1$. If, however, k is less than 1, the result is to favor loss in the U^{238} chain; hence the data will trend to a point below the origin. Trends of this latter form are unique to intermediate daughter loss models, and if such a pattern is ever observed in natural systems it will be a strong indication that intermediate daughter loss has occurred.

2. Rate of loss as a function of the concentration. In this case the possible effect of radiation damage is neglected. Taking emanation loss as an example, the assumption is made that the loss is directly proportional to the total concentration of the daughter element in the crystal. Since actinon is much less abundant than radon, the total concentration will be approximately equal to the radon concentration and will decrease with time according to the decay of U^{238}. Equation (3) thus becomes

$$h(t) = 1 - \rho e^{-\lambda_{238} t} \qquad (13)$$

Again the integrations are straightforward, and equation (10) takes the form

$$Y-Y' = \frac{(\lambda_{235}+\lambda_{238})(e^{\lambda_{238}T_o} - e^{-\lambda_{238}T_o})}{2\lambda_{235}(e^{\lambda_{235}T_o} - e^{-\lambda_{238}T_o})}(X-X') \qquad (14)$$

The end points of this line can be determined by assigning the limiting values 0 and 1 to ρ. If $\rho = 0$, the sample is undisturbed and therefore plots on concordia at T_o. If $\rho = 1$, the sample has the maximum possible disturbance. Calculations have been made for a number of true ages and are shown in Figure 18.

Inasmuch as this model is set up to favor early loss, actinon would be lost in proportionately greater amounts than radon during the lifetime of the mineral. Therefore the lines have an apparent lower intersection with concordia above the origin. However, complete loss is not permitted and thus the lower extension of the line is forbidden.

It can be seen from Figure 18 that the apparent lower intersection increases with increasing age of the sample. Instead of the loss decreasing according to equation (13) one could, ad hoc, assume some parameter α instead of λ_{238} to describe the decrease in loss and thereby fit almost any set of data. However, it would be difficult to justify this.

Figure 18

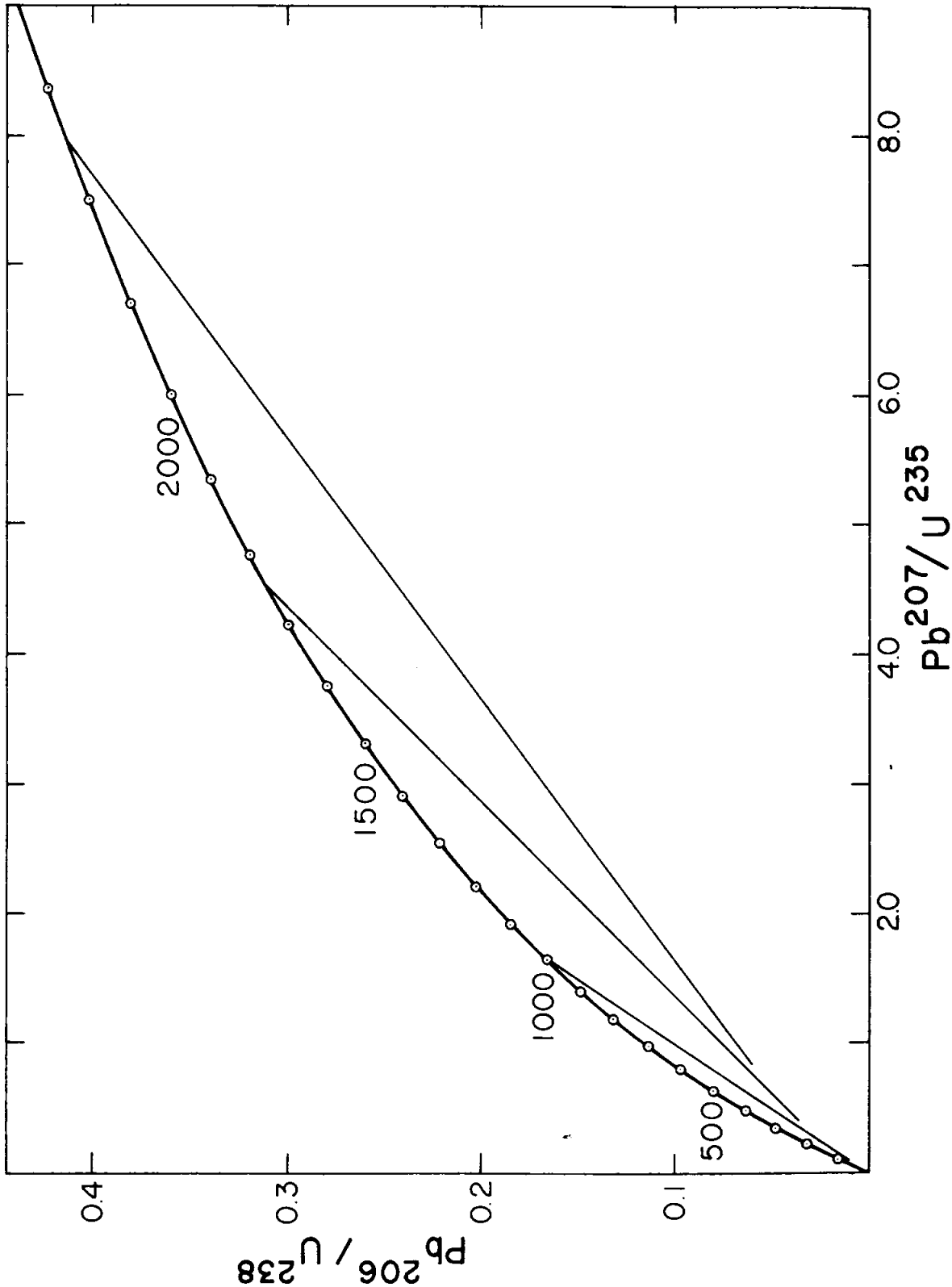

If radiation damage increases the rate of loss, it would offset the results indicated by this model. A similar effect would occur if k were less than 1. The third model illustrates the possible effect of radiation damage alone.

3. Rate of loss as a function of radiation damage. Radiation damage is a poorly understood phenomenon and thus it is difficult to construct a model to fit it. According to the data of Holland and Gottfried (**32**) damage seems to increase until a saturation value is reached, at which point self-annealing or some similar process sets in. Following this idea, it is assumed that the rate of loss of intermediate daughters increases with time and levels off at a saturation value. Since it is not known what governs the rate of increase of damage, a second parameter β will be introduced to accomodate this uncertainty. The function h(t) according to this model will have the form

$$h(t) = \rho + (1-\rho)e^{-\beta t} \qquad (15)$$

In this form constant rate of loss can be seen to be a limiting case, where β has an infinitely large value and thus radiation damage reaches its saturation level infinitely rapidly. The slope of the line on the concordia diagram for a given value of β will be

$$Y-Y' = \frac{(e^{\lambda_{238}T_o}-1) - \frac{\lambda_{238}}{\lambda_{238}+\beta}(e^{\lambda_{238}T_o} - e^{-\beta T_o})}{(e^{\lambda_{235}T_o}-1) - \frac{\lambda_{235}}{\lambda_{235}+\beta}(e^{\lambda_{235}T_o} - e^{-\beta T_o})}(X-X') \qquad (16)$$

Again, the end points of the line can be determined by assigning the limiting values 0 and 1 to ρ. If $\rho = 1$, no loss occurs. If $\rho = 0$, the maximum loss occurs. Figure 19 shows the patterns for three different values of β and a given value of T_o.

This model favors late loss of intermediate daughters and therefore results in greater proportional loss from the U^{238} chain. It provides a limiting contrast to the type of loss illustrated by the second example. Again, if k is less than 1, the effect is to give the lines a steeper slope than shown in Fig. 19.

As was discussed in an earlier paragraph, loss due to radiation damage alone may possibly result in an even stronger bias toward the U^{238} chain than this model suggests. If early loss is governed by slow diffusion, radon (for example) would be lost in some small amount whereas actinon would decay before leaving the lattice. The effect could be mathematically formulated by assigning a time dependence to k.

Summary

It has been shown that intermediate daughter loss can result in linear patterns of discordance on the concordia diagram. The validity of the basic assumptions cannot be established at present. Three limiting cases have been discussed which illustrate likely forms that intermediate daughter loss might take.

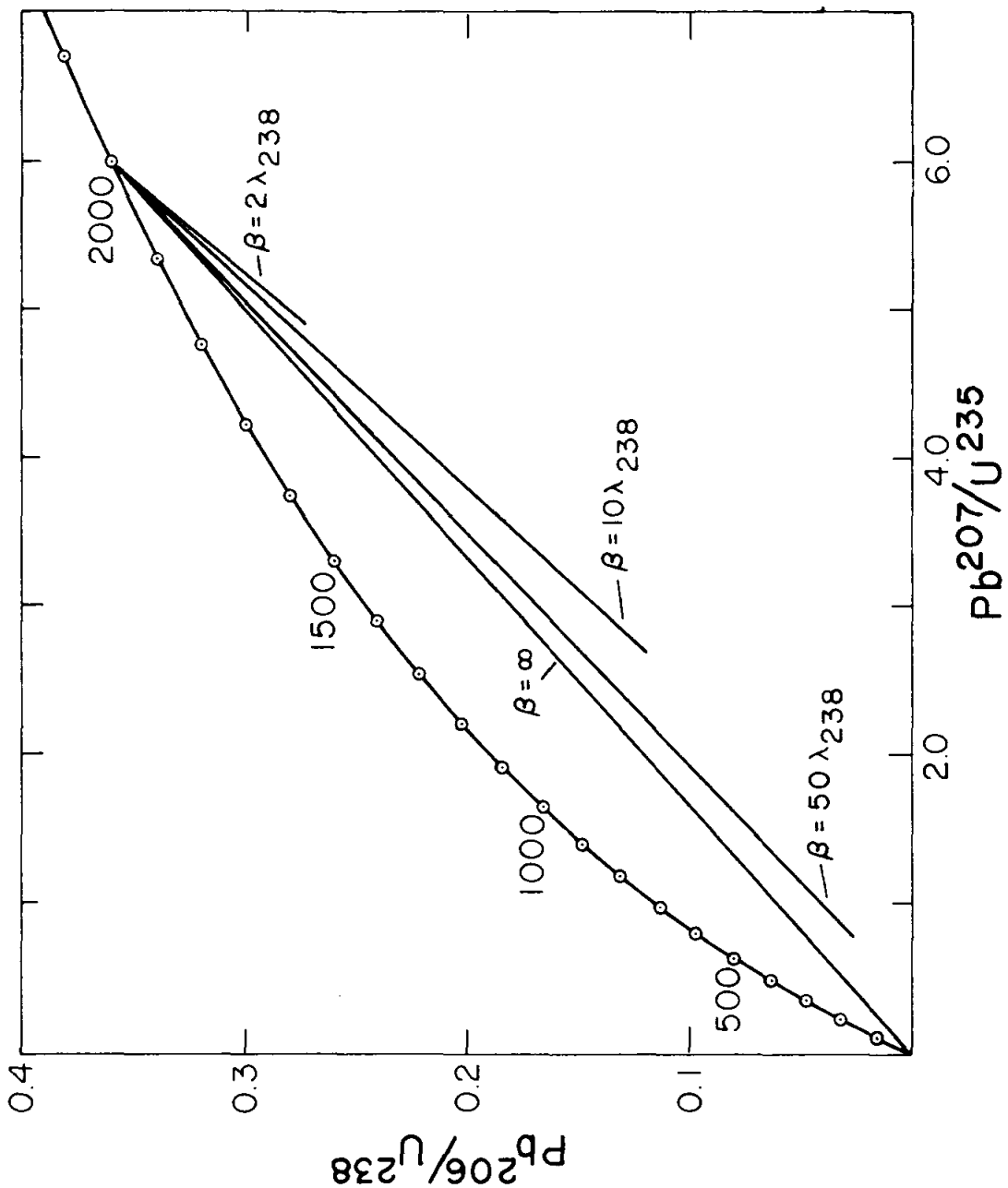
0.4
0.3
0.2
0.1
Pb^{206}/U^{238}
2000
1500
1000
500
$\beta = 2\lambda_{238}$
$\beta = 10\lambda_{238}$
$\beta = \infty$
$\beta = 50\lambda_{238}$
2.0
4.0
6.0
Pb^{207}/U^{235}

Figure 19

It appears from the examples that such loss would probably result in patterns unlike those which have been observed. However, present knowledge of the mechanisms of loss is inadequate to specify with certainty which form of loss predominates in natural materials.

Much of the impetus for investigating this problem has been derived from knowledge of unpublished data on many zircon suites accumulated by L. T. Silver (personal communication). These data suggest that there is no simple and all-inclusive correlation between either the degree of disturbance or the apparent lower intersection and the geologic age or history of the samples. It therefore seems possible that the mechanism of discordance may vary from locality to locality. Indeed, it may be that in any given locality, more than one mechanism has been responsible for the observed discordance.

If a linear pattern is discovered that trends below the origin, intermediate daughter loss is a likely interpretation. In addition, it is felt that intermediate daughter loss should be considered as a possibility for sample suites where 1) the samples are only a few percent discordant, and 2) the trend of the data is approximately toward the origin, or toward an apparent episodic loss age that is much too young for the terrain under consideration.

Considerable work is being done by several workers on the problems of disequilibrium in the radioactive series.

Millard (**51**) at the suggestion of L. T. Silver, has preliminarily investigated Pb^{210} disequilibrium in samples of zircon and this work is continuing. The information obtained by these studies will be highly valuable. However, disequilibrium measurements will always be subject to the uncertainty that modern disturbances, for example due to weathering, may mask the long-term behavior.

APPENDIX A

Sample Processing

Generally 50-70 pounds of rock were required to obtain sufficient quantities of accessory minerals for analysis in this study. Each rock sample was first reduced to fist-size pieces or smaller by crushing with a hammer; reduced further to pea gravel size by means of a jaw crusher; and then passed through a disc pulverizer with a plate separation of 0.01-0.02 inches. The heavy minerals were obtained by passing the sample over a Wilfley table, drying the resulting concentrate in acetone, removing particles of iron and magnetite with a hand magnet, and floating the lighter minerals in tetrabromoethane and methylene iodide. The methylene iodide sinks were rinsed with acetone, dried, and sieved on 100 and 200 mesh Nylon bolting cloth. Isolation of particular minerals from each size fraction was achieved with a Frantz Isodynamic Separator operated at 10^{o} tilt and 20^{o} slope. At these settings allanite was separated in the magnetic fraction at 0.3-0.4 amp.; uranothorite was separated variably between 0.5 and 1.5 amp.; and zircon remained non-magnetic at 1.7 amp. Some of the yield characteristics of this system have been discussed by Silver and Deutsch (**52**).

Zircon samples were acid washed for one hour or more in hot concentrated HNO_3. They were then fused with sodium tetraborate flux, using a J. Lawrence Smith platinum

crucible heated in an electric silicon carbide furnace to about 1150°C. The fused bead was removed from the crucible by solution in dilute HCl, and silica was recovered by digestion in HF and $HClO_4$.

Allanite samples were treated in the same way except that they were not acid washed prior to being fused. Uranothorite samples were dissolved in hot concentrated HNO_3, which sufficed to bring most of the uranium and lead into solution. The residue was digested in HF and $HClO_4$.

Samples for feldspar, total rock, and leach analyses were prepared by crushing a selected hand specimen, usually weighing about 200 grams, in a carefully cleaned, hardened steel mortar to -30 mesh or smaller. Aliquots were separated with a clean, aluminum Jones-type splitter. Potash feldspar was isolated from the total material by flotation in a mixture of tetrabromoethane and acetone adjusted to a specific gravity of 2.60. The sample was then dissolved by digestion in HF and $HClO_4$ and fumed dry. The residue was picked up in 6.5N HCl.

Total rock samples were digested in a similar manner, and the insoluble residue was fused in borax as described above.

Chemistry

The extraction of lead and uranium was performed for most samples by procedures outlined by Silver, McKinney

Deutsch and Bolinger (**34**). The sample in solution was aliquoted by weight into two portions. One of these was extracted for the determination of lead composition. To the other were added suitable lead and uranium spikes for determining the concentrations of these elements.

Briefly, a two-stage dithizone extraction was used for lead. Interfering cations were complexed with ammonium citrate and potassium cyanide. The dithizone was digested in HNO_3 and $HClO_4$ and the residue picked up in dilute ammonium nitrate. Lead sulfide was then precipitated and loaded on a tantalum filament.

Uranium was extracted from a separate portion of solution with Hexone in two stages. Aluminum nitrate served as the salting agent in the first stage and saturated ammonium nitrate in the second. The sample was evaporated in a single tantalum filament as uranyl nitrate.

During the course of the work it became apparent that some lead samples, especially from the zircons, were not giving adequate performance in the mass spectrometer. It seemed likely that the double dithizone extraction procedure did not produce a clean enough separation for these particular samples. Accordingly, with the advice of M. Tatsumoto, a procedure for ion-exchange extraction was set up and used for the later samples. The procedure is straightforward. Analytical grade Dowex 1-X8 anion exchange resin is prepared in a column $0.9cm^2$ x 18 cm. The column is washed once with 50 ml. 8.0N HCl and conditioned with 50 ml. 1.3N HCl.

The sample is precipitated from solution with ammonium hydroxide and the supernate discarded. A few drops of concentrated HCl suffice to redissolve the sample, which is then diluted with 50-75 ml. 1.3N HCl. This is passed through the column and the eluate discarded. The lead is eluted with 50 ml. 8.0N HCl. The effluent is not collected until the color change just reaches the bottom of the resin column. The resulting solution is evaporated to 10 ml. or less, diluted with quadruply distilled water, and extracted once with dithizone, using 5 ml. of ammonium citrate. Subsequent digestion of the dithizone and precipitation of PbS is as before. The yield from this method appears to be 80-90%.

After some experience, it proved possible to isolate lead and uranium simultaneously on a single resin column. The above procedure is followed and lead is obtained. The column is then simply eluted once more with 50 ml. of a very dilute nitric acid solution. The effluent is not collected until the color change reaches the bottom of the column. The resulting solution contains the uranium from the sample and in most cases it is not necessary to perform a secondary extraction. The solution is merely evaporated dry and the uranium is picked up in one drop of HNO_3 and evaporated on the filament.

The ion-exchange method has two important advantages. It requires fewer reagents in less quantity, and it permits the use of the entire concentration aliquot for the

extraction of both lead and uranium.

In order to minimize contamination, all evaporations and digestions were carried out in Pyrex or Teflon evaporating tanks flushed with dry nitrogen gas. All glassware and Teflon ware were cleaned by two-stage washing in hot concentrated nitric acid, followed by rinsing with quadruply distilled water. Platinum was cleaned by washing for three minutes in hot 3:1 aqua regia and rinsing as above. Clean equipment was covered with "Saran Wrap" before being stored.

Frequent checks of contamination are performed in the lead laboratory at C.I.T., largely by Dr. Silver and co-workers. It is found that the level of contamination is usually 0.2 μg. or less for lead, and is negligible for uranium. There are three sources from which lead contamination is most likely to occur: the borax flux, the citrate, and the acid bath used to clean the glassware. The compositions of leads from these sources have been determined and are listed below:

Source	206/204	207/204	208/204
Borax flux	17.83	15.55	37.62
Ammonium citrate	18.14	15.58	37.93
Acid wash	18.68	15.66	38.22

Mass Spectrometry

All isotope ratios were measured on a 12-inch, 60° sector, single-focussing mass spectrometer modified by

McKinney from a design by Inghram. This machine utilizes an electron multiplier and a graphical recorder. The raw data must therefore be corrected for discrimination and for deviations of the recorder shunt resistors from their nominal values. The corrections have recently been determined for this machine by McKinney (**41**) and are listed in Table 17 (Chapter 6).

An extensive evaluation of reproducibility characteristics for this machine was carried out by Chow and McKinney (**42**) by repeated analyses of a shelf lead standard. The reproducibility limits for a single run of a single sample are slightly greater than indicated by their results. A more thorough discussion of the sources and magnitudes of mass spectrometric errors for radiogenic lead samples of this study is presented in Chapter 6. The size of the error limit depends partly on the isotopic composition of the sample, especially with respect to the Pb^{206}/Pb^{204} ratio. Statistical analyses of a number of samples indicate that typical reproducibility limits for the isotope ratios of lead, as measured on this mass spectrometer, are:

Ratio	Common lead	Radiogenic lead
206/204	±0.5%	±1.8%
206/207	±0.25%	±0.30%
206/208	±0.30%	±0.35%

If sufficient intensity of the ion beam is not achieved, or if the beam is unstable, the error is larger.

Isotope Dilution

Concentration measurements for uranium and lead were in all cases performed by the technique of isotope dilution. The amount of spike was measured volumetrically with micropipettes. This method is accurate to one percent or better if the amount of uranium or lead in the aliquot to be spiked is within an order of magnitude of the amount of the spike. The largest source of error occurs in the weighing of the sample aliquot. Hence, for radioactive samples in particular, the ratio of uranium to lead should be more accurate than the concentrations per se, since a single aliquot is spiked for both determinations.

Three lead spikes were available and are described in Table 19. The Pb^{207} and Pb^{208} spikes, chiefly the latter, were used for determining concentrations of radiogenic lead. Both had been made by dissolving specimens of isotopically enriched metal in dilute nitric acid. Concentrations of common lead were determined with Pb^{206} spike, isolated from a uraninite ore. Three different U^{235} spikes were used at various times to determine uranium concentrations. Each had been made from carefully prepared U_3O_8.

A more-or-less regular program of cross-checking spike concentrations is maintained at the C.I.T. laboratory by L. T. Silver. "Reserve" bottles of Pb^{207} and Pb^{208} spikes were set aside for this purpose. A natural uranium spike, made from the metal, is available for cross-checking the U^{235} spikes. All spikes are kept in flasks with

ground-glass stoppers. The lead spikes are in 50 ml. bottles and the uranium spikes in 200 and 250 ml. bottles. It has been found that over a period of a year or so, slight but measurable increases occur in the concentrations of actively used spikes. This is readily accounted for by evaporative losses. An extreme example is shown in Figure 20. The regularity of the apparent increase during the early stages is probably fortuitous, since these measurements lie within mass spectrometric errors. However, there can be no doubt that by the middle of 1962 the concentration had measurably increased. Where the curve breaks sharply upward a 10 ml. portion had been removed from the bottle, apparently inducing unusually large evaporation.

Based on curves such as the one shown in Fig. 20, corrections have been made for a number of samples and are so indicated in the tables of data. A larger uncertainty accompanies this treatment. Referring again to Fig. 20, it is not certain, for example, that the concentration increase from the middle of 1961 to the middle of 1962 was truly linear. The entire increase may have occurred during a short time either at the beginning or at the end of the interval. Therefore in some cases the ratio of lead to uranium carries with it an error assignment equivalent to the uncertainty in specifying the drift in spike concentration.

Table 19

LEAD SPIKE DATA

Spike	Pb Atom Percent 204	206	207	208	Concentration (mols/100 λ)
Pb^{206}	0.06	88.27	8.76	2.91	2.994×10^{-7}
Pb^{207}	0.014	3.52	71.53	24.94	8.231×10^{-8}
Pb^{208}	0.013	1.19	2.77	96.02	9.492×10^{-8}

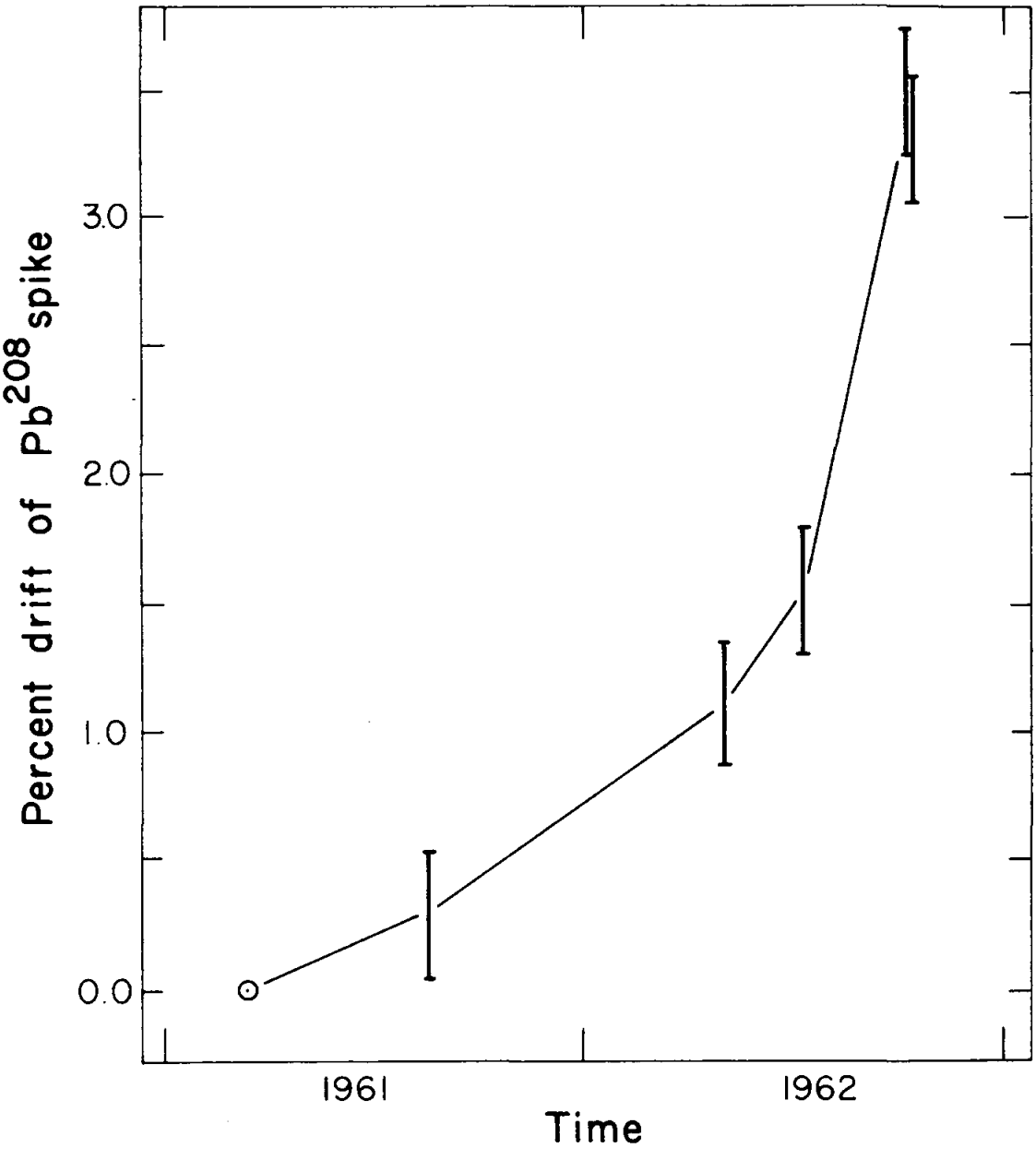

Figure 20

BIBLIOGRAPHY

1. Brown, H., and L. T. Silver (1956), The Possibilities of Obtaining Long-Range Supplies of Uranium, Thorium, and Other Substances from Igneous Rocks, U.S. Geol. Survey Prof. Paper 300, 91-95

2. Larsen, E. S., Jr. (1948), Batholith and Associated Rocks of Corona, Elsinore, and San Luis Rey Quadrangles, Southern California, Geol. Soc. Am. Mem. 29

3. Larsen, E. S., Jr., and D. Gottfried (1961), Distribution of Uranium in Rocks and Minerals of Mesozoic Batholiths in Western United States, U.S. Geol. Survey, Bull. 1070-C

4. Larsen, E. S., Jr., and W. M. Draisin (1948), Composition of the Minerals in the Rocks of the Southern California Batholith, Int. Geol. Congress, Rep't of 18th Session, Great Britain, Part II

5. Patterson, C. C., L. T. Silver, and C. R. McKinney (1956), Lead Isotopes and Magmatic Differentiation, Resumenes de los Trabajos Presentados, Proc. 20th Int. Geol. Congress, Mexico City, Sect. 11-B, 221

6. Larsen, E. S., Jr., D. Gottfried, H. W. Jaffe, and C. L. Waring (1958), Lead-Alpha Ages of the Mesozoic Batholiths of Western North America, U.S. Geol. Survey, Bull. 1070-B

7. Whitfield, J. M., J. J. W. Rogers, and J. A. S. Adams (1959), The Relationship Between the Petrology and the Thorium and Uranium Contents of Some Granitic Rocks, Geochim. et Cosmochim. Acta, 17, 248-271

8. Taylor, H. P., Jr., and S. Epstein (1962), Relationship Between O^{18}/O^{16} Ratios in Coexisting Minerals of Igneous and Metamorphic Rocks. Part 2. Applications to Petrologic Problems. Bull. Geol. Soc. Am., 73, 675-694

9. Tuttle, O. F., and N. L. Bowen (1958), Origin of Granite in the Light of Experimental Studies in the System $NaAlSi_3O_8$-$KAlSi_3O_8$-SiO_2-H_2O, Geol. Soc. Am. Mem. 74

10. MacKevett, E. M. (1951), Geology of the Jurupa Mountains, San Bernardino and Riverside Counties, California, Calif. Div. Mines Sp. Rep't No. 5

11. Burnham, C. W.(1959), Contact Metamorphism of Magnesian Limestones at Crestmore, California, Bull. Geol. Soc. Am., 70, 879-920

12. Gay, P., and R. W. LeMaitre (1961), Some Observations on "Iddingsite", Am. Mineral., 46, 92-111

13. Yoder, H. S., and Th. G. Sahama (1957), Olivine X-ray Determinative Curve, Am. Mineral., 24, 475-491

14. Winchell, A. N., and H. Winchell, Elements of Optical Mineralogy, 4th Ed., J. Wiley and Sons, Inc., N. Y.

15. Eugster, H. P., and D. R. Wones (1962), Stability Relations of the Ferruginous Biotite, Annite, Jour. Petrology, 3, 82-126

16. Stewart, D. B., and E. H. Roseboom, Jr. (1962), Lower Temperature Terminations of the Three-Phase Region Plagioclase-Alkali Feldspar-Liquid, Jour. Petrology, 3, 280-316

17. Yoder, H. S., and H. P. Eugster (1954), Phlogopite Synthesis and Stability Range, Geochim. et Cosmochim. Acta, 6, 157-185

18. Wones, D. R. (1958), The Phlogopite-Annite Join, Carnegie Inst. Wash. Yearbook 57, 194-195

19. Picciotto, E. E. (1950), Distribution de la Radioactivite dans les Roches Eruptives, Bull. Soc. Belge de Geol. de Paléontol. et d'Hydrol., 59, 170-199

20. Larsen, E. S., Jr., N. B. Keevil, and H. C. Harrison (1952), Method for Determining the Age of Igneous Rocks Using the Accessory Minerals, Bull. Geol. Soc. Am., 63, 1045-1052

21. Hurley, P. M., and H. W. Fairbairn (1957), Abundance and Distribution of Uranium and Thorium in Zircon, Sphene, Apatite, Epidote, and Monazite in Granitic Rocks, Trans. Am. Geophys. Union, 38, 939-944

22. Tilton, G. R., C. Patterson, H. Brown, M. Inghram, R. Hayden, D. Hess, and E. Larsen, Jr. (1955), Isotopic Composition and Distribution of Lead, Uranium, and Thorium in a Precambrian Granite, Bull. Geol. Soc. Am., 66, 1131-1148

23. Larsen, E. S., Jr. (1945), Time Required for the Crystallization of the Great Batholith of Southern and Lower California, Am. Jour. Sci., 243-A, Daly Volume, 369-416

24. Aldrich, L. T., G. W. Wetherill, and G. L. Davis (1956), Determinations of Radiogenic Sr^{87} and Rb^{87} of an Interlaboratory Series of Lepidolites, Geochim. et Cosmochim. Acta, 10, 238-240

25. Reynolds, J. H. (1957), Comparative Study of Argon Content and Argon Diffusion in Micas and Feldspars, Geochim. et Cosmochim. Acta, 12, 177-184

26. Silver, L. T., and S. Deutsch (1961), Uranium-Lead Method in Zircons, Ann. New York Acad. Sci., 91, 279-283

27. Wetherill, G. W. (1956), Discordant Uranium-Lead Ages, Trans. Am. Geophys. Union, 37, 320-326

28. Nicolaysen, L. O. (1957), Solid Diffusion in Radioactive Minerals and the Measurement of Absolute Age, Geochim. et Cosmochim. Acta, 11, 41-59

29. Tilton, G. R. (1960), Volume Diffusion as a Mechanism for Discordant Lead Ages, Jour. Geophys. Res., 65, 2933-2945

30. Wasserburg, G. J. (in press), Diffusion Processes in Pb-U Systems, Jour. Geophys. Res.

31. Kulp, J. L., G. L. Bate, and W. S. Broecker (1954), Present Status of the Lead Method of Age Determination, Am. Jour. Sci., 252, 345-365

32. Holland, H. D., and D. Gottfried (1955), The Effect of Nuclear Radiation on the Structure of Zircon, Acta Cryst., 8, 291-300.

33. Wetherill, G. W. (1956), An Interpretation of the Rhodesia and Witwatersrand Age Patterns, Geochim. et Cosmochim. Acta, 9, 290-292

34. Silver, L. T., C. R. McKinney, S. Deutsch, and J. Bolinger (1963), Precambrian Age Determinations in the Western San Gabriel Mountains, California, Jour. Geol., 71, 196-214

35. Gottfried, D., H. W. Jaffe, and F. E. Senftle (1959), Evaluation of the Lead-Alpha (Larsen) Method for Determining Ages of Igneous Rocks, U.S. Geol. Survey Bull. 1097-A

36. Tilton, G. R., and L. O. Nicolaysen (1957), The Use of Monazites for Age Determination, Geochim. et Cosmochim. Acta, 11, 28-40

37. Frondel, C., D. Riska, and J. W. Frondel (1956), X-ray Powder Data for Uranium and Thorium Minerals, U.S. Geol. Survey Bull. 1036-G

38. Fleming, E. H., Jr., A. Ghiorso, and B. B. Cunningham (1952), The Specific Alpha-Activities and Half-Lives of U^{234}, U^{235}, and U^{236}, Phys. Rev., 88, 642-652

39. Stieff, L. R., T. W. Stern, Seiki Oshiro, and F. E. Senftle (1959), Tables for the Calculation of Lead Isotope Ages, U.S. Geol. Survey Prof. Paper 334-A

40. Boardman, W. W., and A. B. Meservey (1948), U^{235} Content of Natural Uranium, K-248, Carbide and Carbon Chemicals Co., K-25 Plant, Oak Ridge, Tenn.

41. McKinney, C. R. (1961), Mass Spectrometer Discrimination (abs.), Am. Geophys. Union, Program of 1st Western Nat. Meet.

42. Chow, T. J., and C. R. McKinney (1958), Mass Spectrometric Determination of lead in Manganese Nodules, Anal. Chem., 30, 1499-1503

43. Greene, R. E., C. A. Kienberger, and A. B. Meservey (1955), U^{235} Content of Natural Uranium, K-1201, Carbide and Carbon Chemicals Co., K-25 Plant, Oak Ridge, Tenn.

44. Russell, R. D., and L. H. Ahrens (1957), Additional Regularities Among Discordant Lead-Uranium Ages, Geochim. et Cosmochim. Acta, 11, 213-218

45. Silver, L. T., and C. R. McKinney (1962), U-Pb Isotopic Studies of a Precambrian Granite, Marble Mountains, California (abs.), Geol. Soc. Am., Program of Cordilleran Sec. Meet.

46. Holmes, A. (1946), The Oldest Known Minerals and Rocks, Trans. Edinburgh Geol. Soc., 14, 176-194

47. Aldrich, L. T., and G. W. Wetherill (1958), Geochronology by Radioactive Decay, Ann. Rev. Nuclear Sci., 8, 257-298

48. Giletti, B. J., and J. L. Kulp (1955), Radon Leakage from Radioactive Minerals, Am. Mineral., 40, 481-496

49. Cherdyntsev, V. V., Abundance of Chemical Elements, Trans. by W. Nichiporuk, U. of Chicago Press, 1961

50. Starik, I. E., O. S. Melikova, V. V. Kurbatov, and V. M. Aleksandrchuk (1955), Byulleten' komissii po opredeleniyu absolutnogo vozrasta geologicheskikh formatsii, 1, No. 22, Acad. Sci., U.S.S.R.

51. Millard, H. (1962), Ph.D. Thesis, California Institute of Technology

52. Silver, L. T., and S. Deutsch (in press), An Experimental Investigation of Discordant Isotopic Ages in Zircons, Jour. Geol.

APPENDIX B

Photograph 1. Contact between coarse-grained and fine-grained Mt. Rubidoux granites.

Photograph 1.

Photograph 2. Coarse-grained Mt. Rubidoux granite: orange-colored "iddingsite" (id) surrounding remnant cores of fayalite (fa) and associated with biotite (bi). Pale green chloritic(?) filaments extending diagonally across picture fill fractures in feldspar crystals and are presumed responsible for the blue-green color of the fresh rock. Plain light, 20X.

Photograph 3. Coarse-grained Mt. Rubidoux granite: partially altered hypersthene (hy) with biotite (bi), magnetite (mg), and hornblende (hb). Plain light, 8X.

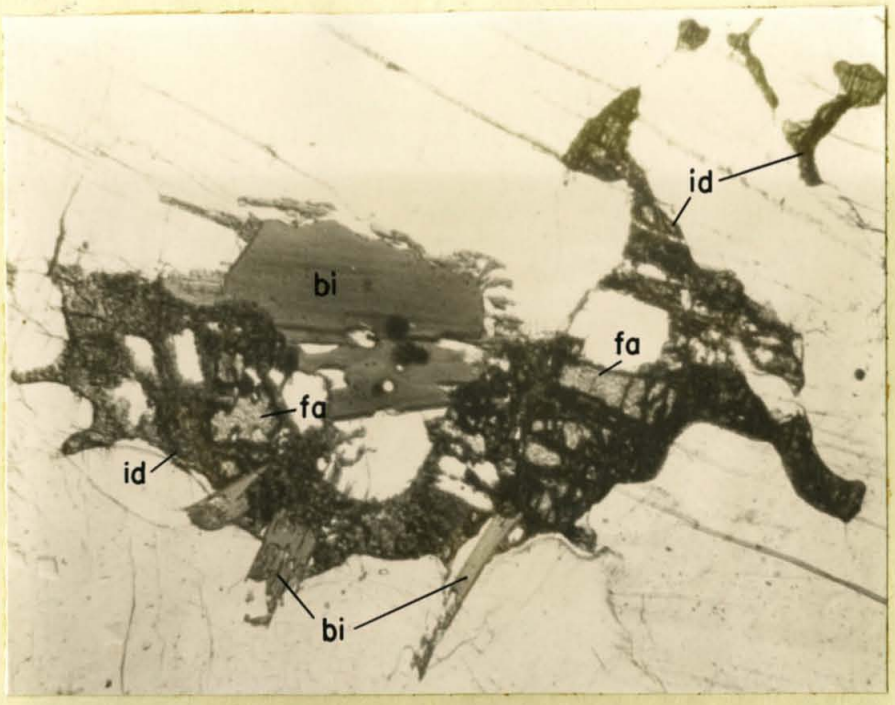

Photograph 2

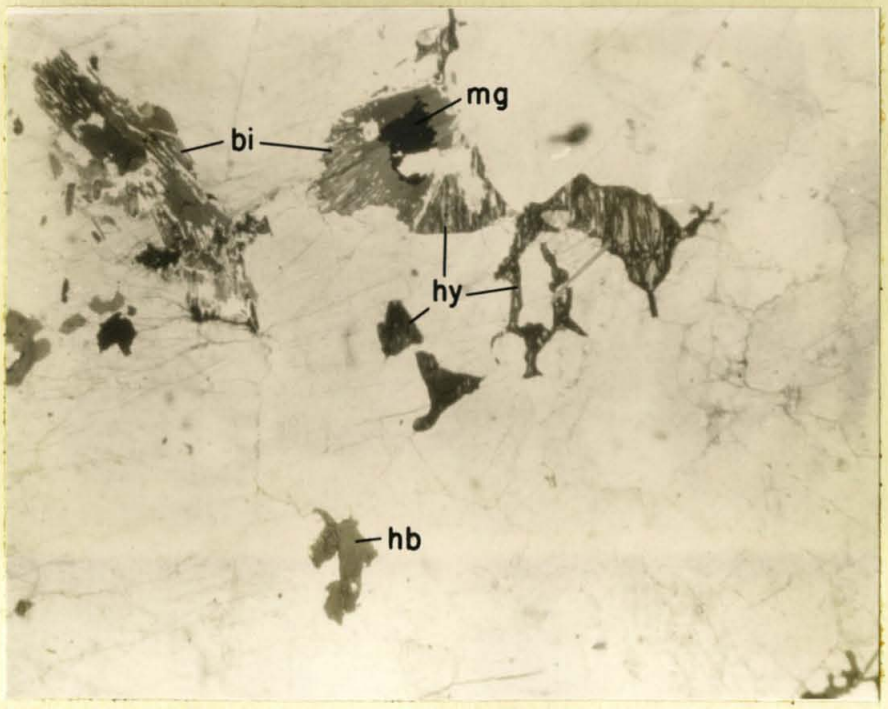

Photograph 3.

Photograph 4. Coarse-grained Mt. Rubidoux granite: olive green chloritic deuteric material with associated magnetite (mg) and biotite (bi). Several sircon crystals (s) are visible. Plain light, 20X.

Photograph 5. Coarse-grained Mt. Rubidoux granite: uranothorite (u) included in biotite. Large grain of "iddingsite" (id) in upper center is situated between biotite and hornblende. Plain light, 20X.

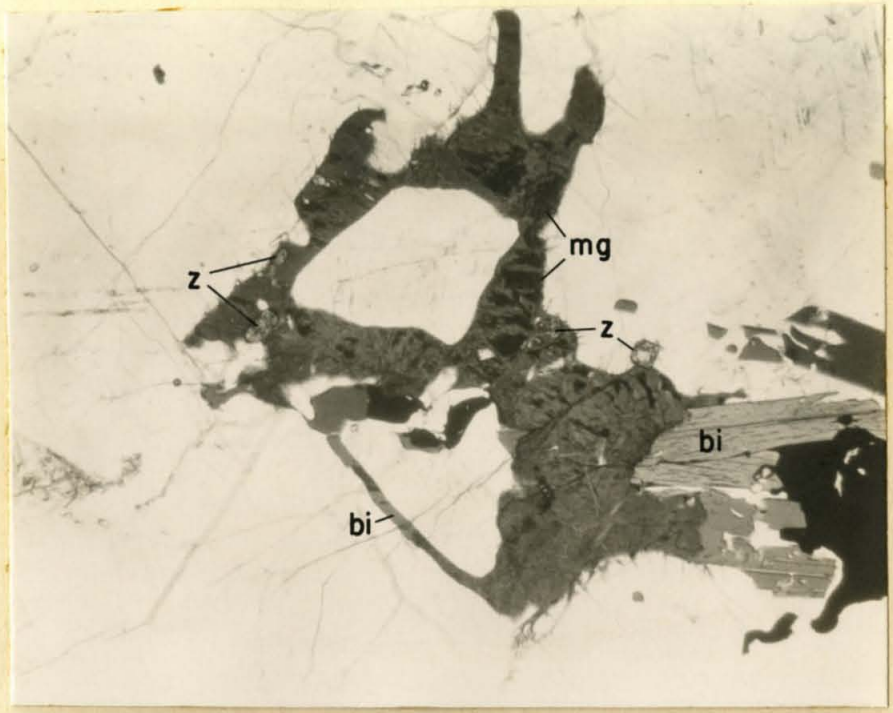

Photograph 4.

Photograph 5.

Photograph 6. General view of collection sites for coarse-grained Mt. Rubidoux granite. SCB-36 is large boulder at center right. SCB-101 is small trench at upper left center (note shovel). SCB-107 and -108 are out of view to the left. Ground surface rises gently behind SCB-101 to about position of power pole, where slope becomes steeper.

Photograph 6.

Photograph 7. Coarse-grained Mt. Rubidoux granite collection site SCB-36. Exposed face shows clear blue-green color characteristic of the unweathered granite, except for a 1-5 mm thick weathering rind on the original surface of the boulder. Samples were collected from fractured portions near hammer.

Photograph 7.

Photograph 8. Weathered coarse-grained Mt. Rubidoux granite collection sites SCB-101A, -101B, and -101C_1. Present ground surface is formed by a disturbed layer above the true A zone. Boundary between B and C_1 zones is irregular but generally slopes slightly upward to the right. Note spheroidally weathered material in lower part of picture, suggesting <u>in situ</u> nature of C_1 zone.

Photograph 8.

Photograph 9. SCB-36 P100-R200 mesh concentrate of zircon and uranothorite. This material has slightly higher magnetic susceptibility than the zircon fractions which were analyzed, and has not been acid washed. Note opaque inclusions in zircons which appear to contribute to magnetic susceptibility. 20X.

Photograph 10. SCB-36 P100-R200 mesh zircon concentrate; corresponding to the analyzed fraction before acid washing. A few grains of uranothorite are present, which would be dissolved in HNO_3. Index of refraction of medium is 1.65. 20X.

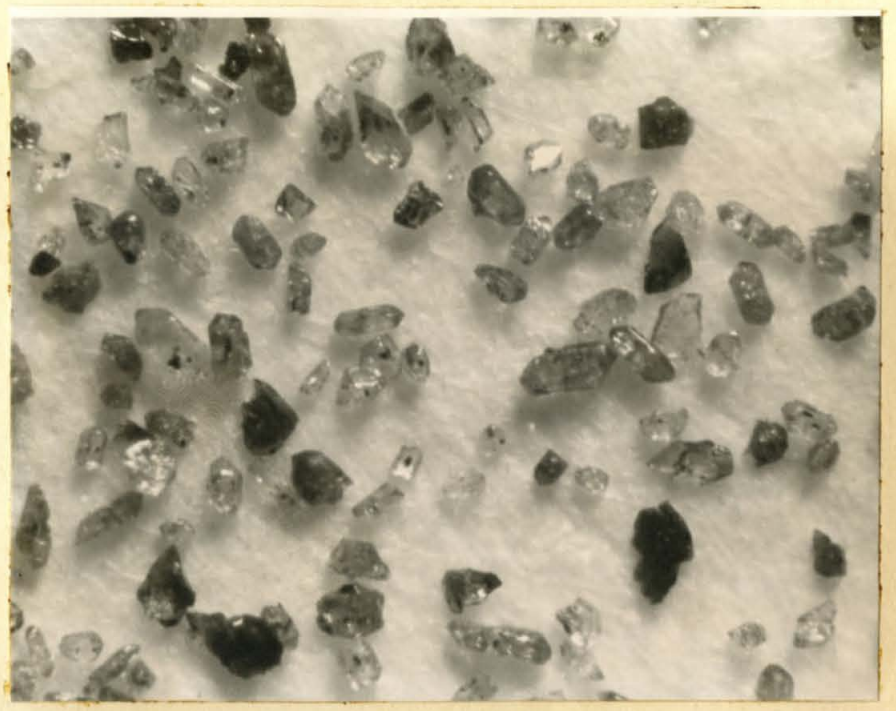

Photograph 9.

Photograph 10.

Photograph 11. SCB-36 P100-R200 zircons, showing diversity of form and typical character of inclusions in analyzed fraction. Index of medium 1.65, 80X.

Photograph 12. SCB-36 P100-R200 zircons. Zoned crystal with core of uranothorite(?). This variety is quite rare. Index of medium 1.65, 80X.

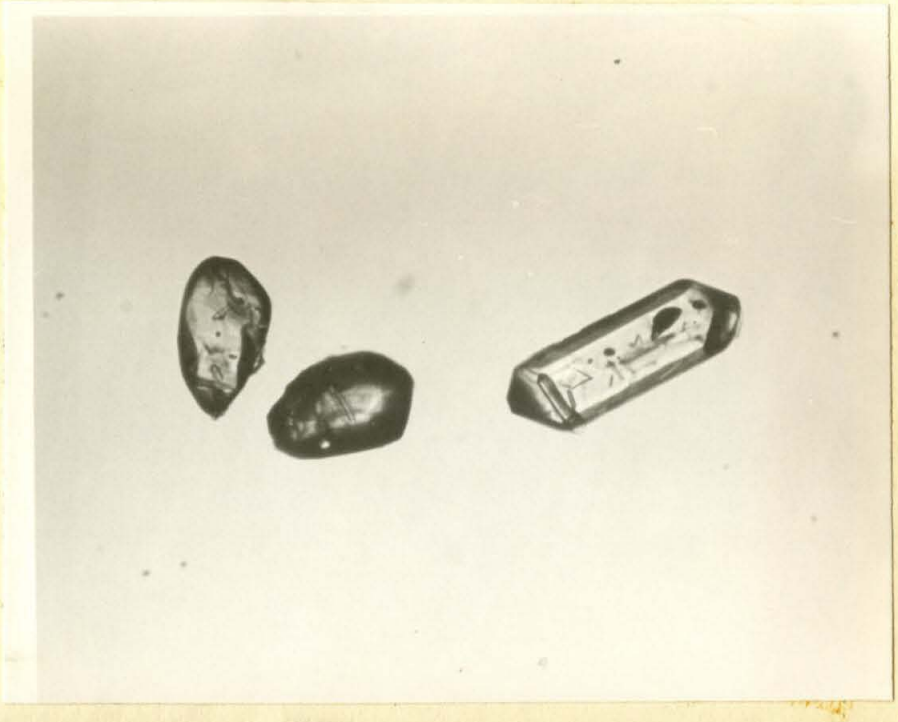

Photograph 11.

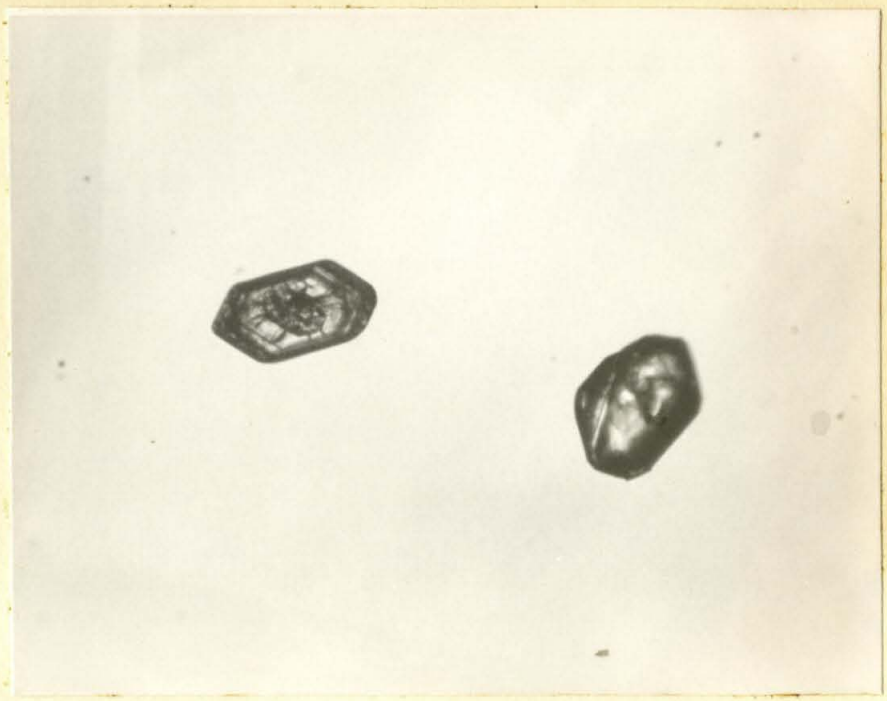

Photograph 12.

Photograph 13. SCB-101C$_3$ F100-H200 mesh acid-washed zircon concentrate; corresponding to analysed fraction. Index of medium 1.65, 20X.

Photograph 14. SCB-101C$_3$ F100-H200 zircons with unusually poor form. Index of medium 1.65, 80X.

Photograph 13.

Photograph 14.

Photograph 15. SCB-1018$_3$ F100-R200 euhedral zircons. Index of medium 1.65, 80X.

Photograph 16. SCB-36 F100-R200 allanite. Note relative homogeneity of grains. Index of medium 1.65, 80X.

Photograph 15.

Photograph 16.

Photograph 17. SCB-36 F100-R200 uranotborite with opaque inclusions. Index of medium 1.65, 80X.

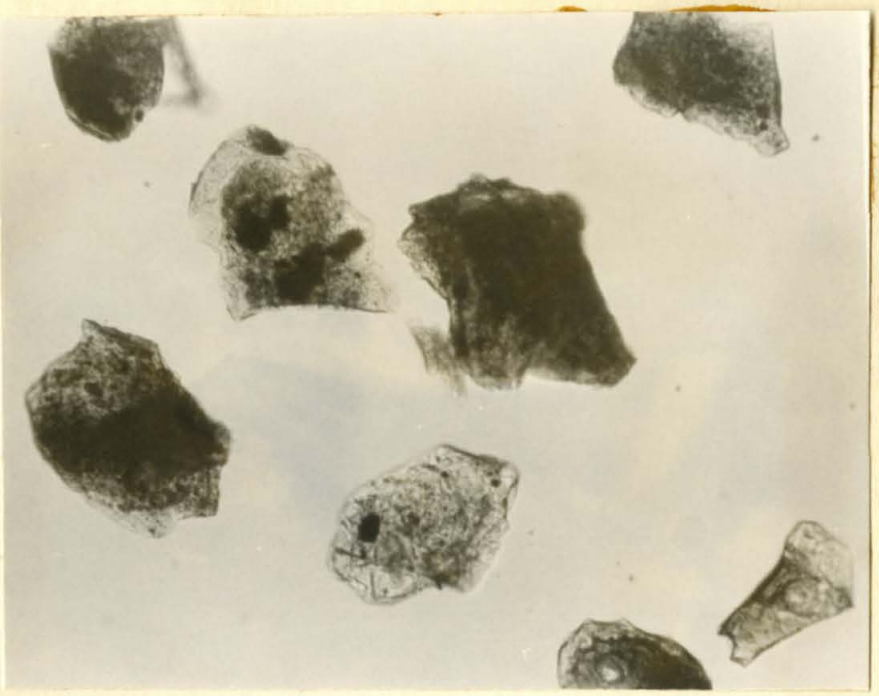

Photograph 17.